Assembly, Spatial Distribution, and Secretion Activity of the Curlin Secretion Lipoprotein, CsgG.

by

Elisabeth Ashman Epstein

A dissertation submitted in partial fulfillment
of the requirements for the degree of
Doctor of Philosophy
(Molecular, Cellular, and Developmental Biology)
in The University of Michigan
2008

Doctoral Committee:

Assistant Professor Matthew R. Chapman, Chair
Associate Professor Kenneth M. Cadigan
Associate Professor Ursula H. Jacob
Assistant Professor Maria B. Sandkvist

Everything should be made as simple as possible, but not any simpler.

- A. Einstein

for my parents

Ken and Rita Ashman

who have always cared for me, encouraged me, and believed in me

Acknowledgements

The work presented in this dissertation was achieved with the support of many people, both in my scientific and personal communities. First, I have been fortunate to have a truly excellent mentor and advisor in Dr. Matt Chapman. Matt has been a steady source of guidance, has supported me both professionally and personally, and has created a lab environment that encourages the sharing of scientific ideas while also fostering independence and creativity. I've been truly honored to be a part of his research group, and I have benefited greatly from the people I've known and worked with here. The members of my dissertation committee, Drs. Ken Cadigan, Ursula Jacob, and Maria Sandkvist have provided invaluable support and feedback, and I thank them for all of their efforts. Dr. Michelle Barnhart was an important source of guidance and scientific knowledge in my first years as a graduate student, and a good friend. Xuan Wang has been a great colleague, giving critical feedback on several of my manuscripts and much excellent scientific expertise, not to mention our late-night discussions in the lab. His friendship has been a highlight of graduate school. Neal Hammer, Daniel Smith, and Ryan Frisch each kept me on my toes in lab meeting where they gave excellent feedback and criticisms of my experimental results, manuscripts, and many helpful ideas. They've also always been ready with a good word of advice or a joke when it is needed. I am grateful for their support

over the years. Kate Parzych was always ready to talk science and take a walk to get some much-needed caffeine. I also appreciate the many helpful discussions I have had with Dr. Robert Bender, as well as his comments on the manuscript published from Chapter II. I have had the privilege of working with three excellent undergraduate students in the Chapman lab: Christina Nisonger, Ingrid Zylinsky, and Margeaux Reizian. These future doctors will probably save the world someday. Fei Li and Yizhou Zhou have also provided criticism on the work presented in Chapter III. I have known them both for only a brief time, but can see that the future of the lab is very bright indeed.

Much of the work presented in this dissertation has been previously published or, at the time of this writing, is in preparation for publication. Much of Chapter I contains was published as a review article {Epstein and Chapman, 2008, Cell Microbiol, 10, 1413-20}. Chapter II was published as {Robinson et al., 2006, Mol Microbiol, 59, 870-81}, and Drs. Lloyd Robinson and John Heuser collected some of the data presented in Chapter II. Chapter III has been submitted for publication while IV is currently in preparation for publication. Margeaux Reizian collected some of data contained in Chapter III, and Lloyd Robinson, Ashley Nenninger, and Neal Hammer each contributed data to Chapter IV. In addition, I gratefully acknowledge Dr. Amy Chang, and members of her laboratory, for their generous and frequent accommodation of my many hours of use of their Olympus microscope. Gregg Sobocinski and Xuan Wang provided technical advice and assistance on electron microscopy, which I used in the generation of data presented in Chapters III and IV. Pamela Wong and Dr. David Thanassi

generously spent time and resources teaching me their liposome permeabilization assays to test pore formation, which is presented briefly in Chapter V.

The Genetics Training Program, NIH National Research Service Award T32GMO7544, generously supported much of my time at the University of Michigan both financially and intellectually. This excellent program helped me grow tremendously as a scientist, and I am particularly thankful for the efforts of Drs. John Moran and Miriam Meisler for their administration of the program and for exponentially increasing my understanding and appreciation of all things genetic.

I am very glad to have been part of the Department of Molecular, Cellular, and Developmental Biology. In particular, Mary Carr has been a huge source of support and helped me navigate the sometimes-confusing waters of funding, health insurance, and Rackham requirements. She has also been a good friend. No work in the department could be done without the efforts of all of the office and building staff, including Diane Durfy, Shelia Dunn, and Ed Grant.

Finally, while this dissertation will focus on my time at the bench, life outside of the lab has been very full and rich these past years, and I thank all of those who have helped make it so. Kaustuv Datta, Jennifer Fuentes, Ashwini Joglekar, Jenn Skidmore, Marya Liimatta, and Chris Rosario welcomed me into an unfamiliar place and made me feel at home here in Ann Arbor. Sukanya Puthambaker has

been a great friend both in and out of Kraus. Drake and Nancy Meadow have been true friends in every way. Therese Maynard has always has left the door open for me, making me feel welcomed and loved. To all the rest of my Michigan family, for things big and small – thank you! A little over five years ago Rachel Rodriguez quit her job and drove with me across the country from the California Central Coast to Ann Arbor, so none of this would have been possible without her. Special thanks are due to the members of the United States Coast Guard and the Port San Luis Harbor Patrol, as without their efforts this dissertation would not have been completed. My parents and brother have always supported me and to them I am very grateful. Neil Epstein understands what it means to go through graduate school and, most of all, has been a huge source of support as I complete this stage of the journey. Finally, I am thankful for all the long talks and sweet days with my grandmother, Geraldine Leger. Her memory is a blessing.

Table of Contents

List of Figures

Figure

List of Tables

Table

Chapter I

Introduction

Amyloid: a convergence of diverse proteins along a common folding pathway

The ability of bacteria to interact with their environment is often mediated by the presence of cell-surface organelles composed of protein polymers. These extracellular protein fibers are implicated in diverse processes like locomotion, attachment to surfaces, natural competence, and host-pathogen interactions (Jonson et al., 2005; Fernandez and Berenguer, 2000). The extracellular environment can be a harsh locale with little energy available for protein folding, and dynamic physical conditions like changing water content, salt concentrations, pH fluctuations, and bombardment with denaturing chemicals. Therefore, assembly of surface structures in the extracellular environment may rely on proteins that can self-assemble without assistance from cellular chaperones, have low energy folding requirements, and are resistant to denaturation and chemical perturbation.

One protein folding assembly pathway that satisfies these conditions is amyloid. Amyloid fibril assembly is a hallmark of diverse neurological diseases such as Alzheimer's disease, Parkinson's disease, Huntington's disease, and bovine spongiform encephalopathy (mad cow disease). Disease-associatedamyloid formation is the result of misfolding and aggregation of

peptides into structurally conserved fibers (Ross and Poirier, 2004). However, amyloid formation is also integrated as a critical element of cellular physiology, and many organisms direct amyloid fiber formation to accomplish important biological tasks (Fowler et al., 2007). Whether the product of disease-associated protein misfolding or a dedicated assembly pathway, all amyloid fibers are characterized by a 'cross-β strand structure, where the β-sheets are oriented anti-parallel to the fiber axis (Nelson et al., 2005). This structure gives rise to common physical properties. Amyloid fibers are self-assembling polymers of protein that are resistant to chemical and temperature denaturation, and to digestion by proteinases (Nordstedt et al., 1994). The β-sheet rich fibers also have similar tinctorial properties: binding to amyloid-specific dyes such as Congo red and Thioflavin T (ThT) are diagnostic of amyloid (Elghetany and Saleem, 1988). Amyloids are abundant in bacterial biofilms, and a recent report suggested that up to 40% of the biomass in activated sludge consists of amyloid-like filaments (Larsen et al., 2007; Larsen et al., 2008).

Much of our knowledge concerning the highly adaptive amyloid fold comes from studies of eukaryotic protein misfolding diseases. Each of these diseases shares a common etiology: the conversion of soluble, non-toxic protein into highly ordered and aggregative fibers. Remarkably, the amyloid-forming proteins of different diseases share little to no sequence homology while the fibers themselves converge on a biochemically similar β-sheet rich conformation. Indeed, a common folding pathway characterizes most amyloid fibers where oligomeric intermediates form that give way to the mature β-sheet rich fibers (Figure 1.1). Conformation-specific antibodies have been isolated that recognize

the transient oligomeric intermediate, but not soluble monomers or mature fibers (Kayed et al., 2003). Conformationally reactive antibodies that were raised against oligomers from the amyloid-forming peptide implicated in Alzheimer's disease (Aβ) also recognize oligomers of non-related amyloid proteins. This suggests that the amyloid folding pathway is remarkably conserved, even comparing diverse proteins (Kayed et al., 2003; Yoshiike et al., 2007; Kayed et al., 2007; Wang et al., 2007).

Evidence is accumulating that suggests that the most toxic species formed by the amyloid folding pathway is the oligomeric intermediate, not the fibers themselves (Caughey and Lansbury, 2003). Further, the conformation of the oligomers as viewed by electron microscopy seems to be quite similar between different amyloid proteins. Indeed, the similar structure of the pre-amyloid oligomers may underlie their common mechanism of toxicity: spherical pre-amyloid oligomers may compromise the integrity of membranes by acting as ion-conducting channels (Caughey and Lansbury, 2003). This model of toxicity has lead to the speculation that the mature amyloid fibers may serve a detoxifying function in cells, and so amyloid formation may offer physiological benefits for cells. The transient oligomeric intermediate species has been detected in the folding of functional amyloids like curli (Wang et al., 2007), and a pre-amyloid oligomer has been implicated in the functional toxicity of the harpins and microcinE492 (Oh et al., 2007; Bieler et al., 2005).

Functional amyloids have been identified in mammals, yeast, and bacteria (Fowler et al., 2007). In bacteria, these amyloids play diverse physiological roles, from the building blocks of the extracellular matrix and determinants of

attachment to mediating toxicity in plants and bacteria – physiological processes that are highly relevant to study in their own right. Functional bacterial amyloids and their disease-associated counterparts converge on a folding pathway that converts soluble proteins to β-sheet rich fibers (Figure 1.1). Notably, the properties that are the most exploited and even beneficial for the organisms that assemble functional amyloids are precisely those characteristics that are the most detrimental when amyloids form in the context of disease. This chapter focuses on some of the best-studied bacterial amyloids and the insights on amyloid formation that we can draw from their respective properties. In particular, we examine bacterial amyloids that appear to functionally favor either the mature, nontoxic amyloid fibers (e.g., curli) or the toxic oligomeric intermediate (e.g., MccE492), as well as survey several newly discovered functional bacterial amyloid-like proteins.

Curli amyloid fibers: biology and pathology

Curli are highly aggregative surface fibers assembled by many *Enterobacteriaceae*, including *Escherichia coli* (Bokranz et al., 2005). First observed in 1989 in fibronectin-binding *E. coli* isolates from bovine fecal samples (Olsen et al., 1989), curli fibers have been shown to mediate interactions between individual bacteria, between bacteria and host tissues, and even to inert surfaces that often resist bacterial colonization, like Teflon and stainless steel (Pawar et al., 2005; Ryu et al., 2004; Uhlich et al., 2006; Bokranz et al., 2005; Gophna et al., 2001; Zogaj et al., 2003). Curli have been implicated in the host-pathogen interaction because they induce the host inflammatory response and

contribute to persistence within the host. Curli are also required for formation of bacterial multi-cellular communities called biofilms (Gophna et al., 2001; Johansson et al., 2001; Olsen et al., 1998; Uhlich et al., 2002). Curli fibers are 4 to 6 nm-wide and are curly, densely tangled masses of extracellular fibers that group cells together (Figure 1.2). Curli, like other amyloid fibers, are resistant to proteinase digestion and are insoluble in when boiled in 1% SDS (Olsen et al., 1989; Collinson et al., 1991). Curli fibers display a characteristic β-sheet rich spectrum when analyzed by circular dichroism spectroscopy and bind the amyloid-specific dyes Congo red and ThT (Chapman et al., 2002).

The Curli Biogenesis Machine

Curli assembly requires the products of at least two divergently transcribed operons: *csgBAC* and *csgDEFG* (Figure 1.2). The *csgBAC* operon encodes the protein subunits of curli fibers, CsgA and CsgB, which must physically interact in order to achieve amyloid assembly (Arnqvist et al., 1992; Collinson et al., 1996; Johansson et al., 2001; Knobl et al., 2001; La Ragione et al., 2001). A third gene in the operon, *csgC*, has no described function nor can a transcript or protein be detected in *E. coli*. A recent report on AgfC, encoded by the *csgC* homolog in *Salmonella spp.,* suggested that this protein might influence the ultra-structural characteristics of curli (Gibson et al., 2007).

CsgA is secreted from cells in a soluble, unfolded state in the absence of CsgB (Hammar et al., 1996). CsgB, which is associated with the bacterial outer membrane, mediates the conversion of soluble CsgA into insoluble and aggregative cell-surface fibers (Hammar et al., 1996; Bian and Normark, 1997;

Hammer et al., 2007; Chapman et al., 2002). Interestingly, CsgA and CsgB need not be expressed from the same cell to display these polymerization activities. Curli fibers assemble on the surface of *csgA*- (CsgB+) cells if grown adjacent to cells secreting CsgA (Hammar et al., 1996; Chapman et al., 2002). This interbacterial complementation demonstrates a model for curli assembly termed 'nucleation-precipitation' and suggests an elegant solution to controlling the process of amyloid formation (Figure 1.2). The cell limits formation of aggregative amyloid fibers to the extra-cellular surface by segregating the activities of nucleation and fiber polymerization into separate proteins that are secreted to the extracellular environment.

The *csgDEFG* operon encodes non-structural proteins essential for production, stability and secretion of the subunit proteins (Chapman et al., 2002; Hammar et al., 1995; Loferer et al., 1997; Robinson et al., 2006). Localization of CsgA and CsgB to the cell surface requires a biogenesis machine composed of at least CsgE, CsgF, and CsgG. CsgD is a transcriptional activator of the *csgBAC* operon, and is also a critical activator of several other operons necessary for biofilm formation, most notably, the cellulose biosynthesis pathway (Gerstel et al., 2003; Gerstel and Romling, 2003; Brombacher et al., 2003). The intergenic region between *csgDEFG* and *csgBAC* is one of the largest in *E. coli*, and the expression of the curli operons is regulated by a complex blend of factors that fine-tune operon expression according to environmental conditions. The interplay between different regulatory factors leads to strain-specific responses to any given condition or set of conditions (Barnhart and Chapman, 2006; Romling, 2005). CsgB, CsgA, CsgE, CsgF, and CsgG each have SEC translocation

sequences that target them for translocation across the cytoplasmic (inner) membrane. Chapter 2 of this dissertation shows that CsgG is an outer membrane localized lipoprotein that is essential for stability and secretion of CsgA and CsgB (Loferer et al., 1997; Robinson et al., 2006). Purified CsgG forms barrel-shaped oligomeric structures (Figure 1.2), and its expression is correlated with pore-like properties such as increased sensitivity to erythromycin (Robinson et al., 2006). CsgG must be localized to the outer membrane in order to stabilize CsgA or CsgB, and CsgG variants localized either to the inner membrane or the periplasm are unable to stabilize or secrete the subunits (Robinson et al., 2006). CsgG interacts with a specific domain at the N-terminus of CsgA; this domain can be used to target non-*csg* proteins to CsgG (Robinson et al., 2006). We also demonstrated that CsgG coimmunoprecipitates with CsgE and CsgF at the outer membrane. CsgG is sufficient to mediate CsgA secretion out of the cell, but CsgE and CsgF are required for efficient curli fiber assembly under most conditions (Hammar et al., 1995; Chapman et al., 2002). The molecular details of CsgE and CsgF function are unclear, although some clues point to their activities. *csgE* mutants do not assemble curli fibers, and the stability of the CsgA and CsgB proteins is greatly reduced relative to the parental wild type (WT) strain (Chapman et al., 2002). *csgF* mutants are deficient in nucleation and exhibit a delay in assembly of curli fibers (Chapman et al., 2002; Hammer et al., 2007). Increased amounts of CsgA are secreted when cells lack CsgF, which suggests that CsgF has a negative effect on CsgA secretion (Chapman et al., 2002; Hammer et al., 2007).

Curli biogenesis is an extremely efficient process, but the mechanism by which assembly is achieved is only beginning to be described. How does the cell prevent internal amyloid assembly (that is, association of CsgA and CsgB prior to their localization to the cell surface)? No accumulation of intracellular intermediates is detected in the absence of CsgG, although the reasons for this remain uncharacterized (Robinson et al., 2006). In addition, the functions of CsgE and CsgF appear to modulate some undefined aspect of CsgG activity. Chapter 4 shows how CsgE directly modulates CsgG activity. Fortunately, *E. coli* is highly amenable to biochemical and genetic analysis, making possible molecular dissection of nucleation and polymerization.

Molecular dissection of curli nucleation and polymerization

The amino acid sequences of CsgA and CsgB contain three readily-identifiable domains: a SEC secretion signal, an N-terminal sequence that, at least for CsgA, targets the protein to CsgG, and an amyloid core domain that is incorporated into amyloid fibers (Robinson et al., 2006; Collinson et al., 1991; Wang et al., 2007). The amyloid core can be further divided into five repeating units. The repeating units are characterized by a five-fold internal symmetry, where each unit is comprised of 19 – 24 amino acids containing conserved serine, glutamine, and asparagine residues (Wang et al., 2007). Interestingly, the CsgA repeating units have different propensities for aggregation, and three of the five units are distinctly amyloidogenic (Olsen et al., 2002; Wang et al., 2007).

CsgA can be readily purified from the culture supernatants of a strain overexpressing both CsgA and CsgG; CsgA is an unstructured, soluble monomer

immediately following purification (Chapman et al., 2002). Purified CsgA self-assembles into amyloid fibers several hours after purification (Wang et al., 2007). Amyloid polymerization of CsgA *in vitro* can be followed in real time by monitoring the fluorescence emitted when the protein is mixed with the amyloid-specific dye ThT (Wang et al., 2007). *In vitro* kinetic studies on CsgA polymerization suggest that the elongation process can happen in three distinct phases: a lag phase, a fast phase, and a stationary phase (Figure 1.1). The lag phase of CsgA polymerization can be abolished by adding a small amount of preformed CsgA fibers, or 'seeds' (Wang et al., 2007).

The amyloid field has long sought to identify the factor(s) that trigger conversion or nucleation of soluble, pre-amyloid monomers into mature amyloid fibers. The curli system is positioned to lend insight into this process because CsgB is the only dedicated nucleator protein described. It has recently been shown that a domain at the C-terminus of CsgB mediates interaction with the outer membrane; truncation of CsgB results in its secretion away from the cells (Hammer et al., 2007). How the C-terminal domain mediates membrane interaction is undefined. The truncated CsgB self-assembles into amyloid fibers *in vitro* and in some conditions can nucleate CsgA into curli fibers *in vivo* (Hammer et al., 2007). Adding the truncated CsgB to an *in vitro* CsgA polymerization reaction abolishes the lag phase and accelerates polymerization, suggesting that CsgB-mediated nucleation of CsgA may occur via presentation of an amyloid-like template to soluble CsgA molecules (Hammer et al., 2007).

The ability of CsgA and CsgB to self-assemble into fibers coupled with the ability of the fibers to seed CsgA amyloid polymerization suggests a template-

driven mechanism for the assembly of curli fibers (Wang et al., 2007; Hammer et al., 2007). First, CsgA may adopt the amyloid conformation presented to it by CsgB at the cell surface. Second, amyloid CsgA can itself act as a template for the subsequent conversion and incorporation of unpolymerized CsgA monomers to the growing tip of the curli fiber (Figure 1.2). It is noteworthy that full-length CsgB does not form fibers *in vivo*, and thus may be an example of a non-fiber forming amyloid protein. The membrane-associated C-terminus of CsgB may prevent CsgB from polymerizing by anchoring the protein to the membrane, but the exact mechanism underlying this aspect of CsgB behavior remains to be elucidated. CsgA, on the other hand, seems to be adapted to polymerize into amyloid fibers and yet to only undergo that process, *in vivo*, when CsgB is available to nucleate it. Elucidation of the molecular details of the CsgB-CsgA interaction and the determinants of CsgA response to nucleation and self-seeding will provide new insights into amyloid assembly.

Amyloid formation of Microcin E492: exploitation of toxic oligomers

Microcin E492 (MccE492) of *Klebsiella pnumoniae* is a toxic, bactericidal protein that assembles into oligomeric pores in the inner membrane of neighboring bacteria. MccE492, which specifically targets Enterobacter species, is imported across the bacterial outer membrane in a receptor-mediated fashion (Destoumieux-Garzon et al., 2003). MccE492 has been shown to form voltage-independent ion channels in planar lipid bilayers (Lagos et al., 1993). The toxicity of the MccE492 peptide changes over the growth cycle of the *K. pnumoniae*: toxicity is greatest during exponential phase and lowest during stationary phase.

No difference in the mass of the peptide, post-translational modification, or protein stability can be detected during these different phases (Bieler et al., 2005).

The change in bactericidal activity of MccE492 when cells transition into stationary phase is proposed to be dependent on amyloidogenesis. MccE492 forms amyloid fibers *in vivo* that correspond to MccE492 toxicity decrease. The assembly of amyloid fibers can be monitored *in vitro*, and corresponds to a loss of toxicity (Bieler et al., 2005). Therefore, the biologically active MccE492 species is presumably a transient pre-amyloid oligomer. A tempting speculation is that the toxic MccE492 species has structural similarity with the toxic, transient oligomeric species formed by disease-associated amyloids. Interestingly, *K. pnumoniae* produces a small protein localized to the inner membrane, MceB, that confers resistance to MccE492 toxicity (Lagos et al., 1999). The mechanism of MceB-mediated immunity has not been reported.

Emerging bacterial amyloids: harpins, chaplins, and MTP

Harpins are virulence factors for plant pathogens such as *Xanthomonas*, *Erwinia*, and *Pseudomonas* species. Harpins are substrates of type III secretion, and they elicit 'hypersensitive response' in the plant host. Hypersensitive response is the generation of cell death in a localized region of plant tissue – presumably to prevent spread of the pathogen. Hypersensitive response is characterized by changes in ion flux followed by production of reactive oxygen species (Heath, 2000). The mechanism by which harpins induce hypersensitive response is unclear and controversial, although evidence suggests these

proteins may compromise membrane integrity (Lee et al., 2001). A recent report shows that harpins from several species could form amyloid-like fibers *in vitro* (Oh et al., 2007). Furthermore, harpin amyloid formation can be linked to the hypersensitive response. The amyloid-forming ability of HpaG, a harpin from *Xanthomonas,* directly correlates with hypersensitive response. A mutant HpaG unable to form amyloid also fails to elicit the hypersensitive response. Interestingly, size exclusion chromatography and visualization by electron microscopy suggests that a tetrameric oligomer is present at the earliest time-points that elicit hypersensitive response, and that the oligomer does not form in the non-toxic mutant (Oh et al., 2007). The sequence determinants of HpaG amyloid formation have not yet been fully reported. HpaG possesses a glutamine-rich prion-like domain, but this domain is dispensable for hypersensitive response (Kim et al., 2004).

Streptomyces coelicolor are soil bacteria that, akin to filamentous fungi, produce aerial hyphae to dispense spores. The biogenesis of aerial hyphae is a physical challenge that requires a dramatic change in the surface hydrophobicity of the organism: the subterranean hyphae are hydrophilic while the aerial hyphae and spores are hydrophobic (Elliot et al., 2003). This change in hydrophobicity is a result of the SDS-insoluble 'surface layer' on the aerial hyphae and spores. The formation of the surface layer requires a group of proteins called chaplins (Claessen et al., 2003). Chaplins in *S. coelicolor* are encoded by *chpA-H* and are necessary for formation of aerial hyphae (Claessen et al., 2003). The chaplins assemble into a network of amyloid fibers in the surface layer; the fibers self-assemble to β-sheet rich fibers *in vitro* and bind amyloid-specific dyes. The

amyloid properties of chaplins might impart a hydrophobic nature to the surface layer and cause a decrease in the surface tension at the air-water interface. The hyphae then could be freed from the soil and continue to grow up into the air (Claessen et al., 2004). The mechanism by which chaplin amyloids assemble and the individual contributions of the eight chaplin proteins to the amyloid network remain largely undefined. Remarkably, addition of crude chaplin-containing cell extract restores formation of aerial hyphae to mutant *S. coelicolor* filaments lacking some of the *chp* genes, an observation reminiscent of the interbacterial complementation phenotype of curliated bacteria (Claessen et al., 2003). Further, there may be a temporal regulation influencing the expression of the genes encoding chaplins (Claessen et al., 2003), suggesting that a coordinated amyloid biosynthesis pathway is at work in the assembly of chaplin amyloids.

A recent report describes the presence of thin, highly aggregative protein fibers on the surface of *Mycobacterium tuberculosis* (Alteri et al., 2007). Electron microscopic analysis of the *M. tuberculosis* pili (MTP) shows fibers that are strikingly similar to curli fibers. MTP are SDS-insoluble and bind Congo red – suggesting that MTP indeed may be an amyloid fiber. The significance of MTP fibers for *M. tuberculosis* physiology is unknown, but more than half of recently examined tuberculosis patients possess antiserum to MTP, suggesting that MTP production may be part of *M. tuberculosis* pathogenesis (Alteri et al., 2007).

Functional amyloids: protein misfolding done right

The discovery of proteinaceous plaques in the brains of deceased dementia patients launched a hundred-year exploration for the factors that mediate the conversion of soluble, nontoxic proteins into aggregative amyloid fibers. Despite this effort, the exact nature of amyloid toxicity and the initiation of amyloid protein aggregation remains unclear. Bacteria utilize amyloid polymerization to accomplish a variety of tasks, from attachment and colonization to toxicity and pathogenesis. Bacteria seem to exploit the toxic intermediate species (in the cases of MccE492 and the harpins) as well as the mature amyloid fiber (as in curli and the chaplins) in positive ways. The study of bacterial amyloid fibers may hold the key to understanding the methods nature has evolved to harness the power of amyloid formation and direct it to beneficial uses.

Secretion and assembly at the Gram-negative outer membrane

There are 5 described classes of extracellular secretion and assembly systems in Gram-negative bacteria, excepting flagella. These include curli fibers, pili assembled by the chaperone-usher (CU) pathway, Type IV pili, and the pili assembled by the Type III and Type IV secretion systems (T3SS and T4SS, respectively) (Economou et al., 2006; Fernandez and Berenguer, 2000; Wu and Fives-Taylor, 2001). These surface structures perform an array of functions, from attachment and biofilm formation to secretion, cell motility and DNA transport. Biogenesis of any surface structure in Gram-negative bacteria requires transport of structural components across the inner and outer membranes from the site of protein synthesis in the cytosol. As of this writing, two general strategies employed to reach the outer membrane and extracellular milleu have been

described. The structural subunits and assembly components of CU pili and curli fibers are targeted across the inner membrane by the general secretory pathway composed of the Sec translocation system and are then are targeted through the periplasm to the outer membrane (Fernandez and Berenguer, 2000). In contrast, the secretion systems supporting assembly of Type IV pili, T3SS pili, and T4SS pili are composed of large, multiprotein complexes that span both inner and outer membranes and are powered by ATP hydrolysis on the cytoplasmic side of the inner membrane (Economou et al., 2006). Each of these secretion systems utilizes a large, pore-like protein at the outer membrane to facilitate transport to the extracellular milieu. All of the systems also require multiple, non-structural proteins to facilitate secretion and assembly.

All outer membrane secretion proteins are synthesized in the cytosol, cross the inner membrane, and must travel through the aqueous periplasm to before finally being assembled into the outer membrane. This route presents a key biophysical challenge: how can hydrophobic protein domains cross an aqueous space? This challenge is thought to a have driven the development of amphipathic, rather than hydrophobic, transmembrane architectures. The known structures of integral outer membrane proteins has revealed that many contain transmembrane domains composed of amphipathic β-strands. The β-strands of monomer or multimeric outer membrane-spanning proteins come together and form a distinct, cone-like β-barrel structure (Galdiero et al., 2007). Recently, an outer membrane transmembrane domain was discovered that is comprised of alpha helices. Wza, the *E. coli* polysachharide translocon, forms an alpha helical barrel across the outer membrane (Dong et al., 2006).

The architecture of outer membrane proteins may underlie certain biochemical properties, such as heat modifiable mobility upon electrophoresis. Resistance to denaturation is a property of many outer membrane-localized multimeric complexes, and two distinct forms of assembly-dependent electrophoretic mobility have been described for outer membrane proteins (Reithmeier and Bragg, 1974; Hardie et al., 1996). The porins and other mono- and oligo-meric β-barrel proteins migrate faster than their predicted monomeric molecular weight when samples are not heated prior to electrophoresis (Hancock and Carey, 1979; Reithmeier and Bragg, 1974). Conversely, folded multimeric complexes, such as the secretin family of proteins, migrate slower than their predicted monomeric molecular weight prior to complete denaturation (Reithmeier and Bragg, 1974; Hardie et al., 1996; Brok et al., 1999).

The trafficking of amphipathic outer membrane proteins (OMPs) requires transport across the hydrophilic environment of the periplasm. This transport requires the actions of specialized multi-protein assembly complexes. One essential system that facilitates assembly of β-barrel type OMPs is the YaeT complex composed of the OMP YaeT and at least three associated OM-lipoproteins: NlpB, YfiO, and YfgL (Kim et al., 2007; Malinverni et al., 2006). YaeT itself is conserved among all organisms producing β-barrel proteins, and so is found in mitochondria, chloroplasts, and Gram-negative outer membranes (Kim et al., 2007). YaeT has several specialized POTRA domains that have been implicated in folding of the nascent β-barrels. The mechanism by which the OMP is inserted into the outer membrane remains unclear, although many OMPs have

specific assembly factors that are also required for OM insertion (Kim et al., 2007). These assembly factors are often lipid-modified proteins.

E. coli lipid-anchored proteins are found in the outer leaflet of the inner membrane and both leaflets of the outer membrane (Tokuda and Matsuyama, 2004). Most lipoproteins are lipid modified on the ultimate N-terminal cysteine of the mature protein. Surface-anchored lipoproteins are often substrates of translocation systems that span both membranes and can direct a lipoprotein from the cytoplasm to the outer leaflet of the outer membrane (Russel, 1998). All other known lipoproteins are targeted across the inner membrane by Sec translocation sequences, and are cleaved by signal II peptidase. Acylation of the ultimate cysteine residue appears to occur during inner membrane translocation (Tokuda and Matsuyama, 2004). Transportation of lipoproteins to the outer membrane occurs by the concerted efforts of five proteins, LolABCDE. Lipoprotein precursors contain a lipoprotein recognition sequence, the lipo-box, centered around the signal II peptidase cleavage site. Within the lipo-box is the acylated cysteine, although the second residue of the mature protein determines the final destination of the lipoprotein. Lipoproteins with an aspartic acid as the second residue of the mature protein are not recognized by the Lol system, and thus are retained in the inner membrane (Hara et al., 2003). Any other residue at the +2 position is recognized first by the inner membrane-spanning LolCDE complex (Narita and Tokuda, 2006). LolCDE is an ABC tranporter that catalyzes the formation of a complex between periplasmic LolA and the lipoprotein (Narita and Tokuda, 2006). The hydrophobic cavity of LolA surrounds the acyl group of the lipoprotein and transports it to LolB in the outer membrane (Oguchi et al.,

2008; Taniguchi et al., 2005). LolB appears to mediate the transfer of the lipoprotein to the outer membrane (Oguchi et al., 2008).

Among the diverse functions of the over 90 described lipoproteins in *E. coli* is to support translocation across the outer membrane. Some lipoproteins, called pilot proteins, serve to support the outer membrane localization and assembly of outer membrane secretion proteins (Burghout et al., 2004; Lario et al., 2005). Interestingly, lipoproteins can also function as secretion pores. For example, the polysaccharide translocon, Wza, is an LolA substrate that passages through the outer membrane (Dong et al., 2006). CsgG is an outer membrane localized lipoprotein that can modulate the stability of curli fiber subunits, CsgA and CsgB (Loferer et al., 1997). The goal of my thesis is to understand the role of CsgG in modulating curli subunit stability, and to understand how other curli assembly proteins affect CsgG. Chapter 2 of this dissertation presents work showing that CsgG is a likely substrate of the Lol transport system, facilitates secretion of curli fiber subunits across the outer membrane and can physically interact with several other proteins in the curli assembly system. Chapter 3 describes the spatial organization of CsgG, and how CsgG organization is coordinated with curli fiber assembly. Chapter 4 shows how one of the CsgG-interacting proteins, CsgE, modulates the secretion properties of CsgG and how CsgE can directly modulate amyloid fiber formation.

Figure Legends

Figure 1.1. The amyloid polymerization pathway proceeds through a common intermediate. **(A)** Hypothetical amyloid folding pathway. Soluble pre-amyloid

peptides (green circles) may accumulate and form a toxic oligomeric common intermediate (tan circles) before the appearance of mature fibers (red circles). Arrow length corresponds to the relative favorability of the folding step. **(B)** Electron micrograph of biologically active pre-amyloid oligomer formed by the harpin HpaG. Purified HpaG oligomers were negatively stained with uranyl acetate before visualization (Oh et al., 2007). Scale bar is 100 nm. **(C)** Electron micrograph of negatively stained amyloid fibers generated by polymerization of a synthetic peptide derived from the sequence of CsgA, the major component of curli fibers (Wang et al., 2007). Scale bar is 6 μm.

Figure 1.2. A secretion and assembly machine directs amyloid fiber formation in *E. coli.* **(A)** Model of curli assembly. Curli biosynthesis requires the products of the divergently transcribed *csgBA* and *csgDEFG* operons. CsgD is a transcriptional activator of the *csgBA* operon. CsgB, CsgA, CsgE, CsgF, and CsgG have SEC signal sequences that target them across the inner membrane (IM). CsgG, CsgE, and CsgF are nonstructural proteins that interact at the outer membrane. CsgA and CsgB are secreted across the outer membrane in a CsgG-dependent manner (see text). CsgB interacts with the outer membrane and presents an amyloid-like template to soluble CsgA (red triangles). CsgA adopts the amyloid conformation (red ovals) and becomes anchored to the cell surface, where it can propagate the β-sheet rich amyloid fold onto unpolymerized CsgA monomers. **(B)** Curli fibers bind the amyloid-specific dye Congo red. Curliated bacteria stain red when grown on media containing the diazo dye Congo red (left), but *csg*- bacteria remain white (right). **(C)** Electron micrograph of curliated

bacteria, where the bacteria were grown for 40 hours at 26 °C prior to analysis (Wang et al., 2007). Scale bar is 1 μm. **(D)** CsgG is the central component of the curlin secretion complex. Rotary shadow electron micrograph of purified CsgG indicates that it assembles into regular barrel-like structures. Scale bar is 100 nm. (Robinson et al., 2006)

Figure 1

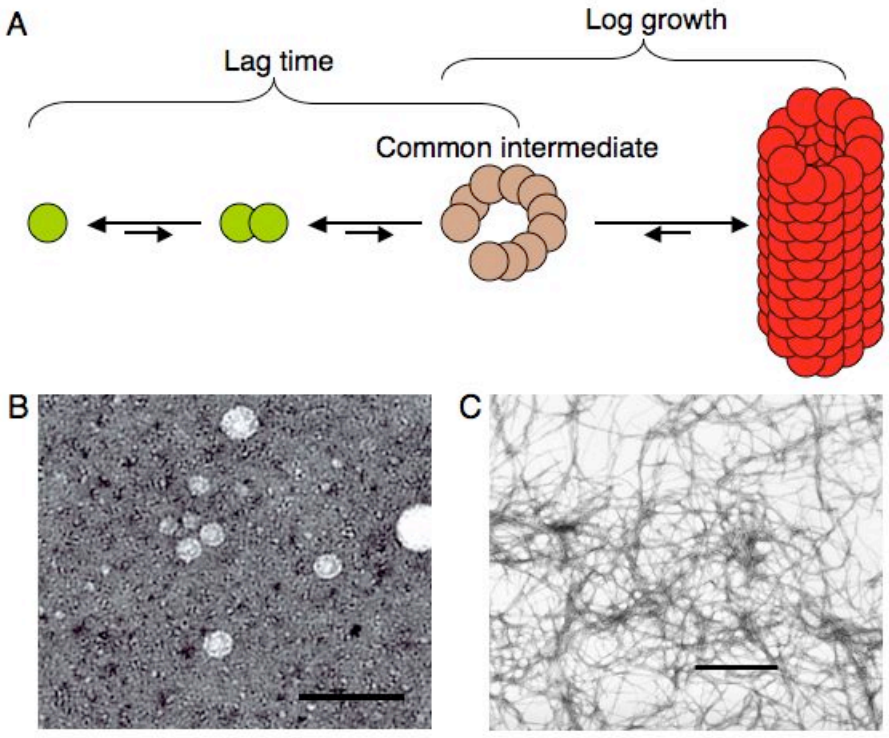

Figure 1.1. The amyloid polymerization pathway proceeds through a common intermediate

Figure 2

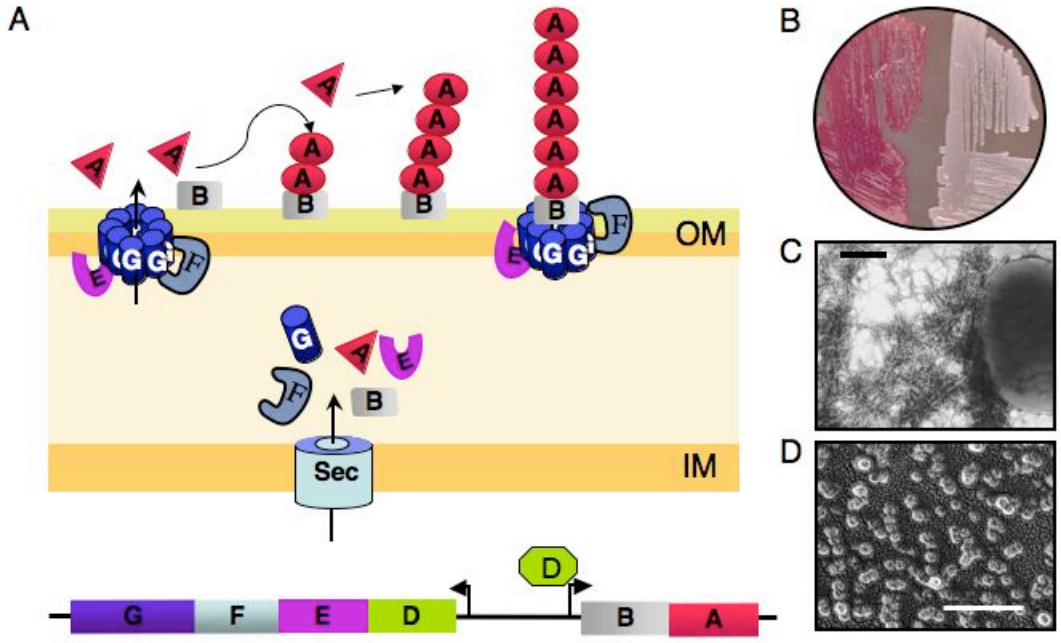

Figure 1.2. A secretion and assembly machine directs amyloid fiber formation in *E. coli.*

References

Alteri, C.J., Xicohtencatl-Cortes, J., Hess, S., Caballero-Olin, G., Giron, J.A., and Friedman, R.L. (2007) *Mycobacterium tuberculosis* produces pili during human infection. *Proc Natl Acad Sci U S A* **104**: 5145-5150.

Arnqvist, A., Olsen, A., Pfeifer, J., Russell, D.G., and Normark, S. (1992) The Crl protein activates cryptic genes for curli formation and fibronectin binding in *Escherichia coli* HB101. *Mol Microbiol* **6**: 2443-2452.

Barnhart, M.M., and Chapman, M.R. (2006) Curli biogenesis and function. *Annu Rev Microbiol* **60**: 131-147.

Bian, Z., and Normark, S. (1997) Nucleator function of CsgB for the assembly of adhesive surface organelles in Escherichia coli. *EMBO J* **16**: 5827-5836.

Bieler, S., Estrada, L., Lagos, R., Baeza, M., Castilla, J., and Soto, C. (2005) Amyloid formation modulates the biological activity of a bacterial protein. *J Biol Chem* **280**: 26880-26885.

Bokranz, W., Wang, X., Tschape, H., and Romling, U. (2005) Expression of cellulose and curli fimbriae by Escherichia coli isolated from the gastrointestinal tract. *J Med Microbiol* **54**: 1171-1182.

Brok, R., Van Gelder, P., Winterhalter, M., Ziese, U., Koster, A.J., de Cock, H., Koster, M., Tommassen, J., and Bitter, W. (1999) The C-terminal domain of the Pseudomonas secretin XcpQ forms oligomeric rings with pore activity. *J Mol Biol* **294**: 1169-1179.

Brombacher, E., Dorel, C., Zehnder, A.J., and Landini, P. (2003) The curli biosynthesis regulator CsgD co-ordinates the expression of both positive and negative determinants for biofilm formation in Escherichia coli. *Microbiology* **149**: 2847-2857.

Burghout, P., Beckers, F., de Wit, E., van Boxtel, R., Cornelis, G.R., Tommassen, J., and Koster, M. (2004) Role of the pilot protein YscW in the biogenesis of the YscC secretin in Yersinia enterocolitica. *J Bacteriol* **186**: 5366-5375.

Caughey, B., and Lansbury, P.T. (2003) Protofibrils, pores, fibrils, and neurodegeneration: separating the responsible protein aggregates from the innocent bystanders. *Annu Rev Neurosci* **26**: 267-298.

Chapman, M.R., Robinson, L.S., Pinkner, J.S., Roth, R., Heuser, J., Hammar, M., Normark, S., and Hultgren, S.J. (2002) Role of *Escherichia coli* curli operons in directing amyloid fiber formation. *Science* **295**: 851-855.

Claessen, D., Rink, R., de Jong, W., Siebring, J., de Vreugd, P., Boersma, F.G., Dijkhuizen, L., and Wosten, H.A. (2003) A novel class of secreted hydrophobic proteins is involved in aerial hyphae formation in Streptomyces coelicolor by forming amyloid-like fibrils. *Genes Dev* **17**: 1714-1726.

Claessen, D., Stokroos, I., Deelstra, H.J., Penninga, N.A., Bormann, C., Salas, J.A., Dijkhuizen, L., and Wosten, H.A. (2004) The formation of the rodlet layer of streptomycetes is the result of the interplay between rodlins and chaplins. *Mol Microbiol* **53**: 433-443.

Collinson, S.K., Clouthier, S.C., Doran, J.L., Banser, P.A., and Kay, W.W. (1996) Salmonella enteritidis agfBAC operon encoding thin, aggregative fimbriae. *J Bacteriol* **178**: 662-667.

Collinson, S.K., Emody, L., Muller, K.H., Trust, T.J., and Kay, W.W. (1991) Purification and characterization of thin, aggregative fimbriae from Salmonella enteritidis. *J Bacteriol* **173**: 4773-4781.

Destoumieux-Garzon, D., Thomas, X., Santamaria, M., Goulard, C., Barthelemy, M., Boscher, B., Bessin, Y., Molle, G., Pons, A.M., Letellier, L., Peduzzi, J., and Rebuffat, S. (2003) Microcin E492 antibacterial activity: evidence for a TonB-dependent inner membrane permeabilization on Escherichia coli. *Mol Microbiol* **49**: 1031-1041.

Dong, C., Beis, K., Nesper, J., Brunkan-Lamontagne, A.L., Clarke, B.R., Whitfield, C., and Naismith, J.H. (2006) Wza the translocon for E. coli capsular polysaccharides defines a new class of membrane protein. *Nature* **444**: 226-229.

Economou, A., Christie, P.J., Fernandez, R.C., Palmer, T., Plano, G.V., and Pugsley, A.P. (2006) Secretion by numbers: Protein traffic in prokaryotes. *Mol Microbiol* **62**: 308-319.

Elghetany, M.T., and Saleem, A. (1988) Methods for staining amyloid in tissues: a review. *Stain Technol* **63**: 201-212.

Elliot, M.A., Karoonuthaisiri, N., Huang, J., Bibb, M.J., Cohen, S.N., Kao, C.M., and Buttner, M.J. (2003) The chaplins: a family of hydrophobic cell-surface proteins involved in aerial mycelium formation in Streptomyces coelicolor. *Genes Dev* **17**: 1727-1740.

Fernandez, L.A., and Berenguer, J. (2000) Secretion and assembly of regular surface structures in Gram-negative bacteria. *FEMS Microbiol Rev* **24**: 21-44.

Fowler, D.M., Koulov, A.V., Balch, W.E., and Kelly, J.W. (2007) Functional amyloid--from bacteria to humans. *Trends Biochem Sci* **32**: 217-224.

Galdiero, S., Galdiero, M., and Pedone, C. (2007) beta-Barrel membrane bacterial proteins: structure, function, assembly and interaction with lipids. *Curr Protein Pept Sci* **8**: 63-82.

Gerstel, U., Park, C., and Romling, U. (2003) Complex regulation of csgD promoter activity by global regulatory proteins. *Mol Microbiol* **49**: 639-654.
Gerstel, U., and Romling, U. (2003) The csgD promoter, a control unit for biofilm formation in Salmonella typhimurium. *Res Microbiol* **154**: 659-667.

Gibson, D.L., White, A.P., Rajotte, C.M., and Kay, W.W. (2007) AgfC and AgfE facilitate extracellular thin aggregative fimbriae synthesis in Salmonella Enteritidis. *Microbiology* **153**: 1131-1140.

Gophna, U., Barlev, M., Seijffers, R., Oelschlager, T.A., Hacker, J., and Ron, E.Z. (2001) Curli fibers mediate internalization of Escherichia coli by eukaryotic cells. *Infect Immun* **69**: 2659-2665.

Hammar, M., Arnqvist, A., Bian, Z., Olsen, A., and Normark, S. (1995) Expression of two csg operons is required for production of fibronectin- and congo red-binding curli polymers in Escherichia coli K-12. *Mol Microbiol* **18**: 661-670.

Hammar, M., Bian, Z., and Normark, S. (1996) Nucleator-dependent intercellular assembly of adhesive curli organelles in Escherichia coli. *Proc Natl Acad Sci U S A* **93**: 6562-6566.

Hammer, N.D., Schmidt, J.C., and Chapman, M.R. (2007) The curli nucleator protein, CsgB, contains an amyloidogenic domain that directs CsgA polymerization. *Proc Natl Acad Sci U S A* **104**: 12494-12499.

Hancock, R.E., and Carey, A.M. (1979) Outer membrane of Pseudomonas aeruginosa: heat- 2-mercaptoethanol-modifiable proteins. *J Bacteriol* **140**: 902-910.

Hara, T., Matsuyama, S., and Tokuda, H. (2003) Mechanism underlying the inner membrane retention of Escherichia coli lipoproteins caused by Lol avoidance signals. *J Biol Chem* **278**: 40408-40414.

Hardie, K.R., Lory, S., and Pugsley, A.P. (1996) Insertion of an outer membrane protein in Escherichia coli requires a chaperone-like protein. *EMBO J* **15**: 978-988.
Heath, M.C. (2000) Hypersensitive response-related death. *Plant Mol Biol* **44**: 321-334.

Johansson, C., Nilsson, T., Olsen, A., and Wick, M.J. (2001) The influence of curli, a MHC-I-binding bacterial surface structure, on macrophage-T cell interactions. *FEMS Immunol Med Microbiol* **30**: 21-29.

Jonson, A.B., Normark, S., and Rhen, M. (2005) Fimbriae, pili, flagella and bacterial virulence. *Contrib Microbiol* **12**: 67-89.

Kayed, R., Head, E., Sarsoza, F., Saing, T., Cotman, C.W., Necula, M., Margol, L., Wu, J., Breydo, L., Thompson, J.L., Rasool, S., Gurlo, T., Butler, P., and Glabe, C.G. (2007) Fibril specific, conformation dependent antibodies recognize a generic epitope common to amyloid fibrils and fibrillar oligomers that is absent in prefibrillar oligomers. *Mol Neurodegener* **2**: 18.
Kayed, R., Head, E., Thompson, J.L., McIntire, T.M., Milton, S.C., Cotman, C.W., and Glabe, C.G. (2003) Common structure of soluble amyloid oligomers implies common mechanism of pathogenesis. *Science* **300**: 486-489.

Kim, J.G., Jeon, E., Oh, J., Moon, J.S., and Hwang, I. (2004) Mutational analysis of Xanthomonas harpin HpaG identifies a key functional region that elicits the hypersensitive response in nonhost plants. *J Bacteriol* **186**: 6239-6247.

Kim, S., Malinverni, J.C., Sliz, P., Silhavy, T.J., Harrison, S.C., and Kahne, D. (2007) Structure and function of an essential component of the outer membrane protein assembly machine. *Science* **317**: 961-964.

Knobl, T., Baccaro, M.R., Moreno, A.M., Gomes, T.A., Vieira, M.A., Ferreira, C.S., and Ferreira, A.J. (2001) Virulence properties of Escherichia coli isolated from ostriches with respiratory disease. *Vet Microbiol* **83**: 71-80.

La Ragione, R.M., Coles, K.E., Jorgensen, F., Humphrey, T.J., and Woodward, M.J. (2001) Virulence in the chick model and stress tolerance of Salmonella enterica serovar Orion var. 15+. *Int J Med Microbiol* **290**: 707-718.

Lagos, R., Villanueva, J.E., and Monasterio, O. (1999) Identification and properties of the genes encoding microcin E492 and its immunity protein. *J Bacteriol* **181**: 212-217.

Lagos, R., Wilkens, M., Vergara, C., Cecchi, X., and Monasterio, O. (1993) Microcin E492 forms ion channels in phospholipid bilayer membrane. *FEBS Lett* **321**: 145-148.

Lario, P.I., Pfuetzner, R.A., Frey, E.A., Creagh, L., Haynes, C., Maurelli, A.T., and Strynadka, N.C. (2005) Structure and biochemical analysis of a secretin pilot protein. *EMBO J* **24**: 1111-1121.

Larsen, P., Nielsen, J.L., Dueholm, M.S., Wetzel, R., Otzen, D., and Nielsen, P.H. (2007) Amyloid adhesins are abundant in natural biofilms. *Environ Microbiol* **9**: 3077-3090.

Larsen, P., Nielsen, J.L., Otzen, D., and Nielsen, P.H. (2008) Amyloid-like adhesins in floc-forming and filamentous bacteria in activated sludge. *Appl Environ Microbiol*

Lee, J., Klusener, B., Tsiamis, G., Stevens, C., Neyt, C., Tampakaki, A.P., Panopoulos, N.J., Noller, J., Weiler, E.W., Cornelis, G.R., Mansfield, J.W., and Nurnberger, T. (2001) HrpZ(Psph) from the plant pathogen Pseudomonas syringae pv. phaseolicola binds to lipid bilayers and forms an ion-conducting pore in vitro. *Proc Natl Acad Sci U S A* **98**: 289-294.

Loferer, H., Hammar, M., and Normark, S. (1997) Availability of the fibre subunit CsgA and the nucleator protein CsgB during assembly of fibronectin-binding curli is limited by the intracellular concentration of the novel lipoprotein CsgG. *Mol Microbiol* **26**: 11-23.
Malinverni, J.C., Werner, J., Kim, S., Sklar, J.G., Kahne, D., Misra, R., and Silhavy, T.J. (2006) YfiO stabilizes the YaeT complex and is essential for outer membrane protein assembly in Escherichia coli. *Mol Microbiol* **61**: 151-164.

Narita, S., and Tokuda, H. (2006) An ABC transporter mediating the membrane detachment of bacterial lipoproteins depending on their sorting signals. *FEBS Lett* **580**: 1164-1170.

Nelson, R., Sawaya, M.R., Balbirnie, M., Madsen, A.O., Riekel, C., Grothe, R., and Eisenberg, D. (2005) Structure of the cross-beta spine of amyloid-like fibrils. *Nature* **435**: 773-778.

Nordstedt, C., Naslund, J., Tjernberg, L.O., Karlstrom, A.R., Thyberg, J., and Terenius, L. (1994) The Alzheimer A beta peptide develops protease resistance in association with its polymerization into fibrils. *J Biol Chem* **269**: 30773-30776.

Oguchi, Y., Takeda, K., Watanabe, S., Yokota, N., Miki, K., and Tokuda, H. (2008) Opening and closing of the hydrophobic cavity of LolA coupled to lipoprotein binding and release. *J Biol Chem*

Oh, J., Kim, J.G., Jeon, E., Yoo, C.H., Moon, J.S., Rhee, S., and Hwang, I. (2007) Amyloidogenesis of type III-dependent harpins from plant pathogenic bacteria. *J Biol Chem* **282**: 13601-13609.

Olsen, A., Herwald, H., Wikstrom, M., Persson, K., Mattsson, E., and Bjorck, L. (2002) Identification of two protein-binding and functional regions of curli, a surface organelle and virulence determinant of Escherichia coli. *J Biol Chem* **277**: 34568-34572.

Olsen, A., Jonsson, A., and Normark, S. (1989) Fibronectin binding mediated by a novel class of surface organelles on Escherichia coli. *Nature* **338**: 652-655.

Olsen, A., Wick, M.J., Morgelin, M., and Bjorck, L. (1998) Curli, fibrous surface proteins of Escherichia coli, interact with major histocompatibility complex class I molecules. *Infect Immun* **66**: 944-949.

Pawar, D.M., Rossman, M.L., and Chen, J. (2005) Role of curli fimbriae in mediating the cells of enterohaemorrhagic Escherichia coli to attach to abiotic surfaces. *J Appl Microbiol* **99**: 418-425.

Reithmeier, R.A., and Bragg, P.D. (1974) Purification and characterization of heat-modifiable protein from the outer membrane of Escherichia coli. *FEBS Lett* **41**: 195-198.

Robinson, L.S., Ashman, E.M., Hultgren, S.J., and Chapman, M.R. (2006) Secretion of curli fibre subunits is mediated by the outer membrane-localized CsgG protein. *Mol Microbiol* **59**: 870-881.

Romling, U. (2005) Characterization of the rdar morphotype, a multicellular behaviour in Enterobacteriaceae. *Cell Mol Life Sci* **62**: 1234-1246.
Ross, C.A., and Poirier, M.A. (2004) Protein aggregation and neurodegenerative disease. *Nat Med* **10 Suppl**: S10-7.

Russel, M. (1998) Macromolecular assembly and secretion across the bacterial cell envelope: type II protein secretion systems. *J Mol Biol* **279**: 485-499.

Ryu, J.H., Kim, H., Frank, J.F., and Beuchat, L.R. (2004) Attachment and biofilm formation on stainless steel by Escherichia coli O157:H7 as affected by curli production. *Lett Appl Microbiol* **39**: 359-362.

Taniguchi, N., Matsuyama, S., and Tokuda, H. (2005) Mechanisms underlying energy-independent transfer of lipoproteins from LolA to LolB, which have similar unclosed {beta}-barrel structures. *J Biol Chem* **280**: 34481-34488.

Tokuda, H., and Matsuyama, S. (2004) Sorting of lipoproteins to the outer membrane in E. coli. *Biochim Biophys Acta* **1693**: 5-13.

Uhlich, G.A., Cooke, P.H., and Solomon, E.B. (2006) Analyses of the red-dry-rough phenotype of an Escherichia coli O157:H7 strain and its role in biofilm formation and resistance to antibacterial agents. *Appl Environ Microbiol* **72**: 2564-2572.

Uhlich, G.A., Keen, J.E., and Elder, R.O. (2002) Variations in the csgD promoter of Escherichia coli O157:H7 associated with increased virulence in mice and increased invasion of HEp-2 cells. *Infect Immun* **70**: 395-399.

Wang, X., Smith, D.R., Jones, J.W., and Chapman, M.R. (2007) In vitro polymerization of a functional Escherichia coli amyloid protein. *J Biol Chem* **282**: 3713-3719.

Wu, H., and Fives-Taylor, P.M. (2001) Molecular strategies for fimbrial expression and assembly. *Crit Rev Oral Biol Med* **12**: 101-115.

Yoshiike, Y., Kayed, R., Milton, S.C., Takashima, A., and Glabe, C.G. (2007) Pore-forming proteins share structural and functional homology with amyloid oligomers. *Neuromolecular Med* **9**: 270-275.

Zogaj, X., Bokranz, W., Nimtz, M., and Romling, U. (2003) Production of cellulose and curli fimbriae by members of the family Enterobacteriaceae isolated from the human gastrointestinal tract. *Infect Immun* **71**: 4151-4158.

Chapter II

The outer membrane-localized CsgG protein mediates secretion of curli fiber subunits

Abstract

Produced by many *Enterobacteriaceae spp.,* curli are biologically important amyloid fibers that have been associated with biofilm formation, host cell adhesion and invasion, and immune system activation. CsgA is the major fiber subunit and CsgE, CsgF, and CsgG are non-structural proteins involved in curli biogenesis. We have characterized the role of CsgG in curli subunit secretion across the outer membrane. Directed mutagenesis of CsgG confirmed that its activity is dependent on localization to the outer membrane. Rotary Shadow electron microscopy of purified CsgG suggested this protein assembles into an oligomeric complex with an apparent central pore. Oligomeric CsgG complexes were confirmed using copurification experiments. Antibiotic sensitivity assays demonstrated that overexpression of CsgG rendered *Escherichia coli* susceptible to the antibiotic erythromycin. A 22 amino acid sequence at the N-terminus of CsgA was sufficient to direct heterologous proteins to the CsgG secretion apparatus. Finally, we determined that CsgG participates in an outer membrane complex with two other curli assembly proteins, CsgE and CsgF.

Introduction

Bacteria use a variety of extracellular fibers to mediate interactions with other cells and with their environment. Assembly of these fibers is complex and often includes chaperon proteins and outer membrane usher-like proteins that are dedicated to the secretion and proper localization of the fiber subunit proteins. Curli are a class of thin (6 to 8 nm), highly aggregated surface fibers that are part of a complex extracellular matrix promoting biofilm and other community behaviors in *E. coli* (Zogaj et al., 2001; Zogaj et al., 2003). Curli also confer binding to fibronectin, laminin, plasminogen and human contact phase proteins (Ben Nasr et al., 1996; Sjobring et al., 1994; Olsen et al., 1989). Among bacterially produced fibers, curli are distinguished by their unusual resistance to chemical and thermal denaturation and by their ability to bind the dyes Congo red (CR) and thioflavin T (ThT). These are properties shared by a growing number of eukaryotic fibers collectively know as amyloids. Amyloid fibers, or the process of amyloid formation, are proposed to cause cell and tissue damage associated with many neurodegenerative diseases (Kayed et al., 2003; Lashuel et al., 2002).

Curliated bacteria stain red when grown on plates supplemented with CR, which provides a convenient way to identify genes important for curli production (Collinson et al., 1993). CR binding has been observed in *Salmonella enterica*, *Klebsiella spp.*, and *Escherichia spp*, and the genes necessary for curli production have been found in numerous clinically important *Enterobacteriaceae* that form biofilms (Zogaj et al., 2003). Curli assembly requires the coordinated effort of proteins encoded by the *csgBA* and *csgDEFG* operons. The *csgBA* operon encodes two homologous proteins (CsgA and CsgB) that are secreted into the extracellular environment (Hammar et al., 1995; Hammar et al., 1996). At

the cell surface, CsgA is assembled into a stable CR-binding amyloid fiber in the presence of CsgB. In the absence of the CsgB nucleator, CsgA is secreted from the cell in a soluble, unassembled state. This soluble CsgA can polymerize into curli fibers if it contacts an adjacent cell expressing the CsgB nucleator (and not expressing CsgA) by interbacterial complementation (Hammar et al., 1996; Bian and Normark, 1997).

The *csgDEFG* operon encodes CsgD, a transcriptional activator of curli synthesis, and three putative assembly factors, CsgE, CsgF and CsgG (Hammar et al., 1995; Romling et al., 1998). Efficient curli assembly requires the CsgE, CsgF and CsgG proteins. CsgG is a lipoprotein localized to the periplasmic side of the outer membrane (Loferer et al., 1997). In the absence of CsgG, CsgA and CsgB are unstable and curli assembly does not occur. At least three models exist to explain these observations. The first suggests that CsgG stabilizes curli subunits in the periplasm, allowing them to be secreted by an unidentified secretion apparatus. The second posits that CsgG assembles into a pore that shuttles curli subunits across the outer membrane. A final model suggests that CsgG stabilizes the subunits in the periplasm and is directly involved in their secretion. The latter model assumes that curli subunits are unstable in the periplasm and that subunit stability is coupled to their secretion across the outer membrane.

Secretins are a well-characterized class of bacterial outer membrane proteins thought to function as secretion pores. Secretins often require accessory lipoproteins called pilot proteins for their oligomerization and/or outer membrane localization (Hardie et al., 1996). Lipoproteins have also been implicated directly

in the secretion step – perhaps as the secretion pore (Schmidt et al., 2001, Bose and Taylor, 2005). Interestingly, while secretins have marked sequence similarity within their C-terminal domains, the lipoproteins hypothesized to function as secretion pores share no apparent sequence similarity (Brok et al., 1999, Schmidt et al., 2001, Bose and Taylor, 2005). In this study, we have characterized the lipoprotein CsgG and our results are consistent with the model that CsgG forms an outer membrane channel that stabilizes the curli subunit proteins by mediating their translocation across the outer membrane. We also demonstrated that CsgG interacted with two periplasmic proteins, CsgE and CsgF, required for efficient curli assembly in vivo. Collectively, our data suggest a new model of curli biogenesis where CsgG is the point of convergence in a pathway enabling curlin subunit secretion.

Results

The role of CsgG in curlin secretion was investigated. CsgG is an outer membrane-localized lipoprotein required for curli production and for CsgA and CsgB stability (Loferer et al., 1997). A convenient measure of subunit secretion is the ability of a cell to act as a CsgA donor or acceptor during interbacterial complementation (Hammar et al., 1995; Chapman et al., 2002). For example, a *csgB*$^{-}$ or *csgF*$^{-}$ strain will secrete soluble CsgA to the cell surface that can be polymerized on the surface of a CsgB^{+} acceptor strain. Since a *csgG*$^{-}$ strain does not assemble curli, interbacterial complementation was used to assess its ability to produce functional CsgA and CsgB proteins. A *csgG*$^{-}$ strain (LSR1) is white when streaked on CR plates. As shown in Fig 2.1A, a *csgG*$^{-}$ strain was unable to

accept CsgA from a *csgB*$^{-}$ (MHR261) donor, nor was it able to donate CsgA to a *csgA*$^{-}$ (MHR204) acceptor strain.

To assess whether CsgG was sufficient for CsgA secretion, CsgA was expressed from a plasmid in the complete *Δcsg* strain, LSR12. In this system, the expression of the Csg proteins is under the control of IPTG. As shown in Fig 2.1B, accumulation of CsgA in the supernatant was observed in strains that expressed CsgG (Fig 2.1B, lanes 2, 3 and 5). Expression of CsgE did not significantly alter CsgA accumulation or secretion under these conditions. Strains expressing CsgE, CsgF and CsgG from a single operon contained on plasmid pMC5 consistently secreted less CsgA than strains expressing CsgG from pMC1 (Fig 2.1B) (Chapman et al., 2002). Notably, CsgE is not required for CsgA secretion when CsgG is overexpressed from the IPTG inducible *trc* promoter (Fig 2.1B), but CsgE is critical for CsgA stability and curli formation when CsgG is expressed at wild type (Wt) levels from the chromosome (Chapman et al., 2002).

The observation that co-expression of CsgA and CsgG is sufficient for CsgA secretion suggests that these proteins interact. CsgA can be divided into at least 3 identifiable domains: the N-terminal Sec-dependent signal sequence, the first 22 amino acids of the mature protein, and a C-terminal domain that is predicted to form the amyloid core of the fiber (Collinson et al., 1999). The N-terminal 22 amino acids of the mature CsgA protein do not constitute an integral part of the fiber (Collinson et al., 1999), but are required for CsgA stability and, possibly, secretion (L. Robinson, unpublished results). To assess whether the mature N-terminal 22 amino acids of CsgA are sufficient for interaction with CsgG, the N-terminal 42 amino acids of premature CsgA (including the CsgA

Sec-dependent signal sequence and the first 22 amino acids of the mature protein) were fused to the mature PhoA protein (Fig 2.1C). This fusion protein was expressed from the *araBAD* promoter in plasmid pAph2. A second PhoA construct was made that lacked the 22 N-terminal residues of CsgA, called pAph1 (Fig 2.1C). A C-terminal HA epitope tag on PhoA allowed for the immunoprecipitation of this protein using α-HA antibodies. Six C-terminal histidine residues were added to CsgG and this fusion construct was cloned behind the *trc* promoter in pTRC99A creating pMC2. This plasmid was able to complement CR-binding and curli formation to a *csgG* null mutant (unpublished data). This construct also drove CsgG expression in cells growing logarithmically in LB media – a condition where expression from *csgBA* and *csgDEFG* promoters is undetectable (Romling et al., 1998a). Loferer et al. (1997) reported that when CsgG was expressed from its native promoter it fractionated exclusively to the Triton-X100 insoluble outer membrane fraction. We have confirmed these results and we have also determined that, when total membranes are treated with sarkosyl, natively expressed CsgG is found almost entirely in the sarkosyl insoluble outer membrane fraction (data not shown). When CsgG is overexpressed from the *trc* promoter significant amounts are found in both sarkosyl soluble and insoluble fractions (Fig 2.1D, lanes 4-7). The sarkosyl soluble protein observed when CsgG is overexpressed may represent CsgG that is associated with the inner membrane or CsgG that is only weakly interacting with the outer membrane at the time of fractionation. LSR12 (C600::Δ*csg*) containing pMC2 was transformed with either pAph1 or pAph2. We found that CsgG was present in the Elugent soluble material derived from the

sarkosyl insoluble fraction when CsgG was expressed with either Wt PhoA (Aph1) or with the CsgA-PhoA fusion protein (Aph2) (Fig 2.1D, lanes 6 and 7). CsgG was specifically immunoprecipitated with α-HA antibodies only when CsgG and the CsgA-PhoA-HA fusion protein (Aph2) were co-expressed (Fig 2.1D, lane 9). CsgG was not immunoprecipitated when co-expressed with Wt PhoA-HA (Fig 2.1D, lanes 8), suggesting that the 22 N-terminal amino acids of CsgA are sufficient for mediating an interaction between CsgG and CsgA.

Purification and Structural Analysis of CsgG. CsgG-his was expressed from pMC2 and purified using affinity chromatography as described in the Materials and Methods. Outer membranes were recovered by detergent extraction and Elugent soluble material was passed over a nickel NTA column. Nickel NTA-purified CsgG migrated near its predicted molecular weight of 29 kDa (Fig 2.2A), although a smaller band was consistently observed in elution fractions that contained full-length CsgG (Fig 2.2A lane 6). The lower molecular weight band is apparently N-terminally truncated CsgG, as this band was recognized by α-His antibodies (data not shown).

Gram-negative outer membrane secretion pores have been resolved by electron microscopy as 12 to 20 nm wide barrel-like structures (Thanassi et al., 1998) (Brok et al., 1999). Observation of purified CsgG-his by rotary shadowing electron microscopy revealed discrete structures of approximately uniform shape and size. The observed structures were 12 to 15 nm wide with an apparent central pore of approximately 2 nm (Fig 2.2C). The structures observed in Fig 2.2C suggest that CsgG forms pore-containing oligomers in the outer membrane.

Although these images suggest that CsgG forms an oligomeric structure, rotary replication can result in an enlargement of the imaged objects, which complicates precise estimation of the size of the oligomer comlex or pore size (Thanassi et al., 1998). Therefore, we utilized two differently tagged versions of CsgG to biochemically confirm CsgG-CsgG interactions. Strain C600 containing inducible plasmids that express CsgG-his (pMC2) and CsgG-HA (pLR92) was grown to mid log phase and induced as described in the Materials and Methods. Outer membrane fractions were collected from strains containing pMC2 alone, pLR92 alone, or pMC2 and pLR92 together. The Elugent soluble material derived from these outer membrane fractions was loaded onto a Ni-NTA column and CsgG-his was immobilized on the column. Proteins were eluted from the column and the eluates were probed with anti-HA antibodies. CsgG-HA was detected in the eluate only when CsgG-his was coexpressed, suggesting that CsgG-his and CsgG-HA formed a complex that was stable throughout Ni-NTA purification (Fig 2.2B).

Antibiotic Sensitivity Assays. We next ascertained whether CsgG expression modified the permeability of the outer membrane by using antibiotic sensitivity assays. Erythromycin does not normally pass the Gram-negative outer membrane because of hydrophobic repulsion forces. Therefore, this bacteriostatic antibiotic can be used to detect the presence of channels in the outer membrane (Schmidt et al., 2001; Augustus et al., 2004). As shown in Fig 2.3A, 30 μg/ml erythromycin did not appreciably affect growth of LSR12 containing vector alone. In contrast, LSR12 containing pMC1 displayed severe growth defects in the presence of erythromycin (Fig 2.3A). Therefore, it appeared

that CsgG expression increased outer membrane permeability, thus allowing erythromycin to enter the cell and poison translation. This is in agreement with our observation that CsgG assembled into pore-like structures with an apparent central cavity of 2 nm, which would be large enough to allow erythromycin to pass. Importantly, bacteria expressing CsgG did not exhibit growth defects in the absence of erythromycin (Fig 2.3A), suggesting that CsgG did not grossly affect membrane integrity. Erythromycin sensitivity was also observed when MC4100 cells overexpressing CsgG were grown on YESCA plates (data not shown). Vancomycin is another antibiotic that is often used to gauge membrane permeability because, like erythromycin, it cannot pass the hydrophobic outer membrane (Schmidt *et al.*, 2001). We observed relatively modest growth inhibition using vancomycin, even in cells overexpressing CsgG from pMC1 (Fig 2.3B), suggesting that CsgG-dependent erythromycin sensitivity is not due to a general membrane defect and may be due to presence of a CsgG pore in the outer membrane. At twice the size of erythromycin (1440 Da vs. 740 Da for erythromycin), we reasoned that vancomycin might not pass through the pore fashioned by CsgG oligomers, although it is possible that chemical differences between the antibiotics are responsible for the exclusion of vancomycin from CsgG-expressing cells.

Lipid modification is required for outer membrane localization. CsgG has been demonstrated to be a lipoprotein localized to the outer membrane. Consequently, it has been suggested that CsgG is targeted to the outer membrane by the LOL transport system (Narita et al., 2004). Bacterial lipoproteins are modified on a

cysteine residue located at the N-terminus (Narita et al., 2004). CsgG contains a conserved N-terminal cysteine residue that is the putative site of lipidation. Expression of lipoproteins with an N-terminal cysteine mutation is toxic to the cell because it titrates the LOL machinery away from other essential lipid proteins (Narita et al., 2004). Therefore, we removed the CsgG lipoprotein signal sequence, including the N-terminal cysteine, and replaced it with the signal sequence from the PhoA protein (Fig 2.4A). The expression of this protein chimera, called CsgGss, was induced in log phase cells and then localized using detergent fractionation. Wild type (Wt) CsgG consistently localized with outer membrane fractions, while CsgGss localized predominately with the soluble periplasmic fraction (Fig 2.4B). The ability of CsgGss to complement a *csgG*$^{-}$ mutant was tested. No CR binding was detected in a *csgG*$^{-}$ mutant, although this strain could be complemented by expression of Wt *csgG* from the *trc* promoter in pMC1 (Fig 2.4C). Partial complementation was achieved when Wt *csgG* was expressed from the *csgBA* promoter in pLR93. In contrast, CsgGss was unable to complement the *csgG*$^{-}$ mutant when expressed from either the *trc* or *csgBA* promoters (Fig 2.4C). Interestingly, the expression of CsgGss abolished the CR positive phenotype of an otherwise Wt strain (Fig 2.4C), suggesting that CsgGss is able to interfere with Wt CsgG function.

Because the CsgA and CsgB proteins are unstable without CsgG, we tested the ability of CsgGss to stabilize the curli subunits in the absence of Wt CsgG. As shown in Fig 2.4D, CsgA and CsgB do not accumulate to Wt levels when CsgGss is expressed in a *csgG*$^{-}$ strain, suggesting that proper CsgG

localization to the outer membrane is required for the chaperone-like activity of CsgG (Fig 2.4D).

Complex with other Csg proteins. CsgG is expressed from an operon along with three other proteins that are known to play a role in curli formation. CsgD is a transcriptional activator required for curli gene expression, while CsgE and CsgF are chaperone-like proteins that facilitate curli formation (Chirwa and Herrington, 2003; Gerstel et al., 2003; Chapman et al., 2002). However, the roles of CsgE and CsgF in curli formation are poorly understood. We tested whether CsgE or CsgF could interact with CsgG at the outer membrane. To facilitate this analysis, the CsgE and CsgF proteins were epitope tagged with AU1 or HA, respectively. These fusion proteins were able to complement CR binding to *csgE* and *csgF* chromosomal deletion strains (data not shown). C600 with pMC2 and pBAD33 or pLR58 (*csgF-HA* in pBAD33) was grown and the expression of CsgF-HA and CsgG-his was induced with arabinose and IPTG. Outer membranes were prepared after 1 hr of induction and CsgF-HA was immunoprecipitated with α-HA antibodies. CsgG was detected in the Elugent soluble outer membrane fraction with or without co-expression of CsgF-HA (Fig 2.5A, lanes 4 and 5), but was specifically co-immunoprecipitated with α-HA antibodies only when CsgF-HA was present. This demonstrated that CsgF and CsgG physically interacted at the outer membrane. C600 containing pMC2 and pBAD33 or pLR169 (*csgE-AU1* in pBAD33) was grown to induce CsgG-his and CsgE-AU1 expression. Proteins contained within the sarkosyl soluble inner membrane and Elugent soluble outer membrane fractions were immunoprecipitated with α-AU1 antibodies. As shown

in Fig 2.5B, CsgE-AU1 and CsgG-his were co-immunoprecipitated with α-AU1 antibodies from the Elugent soluble fractions. Immunoprecipitation of CsgG-his was completely dependent on expression of CsgE-AU1 (Fig 2.5B). CsgG-his was not co-immunoprecipitated with CsgE-AU1 when sarkosyl soluble fractions were used (Fig 2.5B, lanes 6-7 and 10-11). These data suggest that CsgG is an integral part of an outer membrane secretion complex that contains at least two other curli assembly proteins, CsgE and CsgF.

Discussion

Curli biogenesis is a complex process that requires several proteins, including those encoded by the *csg* operons. The lipoprotein CsgG forms an oligomeric structure in the outer membrane that is required for the secretion of the CsgA and CsgB proteins to the cell surface. The localization of CsgG to the outer membrane is dependent on post-translational acylation of the cysteine located at the first residue of the mature protein. Overexpression of CsgG renders logarithmically growing cells susceptible to the hydrophobic antibiotic erythromycin, most likely by a specific change in the permeability of the outer membrane. CsgA secretion and stability is dependent on the N-terminal 22 amino acids of CsgA. These 22 amino acids can also direct non-curli proteins to form a complex with CsgG. CsgE and CsgF also participate in a complex with CsgG, perhaps modifying its secretion activity.

Bacteria use a variety of mechanisms to shuttle proteins to the cell surface, and lipoproteins are often key components of these systems. Lipoproteins that function in protein secretion fall into one of two functionally

distinct classes. The first class represents lipoproteins that chaperone secretin proteins to the outer membrane. Pugsley and colleagues have coined the term "pilot" protein to describe such proteins. The second class of lipoproteins involved in protein secretion is postulated to form an outer membrane pore through which substrate proteins are channeled. Members of several terminal secretion systems predicted to be lipoproteins are directly involved in protein secretion across the outer membrane, including BfpB (Ramer et al., 1996; Schmidt et al., 2001), CfcD (Mundy et al., 2003), and TcpC (Bose and Taylor, 2005). CsgG does not share significant sequence similarity to any of the lipoproteins known to participate in bacterial secretion, yet CsgG homologs are present in many Gram negative bacteria – including many clinically important members of *Enterobacteriaceae* (Zogaj et al., 2003 and our unpublished data).

In the absence of CsgG, the CsgA and CsgB proteins are not secreted to the cell surface, yet they do not accumulate in the periplasmic space (Loferer et al., 1997). Currently, there are at least two models that explain why CsgA and CsgB are unstable in the absence of CsgG. CsgG might act as a chaperone protein, stabilizing CsgA and CsgB in the periplasm until they are secreted to the cell surface. Alternatively, CsgG may simply transport CsgA and CsgB to the cell surface where they are not subject to periplasmic proteases. To clarify the mechanism of CsgG, we asked if CsgG localization to the outer membrane was required for CsgA and CsgB stability. CsgG is modified with a palmitate group after secretion across the inner membrane (Loferer et al., 1997). Therefore, the lipidation-specific signal sequence on CsgG was replaced with a general SEC dependent signal sequence. This protein, called CsgGss, is not lipidated and

localizes to the periplasm instead of the outer membrane. Furthermore, CsgGss is unable to restore curli production in a *csgG*$^{-}$ strain (Fig 2.4C) and it does not act to stabilize the CsgA or CsgB proteins (Fig 2.4D). The failure of CsgGss to stabilize curli subunits cannot be explained by an inability to bind subunits, as CsgGss and the CsgA-PhoA fusion specifically interacted in Far-Western assays (L. Robinson, unpublished data). This suggests that CsgG must localize to the outer membrane in order to stabilize CsgA and CsgB and direct their secretion across the outer membrane. Therefore, stability and secretion of CsgA and CsgB appear to be tightly coupled. CsgA and CsgB may be inherently unstable in the periplasm and CsgG mediated secretion helps to stabilize them by exporting them to the more forgiving extracellular space. The extracellular space is also where curli subunits are proposed to transition into the amyloid state, which might also lead to increased subunit stability (Hammar et al., 1996).

The molecular mechanism behind the dominant negative phenotype observed when CsgGss is expressed along with Wt CsgG is unclear. At least two possibilities exist to explain this result. Since CsgG forms oligomeric structures in the outer membrane, it is possible that CsgGss can form a non-functional complex with Wt CsgG, thereby preventing Wt CsgG activity. As shown in Fig 2.2, CsgG forms oligomeric structures and it is possible that CsgGss participates in this complex. Alternatively, expression of CsgGss may change the cellular environment such that curli formation is inhibited. For example, if CsgGss is not completely folded then inducible cell stress systems may be activated that negatively affect curli formation. One such system is the Cpx system that can be induced by misfolded proteins in the periplasm (Hung et al., 2001; Nevesinjac

and Raivio, 2005; Ruiz and Silhavy, 2005). Not only does the Cpx system upregulate the expression of proteins with protease activity, which might degrade Wt CsgG or the curli subunits, but CpxR has also been shown to downregulate the *csg* operons at the transcriptional level (Prigent-Combaret et al., 2001).

CsgA that has been secreted by CsgG-expressing cells is found is in an unstructured state upon purification (Chapman et al., 2002). The size of the structures observed in Fig 2.2C is in agreement with the idea that the curli subunits may be at least partly unfolded during translocation across the outer membrane. However, the mechanism by which CsgA could be maintained in this unfolded state is unclear. CsgG probably does not work alone during curli assembly, despite the discovery that overexpression of CsgG in logarithmically growing cells results in CsgA secretion (Fig 2.1B), In this experiment, CsgG and CsgA were expressed from inducible promoters and CsgA was almost exclusively found in the extracellular space. CsgE or CsgF did not positively augment CsgA secretion, when CsgG was overexpressed. Yet, CsgE is required for CsgA and CsgB secretion when cells are grown on YESCA plates and the curli proteins are expressed from their native promoters (Chapman et al., 2002). Because CsgE and CsgF interact with CsgG at the outer membrane, it is possible that under native conditions CsgE and CsgF increase the specificity or efficiency of CsgG-mediated secretion. Delineating the molecular details of CsgE and CsgF function during curli formation will help clarify this unique secretion system.

Experimental Procedures

Plasmids, strains, growth conditions, and antibodies. Expression of *csg* genes at wild-type levels from MC4100 chromosome or pLR1-derived plasmids was accomplished by growing cells on YESCA agar (10g Casamino acids, 1g yeast extract, 20 g agar [Fisher, Fairlawn, NJ] in 1L) at 26^{o} C for 48 hours. YESCA agar plates supplemented with 10 μg/ml Congo red (Sigma, St. Louis, MO) were used to monitor curli production on colonies. Expression of genes cloned behind the *trc* promoter in pTRC99A or the *ara* promoter in pBAD33 was induced by addition of 0.4 mM IPTG or 0.4% (w/v) arabinose, respectively. Antibiotics were added at the following concentrations as needed: Kanomycin 50 μg/ml, Ampicillin 100 μg/ml, and Chloramphenicol 20 μg/ml. The *csgBA* promoter was amplified from MC4100 as a BglII/PstI fragment using primers LR1F and LR1R (Table 2.2) and cloned into the BamHI/PstI sites of pACYC177 to create pLR1. An NcoI site incorporated into the reverse primer LR1R allowed cloning of the NcoI/PstI fragment of pLomp4 (Table 2.1) into pLR1, which added BamHI and KpnI sites and created pLR2. Western blots were probed as indicated in the Results with the following antibodies: polyclonal antiserum raised against Ni-NTA purified CsgG-his in rabbits by Proteintech Group, Inc Chicago, IL, rabbit polyclonal antibody raised against the CsgB peptide EGSSNRAKIDQTGDY (Sigma, St. Louis, MO), rabbit polyclonal antibody raised against CsgA (Hammar et al., 1996), or commercially-available antibodies against commonly used epitopes, as indicated when used.

Purification of CsgG. CsgG was purified under non-denaturing conditions from strain C600 containing pMC2 and/or pLR92 as indicated in the results. The

strains were grown with aeration in LB broth containing 100 μg/ml ampicillin and/or 50 μg/ml kanomycin as appropriate. At OD_{600} of 0.6-1.0, *csgG-his* or *csgG-HA* expression was induced with 0.5 mM IPTG and/or 0.04% arabinose for 2 hours. Bacteria were harvested and resuspended in 20 mM Tris·HCl (pH 8.0), lysed with a French press, and outer membrane collected by differential extraction with Sarkosyl (Thanassi and Hultgren, 2000). CsgG was extracted from the sarkosyl insoluble outer membrane fraction by treatment with 0.5% Elugent (Calbiochem, San Diego, CA). The Elugent soluble fraction was applied to a Ni-NTA column (Qiagen, Chatsworth, CA) in 5 column volumes of HNE (20 mM HEPES/300 mM NaCl/0.5% Elugent). The column was washed with 5 column volumes of HNE + 10 mM imidizole. An additional wash of 5 column volumes of HNE + 20 mM imidizole was performed for the co-purification experiment presented in Fig 2B. CsgG bound to the column was eluted with HNE containing 100 mM imidazole.

Electron Microscopy. CsgG was purified for inspection by electron microscopy (EM) analysis as described above with the following modifications: CsgG was extracted from the sarkosyl insoluble outer membrane fraction by treatment with 0.1% of the non-ionic detergent n-dodecyl-beta-D-maltoside (DDM) and the mobile phase of the Ni-NTA column was buffer A (20 mM Tris·HCl pH 8.0/150 mM NaCl/0.1% DDM). Purified CsgG was observed by rotary replication as described by Thanassi et al (1998). Breifly, CsgG purified by Ni-NTA chromatography was adsorbed to mica chips before quick-freezing. These

frozen samples were fractured and deep-etched by exposure to a vacuum. Replicas were constructed by rotary shadowing with platinum.

Cell Fractionation to determine CsgG and CsgGss localization. C600 containing pMC1 or pLR16 was grown with aeration in LB broth and addition of 0.5 mM IPTG to the growth media induced *csgG* or *csgGss* expression. Cells were harvested and 0.5 g cell weight divided into two equal portions and either periplasm or membranes were isolated. The periplasmic fraction was obtained by suspending the cells in 20 mM Tris·HCl pH 8.0/20% sucrose/0.5mM EDTA and 40μL of 25x Protease Inhibitor Tablets (Roche, Indianapolis, IN) was added before treatment with 75μg/mL lysozyme. This suspension was incubated on ice for 40 minutes and the reaction was quenched by addition of 1M $MgCl_2$. Spheroplasts were pelleted by centrifugation at 10,000xg for 20 minutes and the supernatent retained for analysis. Membrane fractions were obtained using a modified protocol originally described by Loferer et al. (1997). Briefly, one half of the cells grown as described above were suspended in 20mM Tris·HCl pH 8.0 and lysed with a French press before separating the periplasm and cytosol from the total membrane fraction by ultracentrifugation at 100,000xg for 1 hour. The inner membrane was then solubilized in 0.5% sarkosyl and the sarkosyl insoluble outer membrane fraction pelleted by centrifugation at 100,000xg for 1 hour. The pellet was suspended in HNE and insoluble material pelleted by centrifugation at 100,000xg for 30 minutes. The Elugent soluble fraction was retained for analysis. The fractions obtained by these procedures were subjected to SDS-PAGE and

the presence of CsgG or CsgGss was detected by immunoblotting with rabbit anti-CsgG antibodies.

Immunoprecipitation.

Elugent soluble outer membrane material was prepared as described above from the strains described in the Results section. One milliliter of the preparation was combined with anti-HA or anti-AU antibody at the concentration recommended by the manufacturer (Covance, Denver, PA) before rocking one hour at 4°C. 25 μl of Protein A-agarose bead slurry (Sigma, St. Louis, MO) was added and the mixture rocked one hour at 4°C. The beads were pelleted and washed three times in HNE before resuspension in 50 μl 2x SDS loading buffer.

Antibiotic sensitivity assays. Plasmid pTRC99A (empty vector) or pMC1 (P*trc-csgG*) were transformed into LSR12 (MC4100::Δ*csgDEFG*;Δ*csgBA*). Strains were grown to stationary phase in LB, diluted 1:100 in fresh media, and grown with agitation for 30 minutes. At this point, 0.05mM IPTG was added to the cultures, and bacteria were grown another 30 minutes before addition of erythromycin or vancomycin. Antibiotic addition was designated as time zero and OD_{600} measured every thirty minutes for three hundered minutes. The OD_{600} was measured using a Molecular Dynamics UV-Vis spectrophometer.

Figure Legends

Figure 2.1. CsgG is required for interbacterial complementation and CsgA secretion. (A) Interbacterial complementation and CR binding of *csgG*$^{-}$ mutants.

The *csgB*$^+$ acceptor strain MHR204 and the *csgA*$^+$ donor strain MHR261 were streaked from the top of the plate to the bottom. The horizontal cross-streaks were made from left to right with the indicated strains. **(B)** Expression and batch purification of CsgA-his. Supernatants from cells containing pMC3 (*csgA*$^+$) and the indicated plasmids were collected and mixed with 20 μl of Ni-NTA beads. After incubation for 20 minutes at room temperature with gentle rocking, samples were briefly centrifuged to pellet beads, decanted and resuspended in 1X SDS loading buffer. CsgA-his migrated with an apparent molecular mass of approximately 17 kDa and is indicated with an arrow. (**C**) N-terminal sequences of Wt PhoA (Aph1) and the CsgA-PhoA fusion protein (Aph2). An asterisk indicates the predicted signal peptidase II cleavage site. (**D**) Co-immunoprecipitation of Aph2 and CsgG. CsgG-his was detected in cell fractions prepared from cells expressing Aph2 (lanes 3, 5, 7, and 9) or Aph1 (lanes 2, 4, 6, and 8) as described in the Materials and Methods by western blot with α-His antibodies. Samples that were immunoprecipitated (IP) from the Elugent soluble (ES) fraction with α-HA antibodies were loaded into lanes 8 and 9. The sarkosyl soluble (SS) fraction is also shown (lanes 4 and 5). CsgG-his migrates at approximately 30 kDa and the "*" indicates the α-HA IgG protein recognized by the α-His antibody in the immunoprecipitation samples.

Figure 2.2. Purification and structural analysis of CsgG. (A) C600/pMC2 cells were harvested and the Elugent soluble (ES) outer membrane fraction (lane 1) was applied to a Ni-NTA column in 5 column volumes of HNE and 1 mL flow-through (FT) collected (lane 2). The column was then washed with 5 column

volumes HNE containing 10mM imidizole. The first (W1) and last (W2) milliliter of this wash was collected for analysis (lanes 3 and 4). CsgG-his bound to the column was eluted with HNE containing 100 mM imidizole and collected in three 1 mL fractions, E1 – E3 (lanes 5-7). Fractions were resolved by SDS-PAGE and visualized by Coomassie Brilliant Blue staining. The asterisk at 30-kDa indicates the molecular weight of CsgG. **(B)** CsgG forms an oligomer in the outer membrane. Elugent soluble outer membrane fraction from cells expressing CsgG-his (lane 4), CsgG-HA (lane 7), or both (lane 1) were isolated and CsgG-his was purified by Ni-NTA chromatography as described in Materials and Methods. Analysis of the fractions by western blot analysis with α-HA antibodies revealed CsgG-HA in the eluate only when CsgG-his was co-expressed (lane 3). The band at ~ 55 kDa in lane 3 is an unidentified cross-reacting band that is sometimes seen when CsgG is purified from C600. **(C)** Rotary Shadow electron microscopy (EM) analysis of CsgG-his protein reveals donut-shaped structures approximately 13 nm in diameter. Scale bar left panel = 100 nm. Right panel shows enlargements of single particles from the left panel. Scale bar right panel = 15 nm. Rotary shadowing with platinum was performed as described in the Materials and Methods.

Figure 2.3. Antibiotic sensitivity studies. (A) Growth curve of *E. coli* strain C600 containing plasmid pTRC99A or pMC1 in the presence or absence of 30 μg/ml erythromycin. Strains were grown overnight, diluted 1:100 in LB and grown for 30 minutes in the presence of 0.05 mM IPTG, before erythromycin was added (time 0). (B) Growth curve of *E. coli* strain C600 containing plasmid pTRC99A or

pMC1 in the presence or absence of 30 μg/ml vancomycin. Strains were grown overnight, diluted 1:100 in LB and grown for 30 minutes in the presence of 0.05 mg/ml IPTG, before vancomycin was added (time 0).

Fig. 2.4. Lipidation is required for CsgG activity. (A) The N-terminal 21 amino acids of CsgG that encodes a SEC dependent secretion sequence and lipoprotein modification site are shown. The "*" indicates the putative signal peptidase II-dependent cleavage site. Shown in red are the N-terminal 25 amino acids from PhoA that were used to replace the lipoprotein signal sequence of CsgG. (B) Expression and localization of CsgG and CsgGss. Cells containing pMC2 or pLR16 were grown to mid log phase and induced with 0.1 mM IPTG for two hours before being harvested and fractionated as described in the Materials and Methods. CsgG and CsgGss were detected using α-His antibodies. Lanes 1 and 2 are whole cell lysates, lanes 3 and 4 are periplasmic fractions and lanes 5 and 6 are Elugent soluble outer membrane fractions. Equal amounts of CsgG-his and CsgGss-his fractions were loaded. (C) CR binding of *csgG*- strains containing the indicated plasmids after 48 hours of growth at 26° C on YESCA plates. (D) Western analysis using α-CsgA or α-CsgB antibodies. Whole cell lysates of cells grown for 48 hours on YESCA plates were treated with formic acid as described by Chapman et al. (2002) and probed with α-CsgA or α-CsgB antibodies. The "*" indicates a non-specific protein recognized by the α-CsgB antibody.

Fig. 2.5. CsgG interacts with CsgE and CsgF at the outer membrane. (A) Cells expressing CsgG-his and CsgF-HA were fractionated and then immunoprecipitated with α-HA antibodies where indicated. Samples were blotted and probed with α-His antibodies to detect CsgG. CsgG migrates at approximately 30 kDa and is indicated with an arrow. (B) Cells expressing CsgG-his and CsgE-AU1 were fractionated prior to immunoprecipitation with α-AU antibodies. CsgG-his migrates at approximately 30 kDa and the "*" indicates the IgG protein in the immunoprecipitation samples recognized by the α-His antibody. (WC = whole cells, SS = sarkosyl soluble fraction, ES = Elugent soluble fraction, IP = immunoprecipitation.)

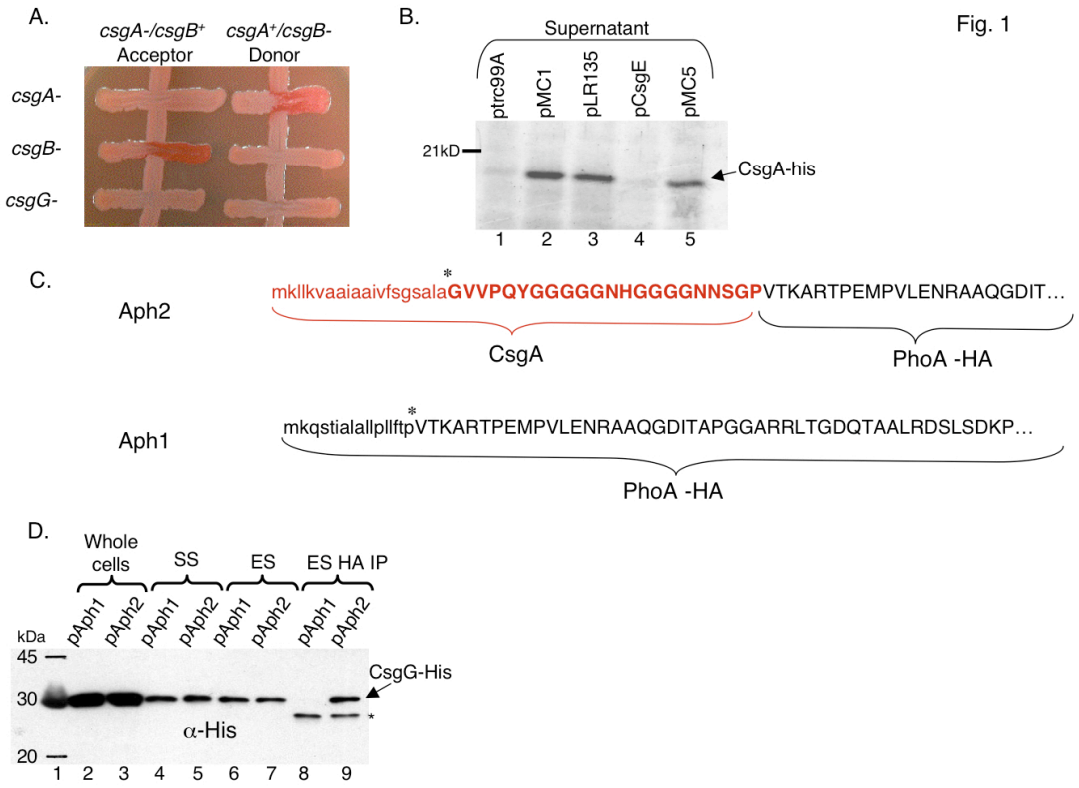

Figure 2.1. CsgG is required for interbacterial complementation and CsgA secretion

.

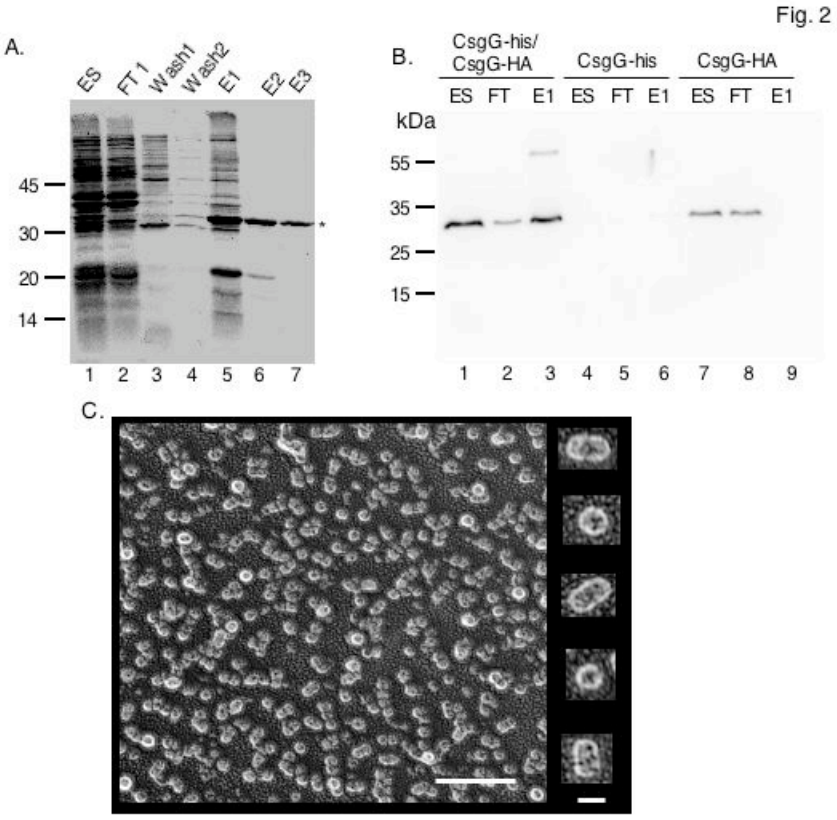

Figure 2.2. Purification and structural analysis of CsgG.

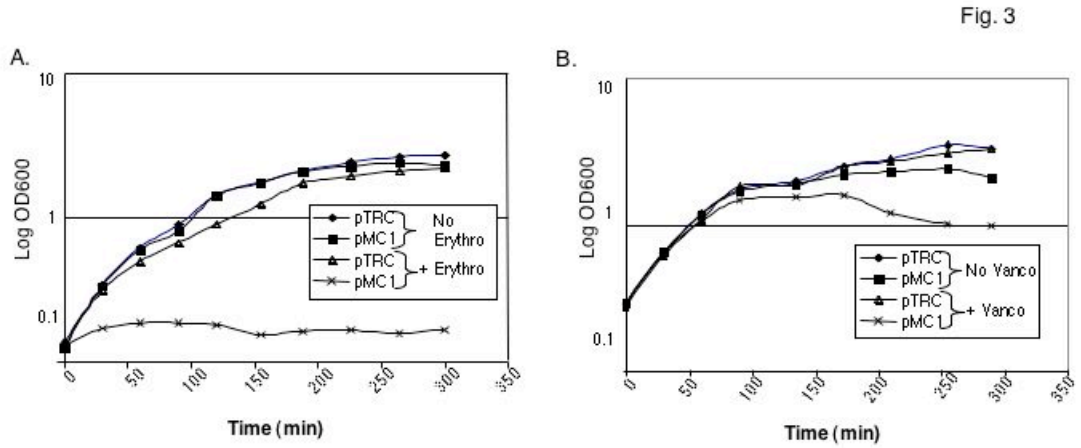

Figure 2.3. Antibiotic sensitivity studies.

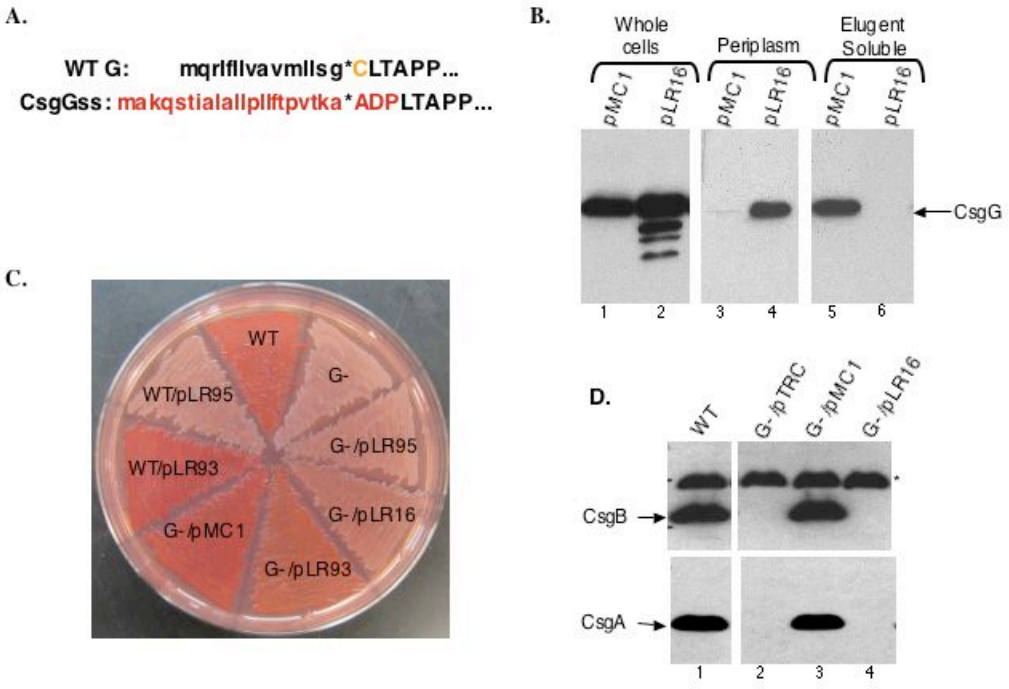

Fig. 2.4. Lipidation is required for CsgG activity.

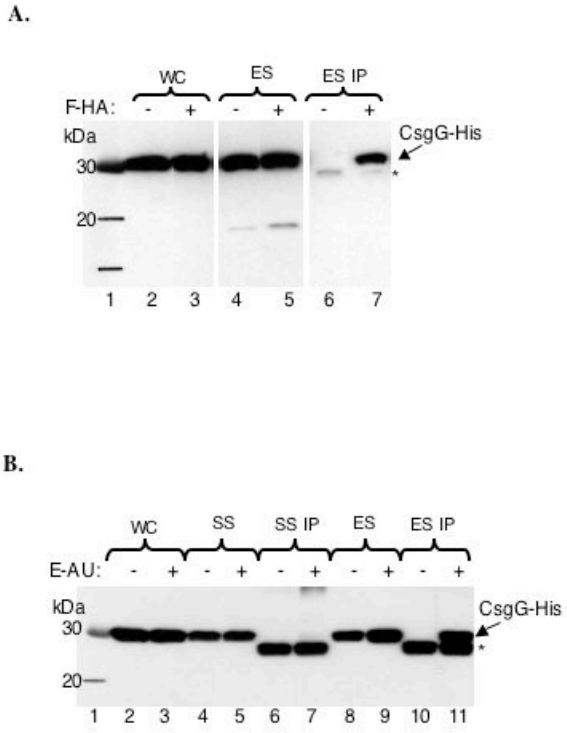

Fig. 2.5. CsgG interacts with CsgE and CsgF at the outer membrane.

Strain /Plasmid	Relevant characteristics
C600	F- *thr leu thi lac tonA*
LSR12	C600::Δ*csgDEFG*Δ*csgBA*
MC4100	F-*ara*D139 Δ(*argF-lac*)U169 *rsp*L150(s*trR*) *rel*A1*flb*B5301 *deo*C1 *pts*F25 *rbs*R
LSR1	MC4100*csgG::Tn105*
MHR204	MC4100*csgA::*Tn105
LSR10	MC4100::Δ*csgA*
MHR261	MC4100::Δ*csgB*
pTrc99A	Expression vector
pMC1	*csgG* cloned into pTrc99A
pLR15	*csgG* amplified from pMC1 with Trc5F and LR15R cloned into pTrc99A
pLR135	*csgE* amplified with LR135F and LR135R and cloned into KpnI/PstI sites of pLR15
pLR16	DNA fragment encoding the PhoA signal sequence amplified with PhoSSF and LR16R1 cloned into pTrc99A; sequence encoding mature CsgG with C-terminal 6his epitope amplified with LR16F2 and GhisR and cloned into BamHI/PstI sites of pTrc99A.
pCsgE	*csgE* amplified with PEF and PER and cloned into the NcoI/BamHI sites of pTrc99A.
pMC5	*csgEFG* cloned into pTrc99A
pMC2	*csgG-6his* amplified with Trc5F and GhisR and cloned into pTrc99A.
pLomp4	DNA fragment encoding the signal sequence of *E. coli* Lpp fused to residues 41-159 of OmpA cloned pTrc99A.
pBAD33	Expression vector
pLR29	*csgEFG* amplified from pMC5 using LR29F and LR29R and cloned into the KpnI/PstI sites of pBAD33.
pLR46	DNA fragment encoding the N-terminus of PapD amplified with LR46F and LR46R cloned into the KpnI/Bgl2 sites of pLR29.
pLR60	CmR gene lacking an NcoI site amplified from pBAD33 with LR60F and LR60R and cloned into Msc1/Sca1 of pLR46.
pLR92	*csgG-HA* amplified from pMC1 with LR92F and LR92R and cloned into the SacI/PstI sites of pLR60.
pLR169	DNA fragment encoding N-terminal AU-tagged CsgE subcloned into NcoI/PstI sites of pLR92 from similarly digested pLR167.
pLR58	*csgF-HA* amplified with Trc5F and LR58R and cloned into the NcoI/PstI sites of pLR92.
pLR134	DNA fragment encoding the first 42 amino acids of CsgA, containing the sec signal sequence and the first 22 residues of the mature protein, amplified with LR134F and LR134R cloned into the NcoI/PstI sites of pLR92.
pAph2	DNA sequence encoding mature PhoA with a C-terminal HA tag amplified with Aph2F and PhoHAR cloned into pLR134.
pAph1	*phoA-HA* amplified with Aph1F and PhoHAR and cloned into the SacI/PstI sites of pLR92.
pACYC177	Cloning vector
pLR1	*csgBA* promoter amplified with LR1F and LR1R and cloned into the BamHI/PstI sites of pACYC177.
pLR2	The NcoI/PstI fragment of pLomp4 subcloned into pLR1.
pLR7	*csgGss-HA* amplified from pLR16 with PhoSSF and LR7R and cloned into the NcoI/PstI sites of pLR1.
pLR167	DNA fragment encoding N-terminal AU-tagged CsgE amplified with LR169F and Trc3R and cloned into pLR7.
pLR95	The NcoI/PstI fragment of pLR16 containing the *csgGss* chimera subcloned into pLR1.
pLR93	The NcoI/PstI of pMC1 containing *csgG* subcloned into pLR1.
pMC3	*csgA-6his* cloned into pHL3

Table 2.1: Strains and plasmids used in this study.

Name	Sequence
1. Trc5F	GCGCCGACATCATAACGG
2. LR15R	gtttggatccTCAAGGATTCCGGTGGtACCGACATATGG
3. LR135F	ttttGGTaCCACCGGAATCCTGAatgAAACGTTATTTACGCTGGATTG
4. LR135R	gtttctgcaggatccTTAaAATTCATCATGCGCCAAATCGC
5. PhoSSF	gtttccATGgctAAACAAAGCACTATTGCACTGGC
6. LR7R	gtttctgcagttaagcgtagtccggaacgtcgtacgggtaGGATTCtGGTGGAACCGAC
7. LR169F	aaaagatctagatacttatcgttatatcGTTGAGGTAGAAGTCCCGGG
8. LR58R	gtttctgcagttaagcgtagtccggaacgtcgtacgggtaAAAATCGGTTGAGTTATTTTGTAAACC
9. PER	GGATCCTAGAATTCATCATGCCGCCAAATC
10. PEF	ccatggATGAAACGTTATTTACGCTGG
11. GhisR	gtttctgcagtcaatggtgatggtgatggtgGGATTCCGGTGGAACCGAC
12. L16R1	gtttggatccgcGGCTTTTGTCACAGGGGTAAACAG
13. LR16F2	gtttggatccaTTAACCGCCCCGCCTAAAGAAGCC
14. LR29F	gtttggtacCACACAGGAAACAGACCATGG
15. LR29R	gtttctgcagttattagatcttAGGATTCtGGTGGAACCGAC
16. LR46F	gtttggtaccacacaggaaacagaccATGATTCGAAAAAAGATTCTGATGGC
17. LR46R	gtttggatccttaagcgtagtccggaacgtcgtacgggtaGGTTTTAATTGCTGCCGGGC
18. LR60F	ccaATATGGACAACTTCTTCGCCCCCGTTTTCActatggGCAAATATTATACGC
19. LR60R	actGTTGTAATTCATTAAGCATTCTGC
20. LR92F	ttttgagctCACACAGGAAACAGACCATGG
21. LR92R	ttttctgcagttattagatctagattggtaccTTAAGCGTAGTCCGGAACGTC
22. LR134F	gtttccATGgcgAAACTTTTAAAAGTAGCAGCAATTGCAGC
23. LR134R	ttttctgcagtaatggtaccATTTGGGCCGCTATTATTACCG
24. Aph2F	aaaaggtaccCGGACACCAGAAATGCCTGTTC
25. PhoHAR	ttttctgcagTTAagcgtagtccggaacgtcgtacgggtaTTTCAGCCCCAGAGCGGC
26. Aph1F	ttttgagctCACACAGGAAACAGACCATGGcaAAACAAAGCACTATTGCACTGG
27. LR1F	gtttagatctCAGAAGTACTGACAGATGTTGC
28. LR1R	gtttctgcagttattcCATggtgtcaccctggacctgg
29. Trc3R	GATTAATCTGTATCAGG

Table 2.2. Oligonucleotide primers used in this study. Lower case letters indicate sequences that do not hybridize to the template used in the PCR reaction.

References

Augustus, A.M., Celaya, T., Husain, F., Humbard, M., and Misra, R. (2004) Antibiotic-sensitive TolC mutants and their suppressors. *J Bacteriol* **186**: 1851-1860.

Ben Nasr, A., Olsen, A., Sjobring, U., Muller-Esterl, W., and Bjorck, L. (1996) Assembly of human contact phase proteins and release of bradykinin at the surface of curli-expressing Escherichia coli. *Mol Microbiol* **20**: 927-935.

Bian, Z., and Normark, S. (1997) Nucleator function of CsgB for the assembly of adhesive surface organelles in Escherichia coli. *EMBO J* **16**: 5827-5836.

Bose, N., and Taylor, R.K. (2005) Identification of a TcpC-TcpQ outer membrane complex involved in the biogenesis of the toxin-coregulated pilus of Vibrio cholerae. *J Bacteriol* **187**: 2225-2232.

Brok, R., Van Gelder, P., Winterhalter, M., Ziese, U., Koster, A.J., de Cock, H., Koster, M., Tommassen, J., and Bitter, W. (1999) The C-terminal domain of the Pseudomonas secretin XcpQ forms oligomeric rings with pore activity. *J Mol Biol* **294**: 1169-1179.

Chapman, M.R., Robinson, L.S., Pinkner, J.S., Roth, R., Heuser, J., Hammar, M., Normark, S., and Hultgren, S.J. (2002) Role of *Escherichia coli* curli operons in directing amyloid fiber formation. *Science* **295**: 851-855.

Chirwa, N.T., and Herrington, M.B. (2003) CsgD, a regulator of curli and cellulose synthesis, also regulates serine hydroxymethyltransferase synthesis in Escherichia coli K-12. *Microbiology* **149**: 525-535.

Collinson, S.K., Doig, P.C., Doran, J.L., Clouthier, S., Trust, T.J., and Kay, W.W. (1993) Thin, aggregative fimbriae mediate binding of Salmonella enteritidis to fibronectin. *J Bacteriol* **175**: 12-18.

Collinson, S.K., Parker, J.M., Hodges, R.S., and Kay, W.W. (1999) Structural predictions of AgfA, the insoluble fimbrial subunit of Salmonella thin aggregative fimbriae. *J Mol Biol* **290**: 741-756.

Gerstel, U., Park, C., and Romling, U. (2003) Complex regulation of csgD promoter activity by global regulatory proteins. *Mol Microbiol* **49**: 639-654.

Hammar, M., Arnqvist, A., Bian, Z., Olsen, A., and Normark, S. (1995) Expression of two csg operons is required for production of fibronectin- and congo red-binding curli polymers in Escherichia coli K-12. *Mol Microbiol* **18**: 661-670.

Hammar, M., Bian, Z., and Normark, S. (1996) Nucleator-dependent intercellular assembly of adhesive curli organelles in Escherichia coli. *Proc Natl Acad Sci U S A* **93**: 6562-6566.

Hung, D.L., Raivio, T.L., Jones, C.H., Silhavy, T.J., and Hultgren, S.J. (2001) Cpx signaling pathway monitors biogenesis and affects assembly and expression of P pili. *EMBO J* **20**: 1508-1518.
Kayed, R., Head, E., Thompson, J.L., McIntire, T.M., Milton, S.C., Cotman, C.W., and Glabe, C.G. (2003) Common structure of soluble amyloid oligomers implies common mechanism of pathogenesis. *Science* **300**: 486-489.

Lashuel, H.A., Hartley, D., Petre, B.M., Walz, T., and Lansbury, P.T.J. (2002) Neurodegenerative disease: amyloid pores from pathogenic mutations. *Nature* **418**: 291.

Loferer, H., Hammar, M., and Normark, S. (1997) Availability of the fibre subunit CsgA and the nucleator protein CsgB during assembly of fibronectin-binding curli is limited by the intracellular concentration of the novel lipoprotein CsgG. *Mol Microbiol* **26**: 11-23.

Mundy, R., Pickard, D., Wilson, R.K., Simmons, C.P., Dougan, G., and Frankel, G. (2003) Identification of a novel type IV pilus gene cluster required for gastrointestinal colonization of Citrobacter rodentium. *Mol Microbiol* **48**: 795-809.

Narita, S., Matsuyama, S., and Tokuda, H. (2004) Lipoprotein trafficking in Escherichia coli. *Arch Microbiol* **182**: 1-6.

Nevesinjac, A.Z., and Raivio, T.L. (2005) The Cpx envelope stress response affects expression of the type IV bundle-forming pili of enteropathogenic Escherichia coli. *J Bacteriol* **187**: 672-686.

Olsen, A., Jonsson, A., and Normark, S. (1989) Fibronectin binding mediated by a novel class of surface organelles on Escherichia coli. *Nature* **338**: 652-655.

Prigent-Combaret, C., Brombacher, E., Vidal, O., Ambert, A., Lejeune, P., Landini, P., and Dorel, C. (2001) Complex regulatory network controls initial adhesion and biofilm formation in Escherichia coli via regulation of the csgD gene. *J Bacteriol* **183**: 7213-7223.

Ramer, S.W., Bieber, D., and Schoolnik, G.K. (1996) BfpB, an outer membrane lipoprotein required for the biogenesis of bundle-forming pili in enteropathogenic Escherichia coli. *J Bacteriol* **178**: 6555-6563.

Romling, U., Bian, Z., Hammar, M., Sierralta, W.D., and Normark, S. (1998) Curli fibers are highly conserved between Salmonella typhimurium and Escherichia coli with respect to operon structure and regulation. *J Bacteriol* **180**: 722-731.

Ruiz, N., and Silhavy, T.J. (2005) Sensing external stress: watchdogs of the Escherichia coli cell envelope. *Curr Opin Microbiol* **8**: 122-126.

Schmidt, S.A., Bieber, D., Ramer, S.W., Hwang, J., Wu, C.Y., and Schoolnik, G. (2001) Structure-function analysis of BfpB, a secretin-like protein encoded by the bundle-forming-pilus operon of enteropathogenic Escherichia coli. *J Bacteriol* **183**: 4848-4859.

Sjobring, U., Pohl, G., and Olsen, A. (1994) Plasminogen, absorbed by Escherichia coli expressing curli
or by Salmonella enteritidis expressing thin aggregative fimbriae, can be activated by simultaneously captured tissue-type plasminogen activator (t-PA). *Mol Microbiol* **14**: 443-452.
Thanassi, D.G., and Hultgren, S.J. (2000) Assembly of complex organelles: pilus biogenesis in gram-negative bacteria as a model system. *Methods* **20**: 111-126.

Thanassi, D.G., Saulino, E.T., Lombardo, M.J., Roth, R., Heuser, J., and Hultgren, S.J. (1998) The PapC usher forms an oligomeric channel: implications for pilus biogenesis across the outer membrane. *Proc Natl Acad Sci U S A* **95**: 3146-3151.

Zogaj, X., Bokranz, W., Nimtz, M., and Romling, U. (2003) Production of cellulose and curli fimbriae by members of the family Enterobacteriaceae isolated from the human gastrointestinal tract. *Infect Immun* **71**: 4151-4158.

Zogaj, X., Nimtz, M., Rohde, M., Bokranz, W., and Romling, U. (2001) The multicellular morphotypes of Salmonella typhimurium and Escherichia coli produce cellulose as the second component of the extracellular matrix. *Mol Microbiol* **39**: 1452-1463.

Chapter III

Spatial clustering of the curlin secretion lipoprotein requires curli fiber assembly

Abstract

Gram-negative bacteria assemble functional amyloid surface fibers called curli. CsgB nucleates the major curli subunit protein, CsgA, into a self-propagating amyloid fiber on the cell surface. The CsgG lipoprotein is sufficient for curlin transport across the outer membrane, and is hypothesized to be the central molecule of the curli fiber secretion and assembly complex. We tested the hypothesis that the curli secretion protein, CsgG, was restricted to certain areas of the cell to promote the interaction of CsgA and CsgB during curli assembly. Here, electron microscopic analysis of curli-producing strains showed that relatively few cells in the population contacted curli fibers, and that curli emanated from spatially discrete points on the cell surface. Microscopic analysis revealed that CsgG was surface exposed and spatially clustered around curli fibers. CsgG localization to the outer membrane and exposure of the surface domain were not dependent on any other *csg*-encoded proteins, but the clustering of CsgG required the *csg*-encoded proteins CsgE, CsgF, CsgA and CsgB. CsgG formed stable oligomers in all the *csg* mutant strains, but these oligomers were distinct from the CsgG complexes assembled in WT cells. Finally, we found that efficient fiber assembly was required for the spatial

clustering of CsgG. These results suggest a new model where curli fiber formation is spatially coordinated with the CsgG assembly apparatus.

Introduction

Escherichia coli and other enteric bacteria assemble highly aggregative fibers on their cell surfaces called curli (Olsen et al., 1989; Arnqvist et al., 1992; Hammar et al., 1995; Collinson et al., 1996). Curli fibers are critical determinants of attachment during biofilm formation and they are potent inducers of host immune response (Herwald et al., 1998; Olsen et al., 1998; Prigent-Combaret et al., 2000; Bian et al., 2000). Curli are structurally and biochemically similar to amyloid fibers (Chapman et al., 2002). Amyloid fibers are most readily associated with neurodegenerative ailments such as Alzheimer's disease; yet some cells are able to assemble functional amyloids without eliciting cytotoxicity. Functional amyloids have been identified in organisms ranging from bacteria to mammals and they fulfill many diverse physiological functions (Fowler et al., 2007).

Curli biogenesis requires the coordinated efforts of proteins encoded by two divergently transcribed operons. *csgBAC* encodes the structural subunits of the fiber, CsgA and CsgB. A third gene in the operon, *csgC*, has no reported role in *E. coli* curli biosynthesis, but the *csgC* homolog in *Salmonella enteritidis* may be important for curli ultrastructural properties (Gibson et al., 2007). *csgDEFG* encodes proteins necessary for the production, secretion and assembly of CsgA and CsgB. CsgD is a transcriptional activator of the *csgBAC* operon. CsgG is an outer membrane-localized lipoprotein that is required for the secretion of CsgA and CsgB to the cell surface (Robinson et al., 2006). CsgE and CsgF can interact

with CsgG at the outer membrane, modulate the stability of CsgA and CsgB, and are required for efficient curli assembly (Chapman et al., 2002; Robinson et al., 2006). However, the precise molecular action of CsgE and CsgF remains unclear.

One model of curli assembly is the nucleation-precipitation pathway, which begins with the CsgG-mediated export of pre-amyloid CsgA and CsgB to the extracellular milieu (Robinson et al., 2006; Loferer et al., 1997). At the cell surface, CsgB presents an amyloid template to CsgA and 'nucleates' soluble CsgA into insoluble amyloid curli fibers (Hammar et al., 1996; Bian and Normark, 1997; Hammer et al., 2007). Remarkably, CsgA and CsgB do not have to be expressed from the same cell in order for curli to be assembled. Some CsgA expressed by a 'donor' cell can polymerize when it contacts a CsgB-expressing 'acceptor' cell in a process termed interbacterial complementation (Hammar et al., 1996). *In vitro* polymerization experiments with purified CsgA and CsgB further suggest that physical contacts between these proteins drive efficient polymerization (Hammar et al., 1996; Hammer et al., 2007).

We investigated the possibility that the curli secretion protein, CsgG, was restricted to certain areas of the cell to promote the interaction of CsgA and CsgB during curli assembly. Studies in many bacterial systems have revealed non-uniform distribution of proteins involved in chemotaxis, cell division, and secretion (Buddelmeijer et al., 1998; Maddock and Shapiro, 1993; Brandon et al., 2003). Spatial restriction, rather than random diffusion, may facilitate the protein-protein interactions required to achieve many cellular processes. For example, the enteropathogenic *E. coli* bundle-forming pili secretion apparatus is polarly

localized (Hwang et al., 2003). Also, the *Myxococcus* type IV pilus secretin, PilQ, is found exclusively at the poles (Nudleman et al., 2006). The ExPortal system in *S. pyogenes*, which serves as the major site of protein secretion, is also spatially localized to discrete regions of the cell. Coupled to the ExPortal are chaperone-like proteins that facilitate folding of newly secreted proteins, suggesting spatial and temporal coordination of protein secretion and folding (Campo et al., 2004; Rosch and Caparon, 2005). We found that CsgG was organized into foci in curli producing cells and that this organization requires efficient fiber polymerization. We also found that CsgG contains a domain that is exposed to the cell surface and that it forms a heat and SDS resistant complex in the outer membrane. Finally, we show that other CsgG-interacting proteins are required for the spatial restriction of CsgG, which provides the first molecular evidence of how CsgG may be modulated by other *csg*-encoded proteins.

Results

CsgG is spatially restricted into clusters on curli-producing cells

The major curli fiber subunit, CsgA, is secreted as a soluble protein that is nucleated by outer membrane-associated CsgB into a highly ordered and aggregative amyloid fiber (Hammar et al., 1996; Chapman et al., 2002; Wang et al., 2007; Hammer et al., 2007). Curli fibers have a distinct morphology that can be readily observed by electron microscopy (EM); the fibers are 4- to 6-nm wide unbranched filaments that form densely tangled masses that interconnect cells (Olsen et al., 1989; Chapman et al., 2002). EM of MC4100 (wild-type strain; WT) cells revealed that curli emanated from discrete regions of the cell surface,

although the location varied among individual cells (Fig. 3.3.1). Of 660 cells examined, 39% of cells contacted curli fibers while 61% lacked fibers entirely. The non-uniform distribution of curli fibers within the population of WT cells led us to investigate whether the distribution of CsgG was likewise restricted to curli-producing cells. First, however, we developed methods to detect CsgG spatial distribution in curli-producing cells.

It was proposed that CsgG is localized to the inner leaflet of the outer membrane (Loferer et al., 1997), but the ability of CsgG to support secretion of CsgA into culture supernatants suggested that CsgG might have an extracellular domain (Robinson et al., 2006). Intact cell immuno-dot blotting was used to test the hypothesis that CsgG was at least partially exposed to the cell surface (Fig. 3.2). Equal numbers of intact cells were spotted onto a nitrocellulose membrane and probed with α-CsgG antibodies. α-CsgG antibodies reacted with WT intact cells while no signal was detected in *csgG* cells. The CsgG signal was restored when *csgG* was transformed with plasmids encoding CsgG or CsgG-his from pMC1 or pMC2, respectively (Fig. 3.2, left panel). Intact cells were also probed with antibodies specific for the periplasmic protein DsbA to assess outer membrane integrity. α-DsbA antibodies did not react with intact cells, but sonication of cell samples resulted in detection of α-DsbA-reactive material after dot blotting (Fig. 3.2, center panel). There was no α-DsbA signal in sonicates of a *dsbA* mutant strain JP120 (data not shown). The observation that α-CsgG antibodies recognized intact cells supported the hypothesis that part of CsgG was exposed to the cell surface. Interestingly, dot blots probed with α-hexahistindine antibodies recognized *csgG*/pMC2 sonicates, but not intact cells

(Fig. 3.2, right panel). Since pMC2 encodes CsgG with a C-terminal hexahistidine epitope, we concluded that the C-terminal region of CsgG was inside the cell.

Because CsgG is essential for curlin stability and secretion, and since curli assembly requires CsgA and CsgB interaction (Loferer et al., 1997; Robinson et al., 2006), we predicted that CsgG would be spatially coordinated around the cell so that CsgA and CsgB could efficiently contact each other on the cell surface. Indirect immunofluorescence microscopy (IFM) was used to determine if CsgG was localized to distinct regions around the cell. Antibodies directed to CsgG in WT cells revealed distinct immunofluorescent punctate groups (Fig. 3.3A). We found that approximately 30% of the 1191 cells examined displayed α-CsgG-stained foci. WT cells either displayed a punctate signal or lacked signal altogether, and each cell generally displayed three or fewer foci. α-CsgG foci were detected in groups of aggregated bacteria and in isolated bacteria (Fig. 3.7). Only about 2.5% of *csgG* mutant cells displayed α-CsgG foci (Fig. 3B). In the few *csgG* cells containing IFM signal, generally only a single, faint α-CsgG focus was observed. The punctate α-CsgG stain was specific for CsgG in WT cells, as omission of the primary antibody dramatically reduced the number of cells with fluorescent signal (6.2% of 484 cells displayed punctate fluorescent staining).

We next used immuno-electron microscopy (IEM) to determine if CsgG co-localized with curli fibers. Cells were grown under curli inducing conditions and equal numbers of cells were probed with α-CsgG antibodies and α-rabbit secondary antibodies conjugated to 10-nm gold particles before being negatively

stained with uranyl acetate. Every curliated cell of the several hundred observed also had gold particles on its surface (Fig. 3C). A majority of these particles were grouped near the cell location from where curli emanated, while very few particles were observed elsewhere on the surface of the cell (Fig. 3C). In addition, we observed gold particles bound to the fibers themselves, which might be due to non-specific staining, or indicate that CsgG can be dislodged from the cell surface during curli assembly (Fig. 3C). In 17 cells examined at high magnification, 100 α-CsgG-directed gold beads were observed randomly distributed over the cell surface, while more than 340 gold beads were localized to the region of the cell from where curli fibers emanated. Cell-associated gold particles were rarely observed when the α-CsgG antibody was omitted from the preparation (Fig. 3D). WT cells in the population that were not observably producing curli fibers either lacked α-CsgG signal entirely or contained fewer gold beads which were not spatially restricted in any obvious way. Therefore, we concluded that CsgG was clustered into foci in curli-producing cells.

Surface-exposed CsgG is spatially dispersed in csg mutants

An intriguing aspect of curli biogenesis is the interdependence of protein stabilities between the *csg*-operon encoded proteins. For example, deletion of *csgG* or *csgE* results in decreased stability and secretion of CsgA and CsgB and, conversely, deletion of *csgF* results in augmented CsgA secretion and stability (Chapman et al., 2002; Loferer et al., 1997; Hammer et al., 2007). Furthermore, overexpression studies showed that CsgG interacts with itself and with CsgA, CsgF and CsgE at the outer membrane (Robinson et al., 2006), although the

molecular consequences of these interactions are unclear. Because several *csg* mutant phenotypes appear to converge at the step of secretion, we examined the spatial organization of CsgG at the outer membrane in different *csg* mutant backgrounds (Fig. 3.4). Each of the *csg* mutant strains examined displayed a dramatic decrease in the number of cells containing CsgG foci (Fig. 3.4A). 30.0% of WT cells had punctate α-CsgG staining compared to 7.2% of *csgE*, 3.6% of *csgF*, 2.1% of *csgB*, and 2.31% of *csgA* cells (Fig. 3.4B). We never observed a significant level of diffuse immunofluorescent signal in any of the WT or mutant cells, leading us to further investigate the cause of the loss in IFM signal. Despite the fewer number of CsgG punctate groups in the *csg* mutant strains compared to WT, western blotting indicated that WT and *csg* mutant strains had similar amounts of CsgG in the outer membrane, inner membrane, cytoplasm/periplasm and whole cell fractions (Fig. 3.4C and data not shown).

Since protein instability or mislocalization did not account for the decrease in CsgG IFM stain that was observed in the *csg* mutant strains, we tested if CsgG surface accessibility was altered in the *csg* mutant strains. The polyclonal α-CsgG antibody reacted with intact cells of each strain tested (Fig. 3.4D), indicating CsgG was still surface exposed in *csg* mutant strains. A slight decrease in α-CsgG signal was evident in *csgE* and *csgF* samples. To test the possibility that the outer membrane prevented the α-CsgG antibody from reaching CsgG in any of the *csg* mutant strains, we performed α-CsgG IFM on permeabilized cells. However, no change in the relative levels of α-CsgG IFM signal was evident in any strain when membranes were permeabilized with Triton-X100 before probing with antibodies (data not shown). Therefore, the loss

of CsgG foci was not due to gross changes in protein stability, mislocalization, or exposure of CsgG to the cell surface. To further test the hypothesis that exposure of CsgG to the cell surface was independent of any *csg*-encoded protein, we also probed intact *csgBACcsgDEFG* (*csgA*-*G*) cells expressing CsgG from the plasmid pMC1 with α-CsgG antibodies. The α-CsgG antibody reacted readily with *csgA*-*G*/pMC1 cells (Fig. 3.4D).

Taken together, these results indicated that the CsgG produced in *csgA*, *csgB*, *csgE*, and *csgF* cells was spatially dispersed in the outer membrane, and not localized into punctate clusters. We used α-CsgG IEM to confirm this notion. We saw two distinct populations of *csg* mutant cells by IEM: some cells showed many α-CsgG beads while many cells had very few α-CsgG beads or lacked gold beads altogether. A similar pattern was observed for WT cells (Fig. 3.2). As shown in Fig. 3.4E, α-CsgG-directed gold beads, when present, were randomly distributed on the cell surface of *csg* mutant strains. Therefore, we conclude that *csg*-encoded proteins were required for spatial restriction of CsgG and that the loss of α-CsgG IFM signal in the *csg* mutant strains was due to a more uniform spatial distribution of CsgG on the surface of the cells, which lowered the IFM signal intensity to below background levels.

CsgG multimers are resistant to denaturation with heat and detergent

Resistance to denaturation is a property of many outer membrane-localized multimeric complexes, and two distinct forms of assembly-dependent electrophoretic mobility have been described for outer membrane proteins (Reithmeier and Bragg, 1974; Hardie et al., 1996). We have previously shown

that differently tagged CsgG constructs can co-purify and co-immunoprecipitate when overexpressed in the same cell, suggesting that CsgG can interact with itself at the outer membrane (Robinson et al., 2006). To examine the possibility that an assembly defect contributed to the loss of spatial clustering of CsgG expressed in the *csg* mutant strains, we examined the assembly status of CsgG in the various CsgG-expressing strains. WT and isogenic *csgE, csgF*, *csgB*, and *csgA* strains were grown on YESCA plates at 26°C for 48 hours and then cells-free suspensions (CFS) were prepared as described in the Materials and Methods. Freshly prepared CFS was suspended in SDS sample buffer and incubated for 10 minutes at various temperatures between 22° and 95°C before loading onto a discontinuous 5%-8% SDS-PAGE gel (Fig. 3.5). CsgG solubilized from WT cells migrated as a single high molecular weight species higher than the 170 kDa standard in the 8% resolving gel at temperatures at below 55°C (Fig. 3.5A and B lanes 1 and 2 and Figure S2A). An intermediate molecular weight CsgG species that migrated between the 170 and 130 kDa standards was detected when WT samples were heated at temperatures greater than 55°C (Fig. 3.5A and B, lane 3 and Fig. 3.8A). The 30 kDa CsgG monomer was only detected when the samples were heated to 95°C for ten minutes (Fig. 3.5A and B, lane 4).

Surprisingly, CsgG in unheated samples obtained from *csgE*, *csgF*, *csgB*, or *csgA* strains resolved by SDS-PAGE did not migrate exclusively as a single, high molecular weight band, as was detected in WT samples. Rather, various amounts of the intermediate molecular weight CsgG species migrating between the 170 and 130 kDa standards were detected in unheated samples from *csg*

mutant cells (Fig. 3.5A lanes 6, 10, and 5B lanes 6 and 13). Notably, detection of monomeric CsgG in any strain required that that the samples be heated to 95°C prior to electrophoresis (Fig. 3.5A, lanes 3, 9, 13, and 5B lanes 4, 9 and 13), suggesting that the intermediate species was an SDS-stable CsgG oligomer. A 45 kDa CsgG species was detected in heated and unheated *csgE*, *csgF*, and *csgB* samples (Fig. 3.5A lanes 6-13 and 5B 10-13). We did not observe this band in the WT, *csgG*, or *csgA* samples. The 45 kDa band did not react with antibodies raised against CsgA (data not shown), and its identity remains unclear. The loss of the single high molecular weight CsgG-containing complex in the *csg* mutant strains suggests that all of these proteins are either directly or indirectly required for the assembly of the high molecular weight CsgG species. Importantly, antibodies raised against CsgA, CsgE or CsgF did not react with the high molecular weight or intermediate CsgG bands (data not shown).

CsgG expressed from the plasmid pMC1 in the *csgA-G* strain migrated predominately as the intermediate molecular weight species between the positions of the 170 and 130 kDa standards when incubated at temperatures below 95°C, which suggested that an SDS-resistant CsgG species can assemble in the absence of all of the other *csg*-encoded proteins (Fig. 3.8A, lanes 6-9). We next overexpressed CsgG in each of *csg* mutant strains to test whether variations in CsgG protein concentration could account for the shift in CsgG electrophoretic mobility in these strains. Overexpression of CsgG in any strain did not increase the amount of the high molecular weight CsgG species, although the intermediate molecular weight species accumulated (Fig. 3.21B and data not shown), raising the possibility that a stoichiometric relationship between CsgG

and other proteins may be required for the stable production of the high molecular weight species. The presence of the intermediate molecular weight CsgG species in the absence of any or all *csg* proteins suggests that a CsgG oligomer can assemble independently of other curli biogenesis proteins, but that the properties of this oligomer are distinct from the CsgG complexes formed in WT cells. These data also suggest that, since CsgG expressed in the various *csg* mutant strains is spatially dispersed, the CsgG complex represented by the intermediate molecular weight species observed in the *csg* mutant strains is likewise dispersed in the outer membrane.

Fiber assembly is required for CsgG clustering

Since we detected spatially restricted CsgG foci in curli-producing WT cells only, we investigated the relationship between fiber assembly and CsgG spatial restriction. Because CsgG clusters were absent from CsgG-expressing strains deficient in curlin secretion (*csgE*) or fiber assembly (*csgE*, *csgB*, *csgA*, *csgF*) we reasoned that CsgA polymerization into curli fibers was essential for CsgG spatial localization. We examined CsgG clustering by IEM and IFM in *csgA* cells expressing CsgA or a CsgA mutant that was unable to polymerize into fibers. CsgA-ΔR1 is missing 23 residues that comprise the first of five CsgA amyloidogenic domains and is unable to polymerize into fibers after it is secreted from the cell (Wang et al., 2008; and Fig. 3.6B). When *csgA* cells were transformed with plasmid pCsgA-his expressing wild type CsgA, 23% of 579 cells contained α-CsgG foci by IFM (Fig. 3.6C, inset) and α-CsgG-directed gold beads were clustered with curli fibers in *csgA*/pCsgA cells as observed with IEM (Fig.

3.6C). In contrast, only 10% of 567 *csgA* cells expressing CsgA-ΔR1-his displayed α-CsgG foci and clusters by IFM and IEM (Fig. 3.6D). Therefore, curli subunit secretion alone is not sufficient to mediate CsgG clustering, and secretion must be accompanied by CsgA polymerization into a fiber for CsgG clusters to form.

Discussion

Curli fiber assembly occurs by a process termed 'nucleation-precipitation' where soluble CsgA and CsgB interact at the cell surface to form insoluble amyloid fiber aggregates. A key event preceding nucleation-precipitation is the transportation of CsgA and CsgB to, and across, the outer membrane. CsgA and CsgB stability and secretion depends on the outer membrane localized lipoprotein CsgG (Loferer et al., 1997; Robinson et al., 2006). Here, we report that CsgG is spatially restricted on the cell surface and that other *csg*-encoded proteins are required for organization of CsgG around the cell.

We found that CsgG formed SDS-resistant multimers and was clustered into spatially discrete foci that were exposed to the extracellular surface. Furthermore, we observed that curli fibers emanated from spatially discrete regions of WT cells (Fig. 3.1). Immunogold-labeling revealed that CsgG was most abundant at the point(s) of the cell where curli emanated from the surface (Fig. 3). Additionally, we observed some binding of the gold-labeled α-CsgG antibodies to the fibers themselves, suggesting that CsgG may become dislodged from the membrane during curli assembly. However, fiber-associated CsgG likely only a minor fraction of the population, since CsgG-his is not

recognized by an α-his antibody added to the outside of cells (Fig. 3.2). The spatial restriction of CsgG into foci around curli fibers suggests a model where CsgA and CsgB fiber assembly is coordinated with CsgG spatial organization.

What mechanisms may be responsible for the clustering of CsgG around curli fibers? One possibility is that CsgG is spatially restricted prior to CsgA or CsgB secretion. In this scenario, CsgA and CsgB are secreted to the same location of the cell surface, perhaps facilitating the high efficiency of curli assembly. Another possibility is that CsgG is not restricted into foci until after secretion of CsgA and CsgB begins. The post-secretion aggregation of CsgA and CsgB into fibers may itself result in the clustering of CsgG around the fibers. Our data favors the later model. First, we did not observe spatially clustered CsgG foci in CsgG-expressing strains deficient in curlin secretion or curli assembly (Fig. 3.4). Further, CsgG foci were not evident when we transformed *csgA* cells with a plasmid encoding CsgA-ΔR1, a CsgA mutant protein that is stable and secreted, but defective in fiber assembly (Wang et al., 2008; Figure 6).

We also found that the loss of CsgE, CsgF, CsgA, or CsgB resulted in loss of spatially clustered CsgG foci, with little change in CsgG surface exposure or targeting to the outer membrane (Fig. 3.4). Stable CsgG oligomers likely form independently of other *csg*-encoded proteins, since slow-migrating SDS-resistant CsgG species were detected in all strains expressing CsgG (Fig. 3.5). However, the CsgG complexes formed in WT cells were slower migrating than the CsgG complexes observed in strains lacking CsgE, CsgF, CsgB, or CsgA (Fig. 3.5). Overexpression of CsgG in the absence of all of the *csg* proteins did not increase the relative amount of high molecular weight CsgG, as overexpressed CsgG

migrated predominately as the intermediate molecular weight species (Fig. 3.8). Therefore some parameter besides CsgG concentration determines formation of the highest molecular weight species. Taken collectively, our data suggests two distinct phases of CsgG assembly and organization: (1) CsgG is targeted to the outer membrane and exposes the surface-accessible domain in the absence of any or all of other *csg* encoded proteins, and (2) spatial restriction of CsgG into microdomains and assembly of the highest molecular weight CsgG complexes requires curli fiber polymerization supported by the other *csg* encoded proteins. Since CsgG physically interacts with CsgE, CsgF and CsgA (Robinson et al., 2006) any, or all, of these proteins may contribute to CsgG spatial restriction. However, genetic analyses to determine exactly which of these CsgG-interacting proteins is required for either the assembly of CsgG multimers or spatial restriction of CsgG were difficult as deletion of any single *csg* encoded protein results in loss of multiple other *csg*-encoded proteins from the cell surface (Chapman et al., 2002; Hammer et al., 2007).

Previous results indicated that the N-terminal cysteine of CsgG was lipidated, and that lipidation was required for the transport of CsgG to the outer membrane (Loferer et al., 1997; Robinson et al., 2006). We showed that CsgG contained a domain exposed to the cell surface (Fig. 3.2), and a previous study indicated that CsgG had a periplasmic domain (Loferer et al., 1997). Surface-exposed lipoproteins have been identified in several bacterial species, including *Escherichia*, *Klebsiella* and *Neisseria spp.* Membrane-spanning lipoprotein translocons are not unprecedented. For example, the lipoprotein Wza is an *E. coli* polysaccharide translocon that spans the outer membrane (Drummelsmith

and Whitfield, 2000). CsgG and Wza are topologically similar as both have periplasmic and surface-exposed domains (Figure 2; Drummelsmith and Whitfield, 2000; Loferer et al., 1997) and are also functionally similar, as both have been implicated as conduits for secretion across the outer membrane (Dong et al., 2006; Robinson et al., 2006). Importantly, CsgG lacks any apparent amino acid sequence similarity with either Wza or any other family of proteins (data not shown), and the architecture of the CsgG membrane-spanning domain(s) remains unclear. Future exploration of the domain architecture of CsgG and definition of the residues governing the contacts between CsgG and its many interacting proteins will help clarify the biology of this unique lipoprotein. One outstanding question in the biosynthesis of functional amyloids is how cells control amyloid fiber aggregation without any apparent cellular toxicity. In the curli biogenesis system, the activities of nucleation and polymerization are separated into two different proteins, CsgB and CsgA, respectively. This suggests that the cell can avoid unregulated fiber polymerization by keeping CsgA and CsgB separated until they reach the cell surface. The fiber-dependent spatial clustering of CsgG suggests an elegant mechanism to regulate the segregation of CsgA and CsgB: only when the *csg*-encoded proteins interact with CsgG does spatial restriction occur and CsgA and CsgB interaction occur. These results support a model where CsgG is the center of a curli assembly platform, although very little is known about the molecular nature of the protein-protein interactions that facilitate CsgG ultrastructural changes. In particular, the mechanisms preventing CsgA and CsgB amyloid assembly on the periplasmic face of the spatially restricted assembly complex remain to be elucidated.

Clarification of how the curli assembly platform forms will help further unravel the mechanism of coordinated curli amyloid biogenesis.

Experimental Procedures

Plasmids, strains, and growth conditions

E. coli strain MC4100 (and its derivations listed in Table 3.1) was grown on YESCA agar (10 g Casamino acids, 1 g yeast extract, 20 g agar per 1L) at 26°C for 36 – 48 hours to induce curli expression (Hammar et al., 1995). YESCA agar with 10 μg/ml Congo red was used to monitor curli production. CsgG and CsgG-his cloned behind the *trc* promoter in pTRC99A (plasmids pMC1 and pMC2, respectively, as described in Table 3.1) were used to overexpress CsgG in cells were grown on YESCA plates. Ampicillin was used at 100 μg/ml when appropriate.

Immunofluorescence Microscopy

CsgG was visualized by indirect immunofluorescence microscopy using a previously described protocol, with some modifications (Buddelmeijer et al., 1998). Briefly, cells grown on YESCA plates were suspended in 1X PBS (pH 7.4) and fixed with 2.5% formaldehyde and 0.04% glutaraldehyde and washed three times in 1X PBS (pH 7.4). Next, fixed cells were incubated with 3% BSA-1X PBS (pH 7.4) at 37°C for 30 minutes. Fixed and blocked cells were incubated at 37°C for 1 hour with rabbit polyclonal antibodies diluted with 3% BSA-1X PBS (pH 7.4) at the following dilutions: 1/1000 α-CsgG (Robinson et al., 2006), 1/1000 α-CsgA (Chapman et al., 2002), or 1/500 α-CsgB (Hammer et al., 2007). Cells were next

washed twice with 1X PBST (pH 7.4) and then incubated at 37°C for 30 minutes with goat α-rabbit IgG conjugated to Alexa-488 (Molecular Probes, OR) diluted 1/400 in 3% BSA-1X PBS (pH 7.4), and then washed twice in 1X PBST (pH 7.4). Cells were suspended with 2 mg/ml 4',6-diamidino-2-phenylindole (DAPI) to stain cellular DNA before spotting onto a glass slide and viewing with an Olympus BX51 fluorescence microscope. Images of the Alexa488 epifluorescence signal were captured with the following parameters: gain = 80 and offset = 24 for all strains observed; exposure was 500 ms when using α-CsgG or α-CsgB antibodies and 250 ms when using α-CsgA antibodies. DAPI signal was captured with a 250 ms exposure at the same gain and offset for all strains and conditions. The two images from each field of view were superimposed using Adobe Photoshop software. The number of cells with Alexa488 signal that co-localized with the DAPI signal was determined. The mean percent of three independent experiments +/- standard error was determined.

Electron Microscopy and immuno-gold labeling

Equal numbers of cells grown on YESCA plates at 26°C for 40 hours were suspended in 1X PBS (pH 7.4). A 20 μL drop of cell suspension was placed on a piece of parafilm and a 200 mesh Formvar-coated grid (Ernest F. Fullam, Inc., NY) was floated on the drop for 2 minutes. The grid was transferred to a 20 μL drop of 1X PBS for an additional 2 minutes before being stained on a drop of freshly prepared 0.5% uranyl acetete (Chapman et al., 2002). Bacteria were observed using a Phillips CM12 scanning transmission electron microscope. Immuno-staining of samples was performed essentially as previously described,

with some modifications (Sauvonnet et al., 2000). Briefly, grids with cells bound as described above were subjected to sequential incubation with the following solutions (20 μL of each solution at room temperature unless noted otherwise): 1% BSA-1X PBS (5 minutes), one of the following antibody solutions (as indicated in the results): 1/500 α-CsgG-0.1% BSA-1X PBS, 1/200 α-CsgA-0.1% BSA-1X PBS, 1/200 α-CsgB-0.1% BSA-1X PBS (60 minuets at 37°C), 0.1% BSA/1X PBS (3 times, 2 minutes each wash), 1/15 α-Rabbit IgG-10nm gold particles (Sigma, MO)-1% BSA/1X PBS (30 minutes at 37°C), and 0.1% BSA/1X PBS (3 times, 2 minutes each wash). Preparations were then fixed with 1% gluteraldehyde/1X PBS (5 minutes) and washed twice with sterile filtered water (5 minutes each wash). Grids were stained with 0.5% uranyl acetate and viewed with a transmission electron microscope.

Cell fractionation, gel electrophoresis, immunoblotting

Cell-free suspensions were generated by passing cells twice through a French press at 14,000-psi, followed by centrifugation at 3000g for 15 minutes to remove unbroken cells. Proteins in the cell free suspensions were solubilized with 0.5% Elugent (Calbiochem, Darmstadt, Germany). Cells were also fractionated by detergent extraction into soluble, inner and outer membrane fractions exactly as previously described (Robinson et al., 2006). Elugent-soluble proteins from the sarkosyl-insoluble outer membrane fraction or the cell-free suspension were suspended in loading buffer containing 1.5% SDS and resolved by 5% stacking/13% or 8% resolving discontinuous SDS-PAGE. Blots were probed with α-CsgG antibodies diluted 1/100,000 in 1% milk-1%BSA-1X TBST as described

(Robinson et al., 2006). Antibodies were removed from blots and reprobed for different antigens by the method described previously (Kayed et al., 2003).

Intact cell dot blotting

Cells were collected off YESCA plates, suspended in 20 mM Tris·HCl (pH 8) and left unperturbed or sonicated for 30 seconds before spotting unto a nitrocellulose membrane. Blots were air dried for 15 minutes before blocking with 1% milk-1% BSA-1X TBST on a shaker for 2 hours at room temperature (RT) or overnight at 4°C. Blots were probed with α-CsgG antibody diluted 1/100,000 in 1% milk-1% BSA-1X TBST (Robinson et al., 2006), α-DsbA antibody diluted 1/3500 in 3% milk-1X TBST (gift of J. Bardwell), α-CsgA antibody diluted 1/5000 in 1% milk-1% BSA-1X TBST (Chapman et al., 2002), α-CsgB antibody diluted 1/500 in 1% milk-1% BSA-1X TBST (Hammer et al., 2007), or commercially available α-hexahistidine antibodies (Covance, NJ) diluted 1/5000 in 1% milk-1% BSA-1X TBST for 1 hour at RT and washed three times (five minutes each) in 1X TBST. Next, blots were probed with goat α-rabbit antibodies conjugated to horseradish peroxidase (Sigma, MO) diluted with 1% milk-1% BSA-1X TBST for 1 hour at RT and washed three times (five minutes each) in 1X TBST.

Figure Legends

Figure 3.1. Curli fibers are non-uniformly distributed on curli-producing cells. Negatively-stained electron micrographs of MC4100 (WT) cells showing the typical asymmetric display of curli fibers or absence of fibers on some cells. Scale bars equal 500 nm.

Figure 3.2. CsgG is exposed to the cell surface. WT, *csgG*, and *csgG* containing plasmids encoding CsgG (*csgG*/pMC1) or CsgG with a C-terminal hexahistidine epitope (*csgG*/pMC2) were grown on YESCA plates for 48 hours at 26°C. Equal numbers of intact or sonicated cells, as indicated, were spotted onto a nitrocellulose membrane before probing with α-CsgG, α-DsbA, or α-hexahistidine epitope antibodies.

Figure 3.3. CsgG is spatially restricted in the outer membrane. (A) Typical images of cells obtained after α-CsgG indirect immunofluorescence staining of WT or **(B)** the isogenic *csgG* mutant. Shown are merged images of cells probed with rabbit α-CsgG primary antibody and goat α-rabbit secondary antibody conjugated to Alexa488 (green) and DAPI-stained nucleoid (blue). Scale bars equal 12.5μm. Quantification of the immuno-fluorescecent foci is presented in Figure 4B (see text). **(C - D)** Typical TEM images obtained after indirect immunogold labeling with 10-nm gold particles of WT cells probed with **(C)** α-CsgG antibodies or **(D)** without primary antibody, as described in the Materials and Methods. Cells were grown on YESCA plates at 26°C for 40 hours to induce curli expression. Scale bars equal 200 nm.

Figure 3.4. Spatial restriction of CsgG requires other *csg*-encoded proteins **(A)** Typical images obtained after α-CsgG IFM staining of *csgE*, *csgF*, *csgB*, or *csgA* cells grown on YESCA plates for 40 hours at 26°C. Shown are merged images of cells stained with DAPI (blue) and Alexa488 α-CsgG signal (green), although no cell-associated Alexa488 signal is evident. Scale bars are equal to

12.5μm. **(B)** Quantification of cell-associated foci after IFM staining. Percent of cells with α-CsgG immunofluorescence stain was determined in WT (1191 cells examined), *csgG* (G-; 528 cells examined), *csgE* (E-; 553 cells examined), *csgF* (F-; 567 cells examined), *csgB* (B-; 549 cells examined), or *csgA* (A-; 329 cells examined) cells by counting the percentage of DAPI stained cells colocalized with Alexa488 punctate dots. The standard error of the mean of three independent experiments is indicated above each bar in the graph. **(C)** WT or *csgE* cells were grown on YESCA plates for 48 hours at 26°C and cell fractions were prepared as described in the Materials and Methods. Equal proportions of fractions containing whole cells (lane 1), high-speed supernatants containing cytosol and periplasm (lane 2), inner and outer membranes (lane 3), sarkosyl soluble inner membranes (lane 4) or sarkosyl insoluble outer membranes (lane 5) were resolved by SDS-PAGE before western blotting with α-CsgG antibodies. Similar results were seen for all *csg* mutant strains examined (data not shown). **(D)** WT, *csgG*, *csgE, csgF*, *csgB*, *csgA*, or *csgA-G*/pMC1 were grown on YESCA plates for 48 hours at 26°C, before an equal number of cells was spotted onto a nitrocellulose membrane and probed with α-CsgG antibodies, as indicated. **(E)** Typical TEM image obtained after indirect immunogold labeling with 10-nm gold particles of *csgA* cells probed with α-CsgG antibodies as described in the Materials and Methods. Cells were grown on YESCA plates at 26°C for 40 hours to induce expression of *csgB* and *csgDEFG* operons. Similar results were obtained with other *csg* mutant strains tested (see Results). Scale bar equals 200 nm.

Figure 3.5. CsgG forms a detergent-stable high molecular weight multimer. **(A - B)** MC4100 (WT) or isogenic mutant strains *csgG*, *csgE*, *csgF*, *csgA*, *csgB* were grown on YESCA plates for 40 hours at 26°C and cells-free suspension was generated as described in the Materials and Methods. Proteins were solubilized in 0.5% Elugent prior to being resuspended in 1X SDS-loading buffer with 2-mercaptoethanol. Samples were incubated for 10 minutes at RT (lanes 1, 5, 6, and 10), 37°C (lanes 2, 7, and 11), 55°C (lanes 3, 8, and 12), or 95°C (lanes 4, 9, and 13) and electrophoresed by 5%-8% discontinuous SDS-PAGE. The gel was transferred to PVDF membrane and probed with α-CsgG antibodies.

Figure 3.6. Fiber polymerization is required for CsgG clustering. (A) Diagram of CsgA functional domains showing the N-terminal CsgG-secretion signal (blue) and the 5 amyloid domains, R1 – R5. **(B)** Diagram of CsgA-ΔR1, which lacks the first of 5 amyloid domains **(C - D)** Typical TEM images obtained after indirect immunogold labeling with 10-nm gold particles of *csgA* cells expressing CsgA (panel **C**) or CsgA-ΔR1 (panel **D**) probed with α-CsgG antibodies as described in the Materials and Methods. Cells were grown on YESCA plates at 26°C for 40 hours to induce expression of *csgB* and *csgDEFG* operons. Inset shows images obtained after α-CsgG IFM staining of *csgA*/pCsgA (579 cells examined) or *csgA*/pCsgA-ΔR1 cells (567 cells examined), as indicated, grown on YESCA plates for 46 hours at 26°C. Shown are merged images of cells stained with DAPI (blue) and Alexa488 α-CsgG signal (green). The percentage of cells examined which contained α-CsgG foci in each strain are indicated.

Figure 3.7. CsgG foci are present in aggregated and non-aggregated cells. Unmerged IFM images of WT cells stained with α-CsgG antibody and α-rabbit-Alexa488. Panel **A** shows the Alexa488 signal, panel **B** is DAPI signal, and panel **C** is a corresponding differential interference contrast (DIC) image. Panel **D** is an overlay of the Alexa488 (green) and DAPI (blue) signals. Scale bars on all images are equal to 12.5μm.

Figure 3.8. CsgG overexpression is not sufficient to restore high molecular weight species in absence of *csg*-encoded proteins.
(A) CFS from WT or *csgA-G*/pMC1 was generated as described in the Materials and Methods. Samples were incubated for 10 minutes at RT (lanes 1 and 6), 37°C (lanes 2 and 7), 42°C (lanes 3 and 8), 55°C (lanes 4 and 9), or 75°C (lanes 5 and 10), then electrophoresed by 5%-8% discontinues SDS-PAGE. Gel was transferred to PVDF membrane and blotted with α-CsgG antibodies. **(B)** CFS from WT or WT/pMC1 were prepared and samples were incubated at the following temperatures before resolving by 5%-8% discontinuous SDS-PAGE: RT (lanes 1 and 4), 42°C (lanes 2 and 5), or 95°C (lanes 3 and 6). Resolved proteins were transferred to PVDF membrane and blotted with α-CsgG antibodies

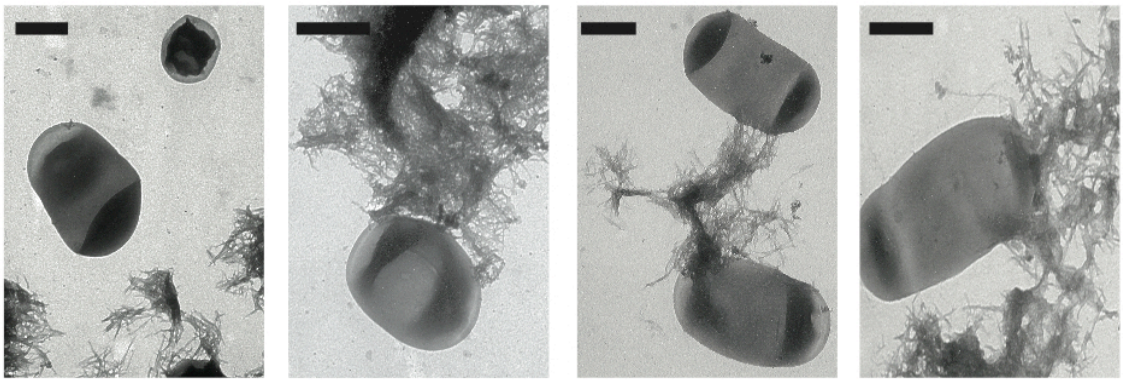

Figure 3.1. Curli fibers are non-uniformly distributed on curli-producing cells.

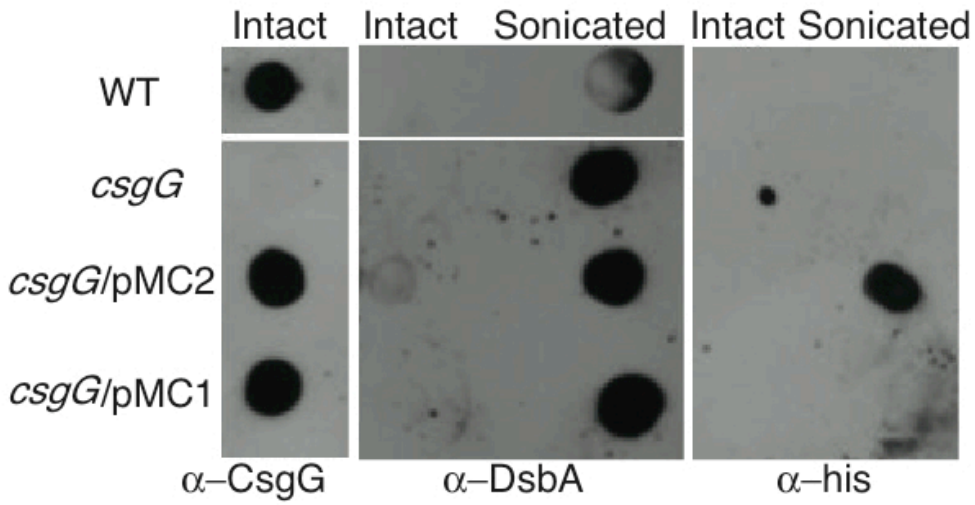

Figure 3.2. CsgG is exposed to the cell surface.

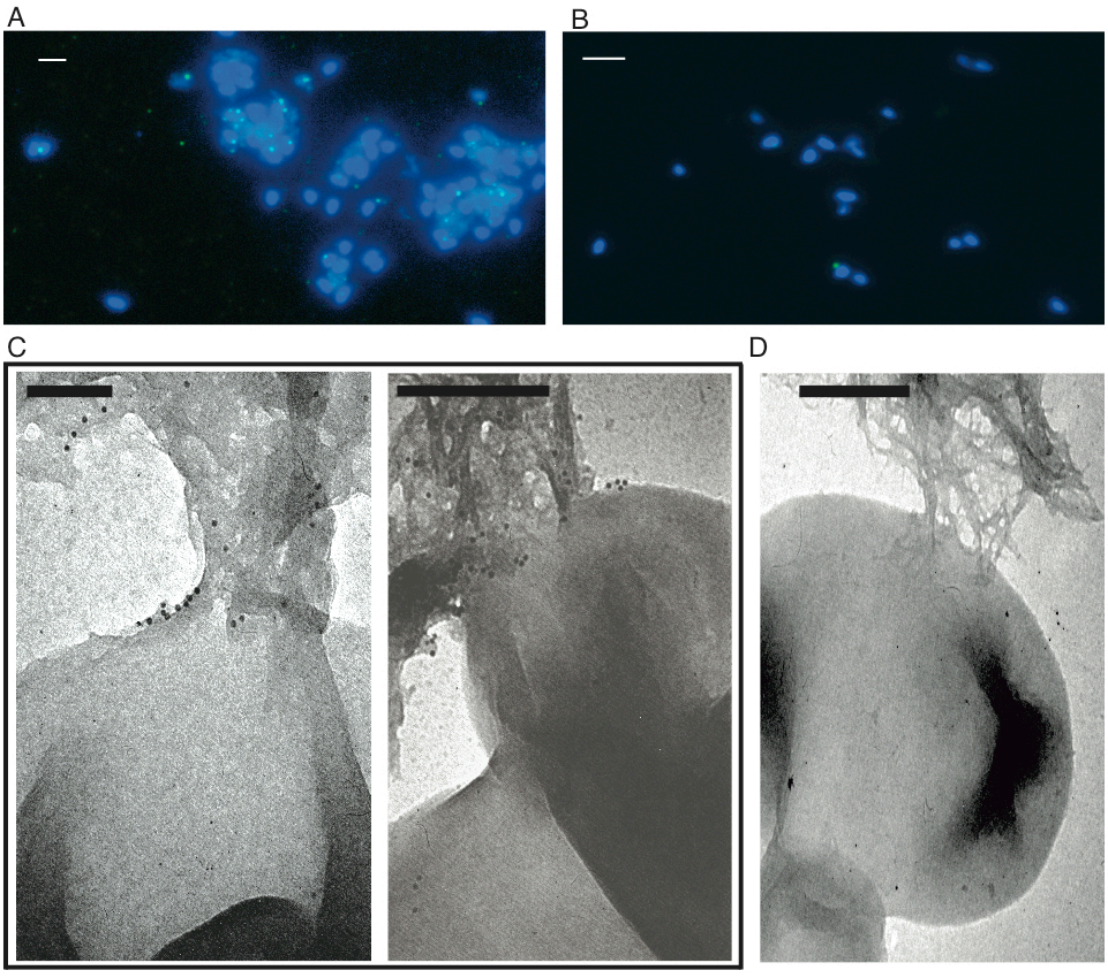

Figure 3.3. CsgG is spatially restricted in the outer membrane.

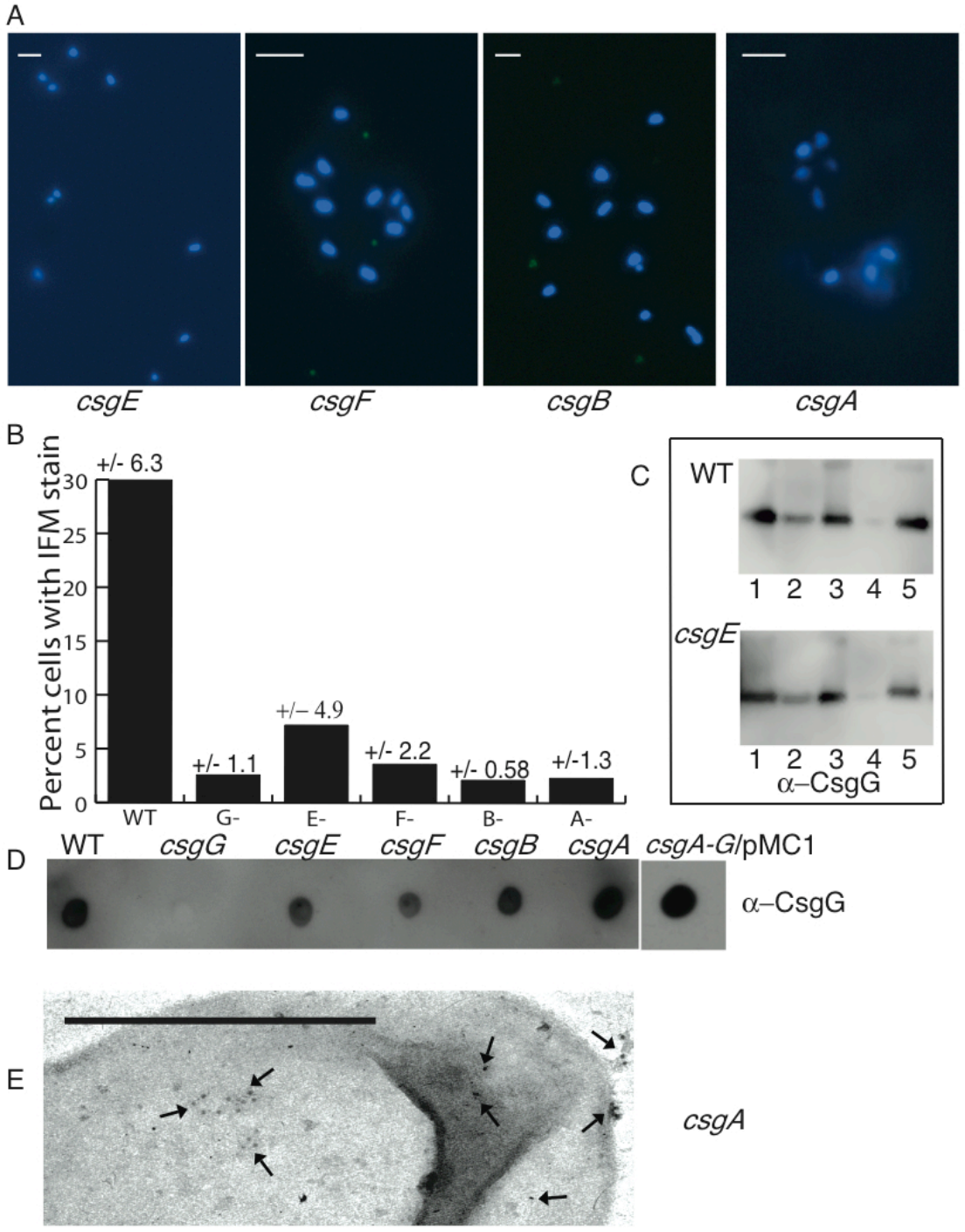

Figure 3.4. Spatial restriction of CsgG requires other *csg*-encoded protein

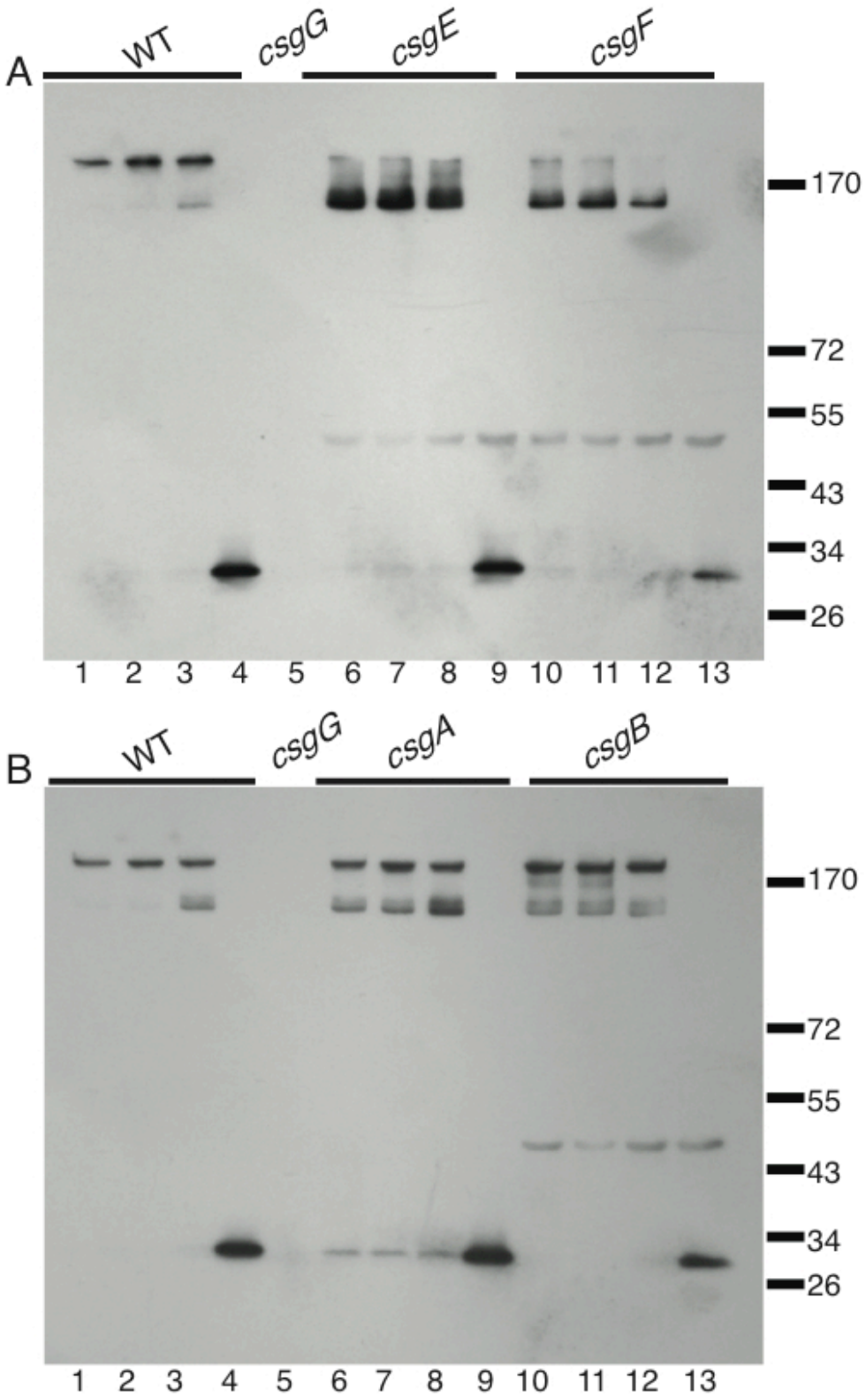

Figure 3.5. CsgG forms a detergent-stable high molecular weight multimer.

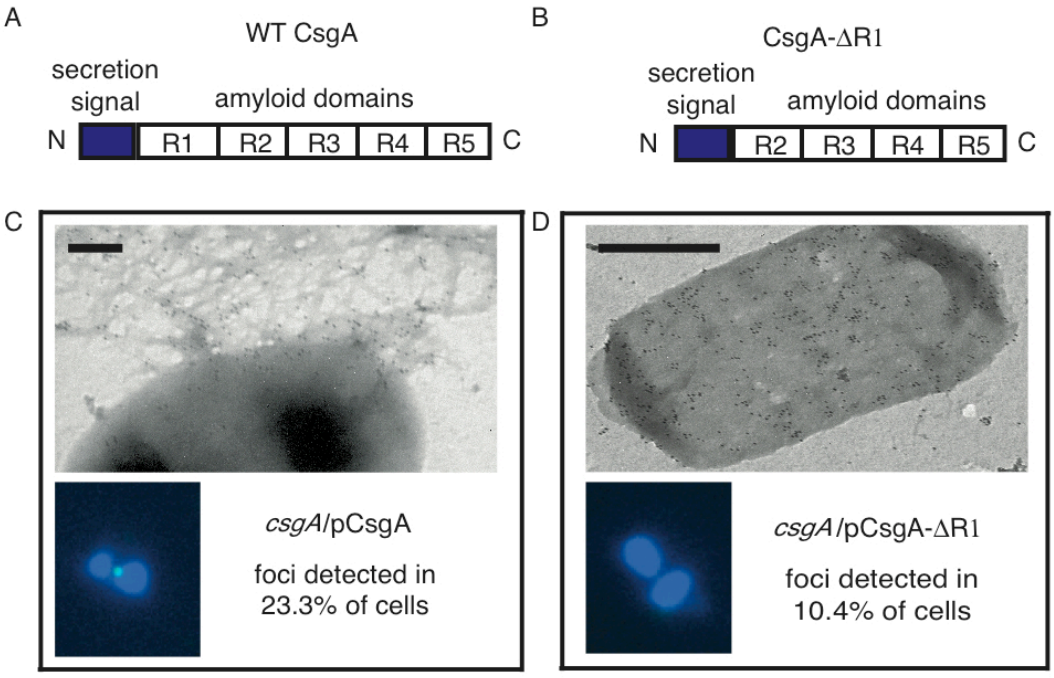

Figure 3.6. Fiber polymerization is required for CsgG clustering.

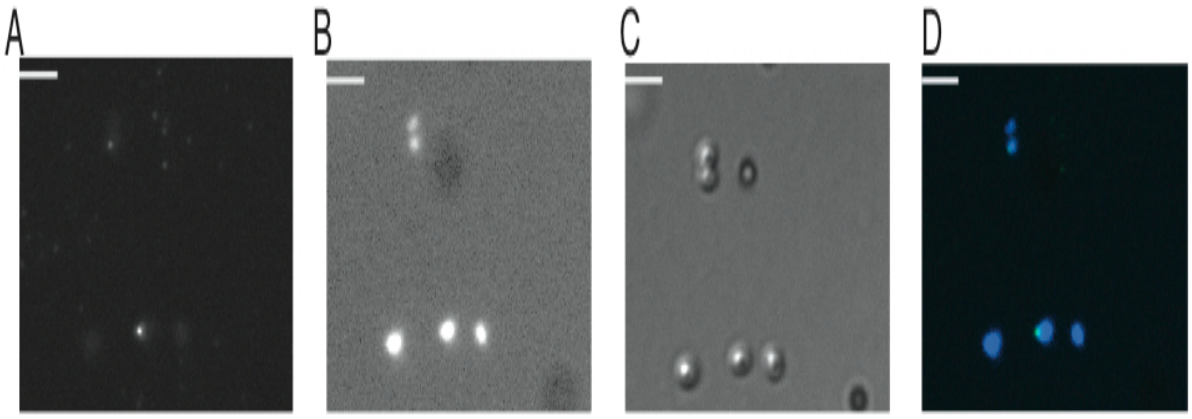

Figure 3.7. CsgG foci are present in aggregated and non-aggregated cells.

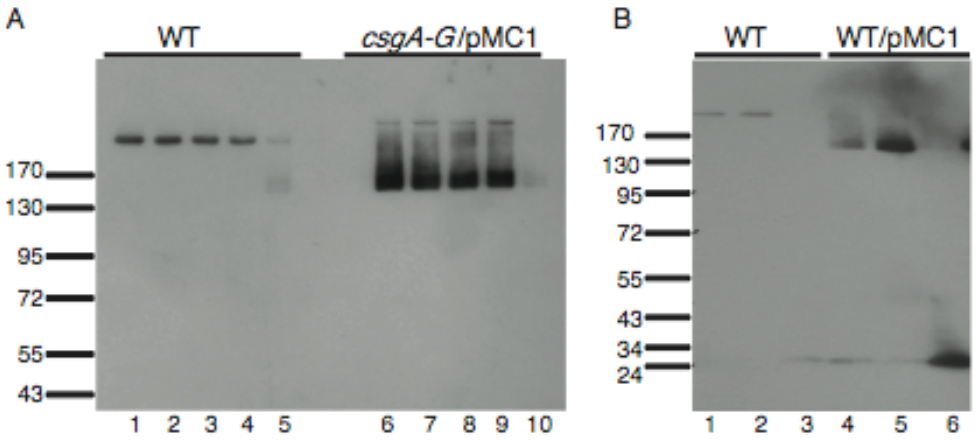

Figure 3.8. CsgG overexpression is not sufficient to restore high molecular weight species in absence of *csg*-encoded proteins.

Strain or Plasmid	Relevant characteristics	Source
MC4100	F-*ara*D139 Δ(*argF-lac*)U169 *rsp*L150(s*trR*) *rel*A1*flb*B5301 *deo*C1 *pts*F25 *rbs*R	Casadaban (1976)
LSR1	MC4100*csgG::Tn105*	Robinson et al. (2006)
LSR10	MC4100::Δ*csgA*	Chapman et al. (2002)
MHR261	MC4100::Δ*csgB*	Hammar et al. (1996)
MHR592	MC4100::Δ*csgF*	Chapman et al. (2002)
MHR480	MC4100::Δ*csgE*	Chapman et al. (2002)
LSR11	MC4100::Δ*csgBACcsgDEFG*	Robinson et al. (2006)
pTrc99A	Expression vector	Pharmacia Biotech
pMC1	*csgG* cloned into pTrc99A	Chapman et al. (2002)
pMC2	*csgG-6his* cloned into pTrc99A.	Robinson et al. (2006)
pHL3	Expression vector	Chapman et al. (2002)
pCsgA	*csgA-6his* cloned into pHL3	Wang et al. (2008)
pCsgA-ΔR1	*csgA-ΔR1-6his* cloned into pHL3	Wang et al. (2008)

Table 3.1: Strains and plasmids used in this study.

References

Arnqvist, A., Olsen, A., Pfeifer, J., Russell, D.G., and Normark, S. (1992) The Crl protein activates cryptic genes for curli formation and fibronectin binding in *Escherichia coli* HB101. *Mol Microbiol* **6**: 2443-2452.

Bian, Z., Brauner, A., Li, Y., and Normark, S. (2000) Expression of and cytokine activation by Escherichia coli curli fibers in human sepsis. *J Infect Dis* **181**: 602-612.

Bian, Z., and Normark, S. (1997) Nucleator function of CsgB for the assembly of adhesive surface organelles in Escherichia coli. *EMBO J* **16**: 5827-5836.

Brandon, L.D., Goehring, N., Janakiraman, A., Yan, A.W., Wu, T., Beckwith, J., and Goldberg, M.B. (2003) IcsA, a polarly localized autotransporter with an atypical signal peptide, uses the Sec apparatus for secretion, although the Sec apparatus is circumferentially distributed. *Mol Microbiol* **50**: 45-60.

Buddelmeijer, N., Aarsman, M.E., Kolk, A.H., Vicente, M., and Nanninga, N. (1998) Localization of cell division protein FtsQ by immunofluorescence microscopy in dividing and nondividing cells of Escherichia coli. *J Bacteriol* **180**: 6107-6116.

Campo, N., Tjalsma, H., Buist, G., Stepniak, D., Meijer, M., Veenhuis, M., Westermann, M., Muller, J.P., Bron, S., Kok, J., Kuipers, O.P., and Jongbloed, J.D. (2004) Subcellular sites for bacterial protein export. *Mol Microbiol* **53**: 1583-1599.

Chapman, M.R., Robinson, L.S., Pinkner, J.S., Roth, R., Heuser, J., Hammar, M., Normark, S., and Hultgren, S.J. (2002) Role of *Escherichia coli* curli operons in directing amyloid fiber formation. *Science* **295**: 851-855.

Collinson, S.K., Clouthier, S.C., Doran, J.L., Banser, P.A., and Kay, W.W. (1996) Salmonella enteritidis agfBAC operon encoding thin, aggregative fimbriae. *J Bacteriol* **178**: 662-667.

Dong, C., Beis, K., Nesper, J., Brunkan-Lamontagne, A.L., Clarke, B.R., Whitfield, C., and Naismith, J.H. (2006) Wza the translocon for E. coli capsular polysaccharides defines a new class of membrane protein. *Nature* **444**: 226-229.

Drummelsmith, J., and Whitfield, C. (2000) Translocation of group 1 capsular polysaccharide to the surface of Escherichia coli requires a multimeric complex in the outer membrane. *EMBO J* **19**: 57-66.

Fowler, D.M., Koulov, A.V., Balch, W.E., and Kelly, J.W. (2007) Functional amyloid--from bacteria to humans. *Trends Biochem Sci* **32**: 217-224.

Gibson, D.L., White, A.P., Rajotte, C.M., and Kay, W.W. (2007) AgfC and AgfE facilitate extracellular thin aggregative fimbriae synthesis in Salmonella Enteritidis. *Microbiology* **153**: 1131-1140.

Hammar, M., Arnqvist, A., Bian, Z., Olsen, A., and Normark, S. (1995) Expression of two csg operons is required for production of fibronectin- and congo red-binding curli polymers in Escherichia coli K-12. *Mol Microbiol* **18**: 661-670.

Hammar, M., Bian, Z., and Normark, S. (1996) Nucleator-dependent intercellular assembly of adhesive curli organelles in Escherichia coli. *Proc Natl Acad Sci U S A* **93**: 6562-6566.

Hammer, N.D., Schmidt, J.C., and Chapman, M.R. (2007) The curli nucleator protein, CsgB, contains an amyloidogenic domain that directs CsgA polymerization. *Proc Natl Acad Sci U S A* **104**: 12494-12499.

Hardie, K.R., Lory, S., and Pugsley, A.P. (1996) Insertion of an outer membrane protein in Escherichia coli requires a chaperone-like protein. *EMBO J* **15**: 978-988.

Herwald, H., Morgelin, M., Olsen, A., Rhen, M., Dahlback, B., Muller-Esterl, W., and
Bjorck, L. (1998) Activation of the contact-phase system on bacterial surfaces--a clue to serious complications in infectious diseases. *Nat Med* **4**: 298-302.

Hwang, J., Bieber, D., Ramer, S.W., Wu, C.Y., and Schoolnik, G.K. (2003) Structural and topographical studies of the type IV bundle-forming pilus assembly complex of enteropathogenic Escherichia coli. *J Bacteriol* **185**: 6695-6701.

Kayed, R., Head, E., Thompson, J.L., McIntire, T.M., Milton, S.C., Cotman, C.W., and Glabe, C.G. (2003) Common structure of soluble amyloid oligomers implies common mechanism of pathogenesis. *Science* **300**: 486-489.

Loferer, H., Hammar, M., and Normark, S. (1997) Availability of the fibre subunit CsgA and the nucleator protein CsgB during assembly of fibronectin-binding curli is limited by the intracellular concentration of the novel lipoprotein CsgG. *Mol Microbiol* **26**: 11-23.

Maddock, J.R., and Shapiro, L. (1993) Polar location of the chemoreceptor complex in the Escherichia coli cell. *Science* **259**: 1717-1723.

Nudleman, E., Wall, D., and Kaiser, D. (2006) Polar assembly of the type IV pilus secretin in Myxococcus xanthus. *Mol Microbiol* **60**: 16-29.

Olsen, A., Jonsson, A., and Normark, S. (1989) Fibronectin binding mediated by a novel class of surface organelles on Escherichia coli. *Nature* **338**: 652-655.

Olsen, A., Wick, M.J., Morgelin, M., and Bjorck, L. (1998) Curli, fibrous surface proteins of Escherichia coli, interact with major histocompatibility complex class I molecules. *Infect Immun* **66**: 944-949.

Prigent-Combaret, C., Prensier, G., Le Thi, T.T., Vidal, O., Lejeune, P., and Dorel, C. (2000) Developmental pathway for biofilm formation in curli-producing Escherichia coli strains: role of flagella, curli and colanic acid. *Environ Microbiol* **2**: 450-464.

Reithmeier, R.A., and Bragg, P.D. (1974) Purification and characterization of heat-modifiable protein from the outer membrane of Escherichia coli. *FEBS Lett* **41**: 195-198.

Robinson, L.S., Ashman, E.M., Hultgren, S.J., and Chapman, M.R. (2006) Secretion of curli fibre subunits is mediated by the outer membrane-localized CsgG protein. *Mol Microbiol* **59**: 870-881.

Rosch, J.W., and Caparon, M.G. (2005) The ExPortal: an organelle dedicated to the biogenesis of secreted proteins in Streptococcus pyogenes. *Mol Microbiol* **58**: 959-968.

Sauvonnet, N., Gounon, P., and Pugsley, A.P. (2000) PpdD type IV pilin of Escherichia coli K-12 can Be assembled into pili in Pseudomonas aeruginosa. *J Bacteriol* **182**: 848-854.

Wang, X., Hammer, N.D., and Chapman, M.R. (2008) The molecular basis of functional bacterial amyloid polymerization and nucleation. *J Biol Chem* **283**: 21530-21539.

Wang, X., Smith, D.R., Jones, J.W., and Chapman, M.R. (2007) In vitro polymerization of a functional Escherichia coli amyloid protein. *J Biol Chem* **282**: 3713-3719.

Chapter IV

The curlin secretion specificity factor CsgE prevents amyloid fiber polymerization

Abstract

Curli are extracellular amyloid fibers produced by *Escherichia coli* that are critical for biofilm formation, host cell interactions, and adhesion to abiotic surfaces. CsgA and CsgB are the major and minor curli subunit proteins, respectively, while CsgE, CsgF, and CsgG participate in the assembly of subunits into fibers. Both the secretion and the stability of curli subunits are dependent upon the small accessory protein CsgE and the outer membrane lipoprotein CsgG. In this investigation we identified functional interactions between CsgE and CsgG in curli subunit secretion. CsgE was found to be completely dispensable for subunit secretion and curli assembly when CsgG was overexpressed in *csgE* mutant cells. When then N-terminus of CsgA was fused to the unrelated periplasmic protein CpxP, CsgG overexpression was sufficient for secretion of the fusion protein, A22-P, into the supernatant. However, wild type (WT) CpxP was also secreted in a CsgG-dependent manner. Coexpression of CsgE along with CsgG had no effect on A22-P secretion but completely blocked the secretion of WT CpxP. When CsgG was expressed at low levels, CsgE drastically augmented the secretion of A22-P. Previous studies indicated that CsgG rendered *E. coli* sensitive to erythromycin. Coexpression of CsgE with CsgG restored

erythromycin resistance, demonstrating that CsgE modifies the putative pore characteristics of CsgG. Taken collectively these data indicate that CsgE interacts with CsgG to enhance its ability to specifically secrete the curli fiber subunits. Finally, using purified proteins, we found that CsgE prohibited the self-assembly of CsgA into amyloid fibers. These results suggest that subunit secretion and fiber polymerization are highly ordered, yet linked, processes.

Introduction

Curli represent a novel class of bacterial surface fibers that are produced by enteric bacteria such as *Escherichia*, *Salmonella*, and *Citrobacter* (Zogaj et al., 2003). Curli promote biofilm formation (Vidal et al., 1998) bind a variety of host proteins including fibronectin and MHC class I molecules (Olsen et al., 1989, Olsen et al., 1998), and induce bacterial internalization by eukaryotic cells (Gophna et al., 2001; Gophna et al., 2002). The biochemical and structural properties of curli are shared with disease-associated fibers called amyloids. Amyloids are characterized as unusually stable β-sheet rich fibrous protein aggregates that bind to Congo red and thioflavin T. Unlike disease-associated amyloid formation, curli assembly is regulated by a dedicated biosynthesis pathway. Because protein misfolding and amyloid formation are associated with several intractable human diseases such as Alzheimer's, Parkinson's, and Huntington's, elucidation of the details of curli biogenesis may provide highly relevant insight into how cells control amyloid formation.

The curli proteins are expressed from the divergently transcribed *csgBAC* and *csgDEFG* operons (Hammar et al., 1995). CsgA, the major fiber subunit,

interacts with the CsgB nucleator protein and polymerizes into a highly insoluble and aggregative amyloid fiber at the cell surface. The transcriptional activator CsgD is required for expression of the *csgBAC* operon, while CsgE, CsgF, and CsgG comprise the curli secretion and assembly machinery. The curli assembly machine functions to secrete soluble CsgA and CsgB, presumably minimizing the toxic effects of amyloidogenesis by restricting curli amyloid formation to the extracellular milieu. However, the mechanism(s) by which the cell prevents internal assembly of curli amyloid fiber has remained elusive.

The 30 kDa lipoprotein CsgG localizes to the outer membrane (OM) and is absolutely required for curli synthesis and subunit stability (Robinson et al., 2006). CsgG has domains in the periplasm as well as on the cell surface, and is spatially clustered around the base of curli fibers (Epstein, 2008 submitted). Consistent with its proposed role as a secretion channel, CsgG forms an SDS-resistant pore-like multimer at the outer membrane and interacts with CsgE, CsgF, and the mature N-terminus of the fiber subunit CsgA (Robinson et al., 2006; Epstein submitted). CsgE and CsgF are small, chaperone-like proteins that may modulate the secretion activity of CsgG. CsgF is a surface-exposed protein that also requires CsgG for its stability and surface localization. Functionally, CsgF is critical for CsgB-mediated nucleation and acts negatively on CsgA secretion (Chapman et al., 2002). The role of CsgE in curli assembly is unclear, although cells lacking *csgE* display phenotypes very similar to *csgG* strains (Chapman et al., 2002).

Like *csgG* cells, deletion of *csgE* results in nearly undetectable levels of the curli subunits, CsgA and CsgB, and also of CsgF (Chapman et al., 2002;

Nenninger submitted). Importantly, CsgG stability and localization to the outer membrane is unaffected in *csgE* cells (Epstein 2008, submitted). Unlike *csgG* strains, *csgE* can assemble a few curli fibers (Chapman et al., 2002). However, the morphology of *csgE* fibers is distinct, with an increased curvature compared to WT curli, which appear straight and rigid (Chapman et al., 2002).

Since the *csgG* and *csgE* phenotypes closely resemble each other, we investigated the role of CsgE in CsgG-mediated secretion. In this work we show that CsgE and CsgG function to in the same pathway in supporting the stability and secretion of CsgA, CsgB and CsgF. We found that CsgG overexpression suppresses the phenotypes of a *csgE* mutant. Also, we show that CsgE modulates the pore-like properties of CsgG and acts as a specificity factor in CsgG-mediated secretion. Finally, we found that CsgE can inhibit the polymerization of purified CsgA into fibers, suggesting a model for how the cell can prohibit intercellular amyloid formation and ensure that secretion of soluble subunits precedes polymerization.

Results

csgE *phenotypes are suppressed by CsgG overexpression*

The phenotypes of cells lacking CsgE or CsgG are remarkably similar. Both strains fail to secrete or assemble curli fibers and are drastically depleted in CsgA, CsgB, and CsgF. Previously, however, we showed that CsgG overexpression alone is sufficient to mediate the secretion of CsgA into culture supernatants and CsgF to the cell surface (Robinson et al., 2006; Nenninger submitted). CsgG is limiting for curlin stability and secretion (Loferer et al., 1997).

Therefore, we examined the possibility that CsgG overexpression alleviates the requirement for CsgE in fiber subunit secretion. To test this hypothesis, the *csgE* mutant was transformed with plasmids that express CsgG at high levels or low levels (pMC1 or pLR93, respectively; see Table 4.1) and streaked on YESCA plates to induce the expression of the *csg* operons. Plates were supplemented with the amyloid-binding dye Congo red (CR) to monitor curli production. As shown in Figure 1A, overexpression of CsgG from pMC1 restored WT levels of CR binding to the *csgE* cells. When *csgG* was expressed from a low copy plasmid (pLR93), little CR binding was observed. CsgF was unable to suppress the *csgE* mutant when expressed either at low or high levels.

To confirm that the CR binding observed when CsgG was overexpressed was due to curli production, Western blot analysis of whole cell lysates was performed using CsgA- and CsgB-specific antisera. Lysates prepared from *csgE* cells overexpressing CsgG contained WT levels of both CsgA and CsgB (Figure 1B). Thus, CsgE is dispensable for curli stability and secretion when CsgG is overexpressed in the presence of other *csg*-encoded proteins, and also suggests that CsgE aids the secretion of CsgB and CsgA.

CsgF is a cell-surface assembly factor that is required for CsgB nucleation activity, although it is not currently thought to be a component of the fiber. CsgF stability is dependent on CsgE and CsgG. Therefore, we next tested if CsgF stability and surface exposure could be restored to *csgE* cells overexpressing CsgG. Fig. 4.1C shows that CsgF stability is restored in *csgE* cells when the cell contained plasmids encoding *csgE* or *csgG*. Surface exposed CsgF is susceptible to degradation by proteins K (PK). *E. coli csgE* mutants containing

plasmids encoding either *csgE* or *csgG* produce PK-sensitive CsgF (Fig. 4.1D), demonstrating that CsgF is both stable and surface exposed in both strains. Therefore, CsgE is dispensable for stability or secretion of CsgA, CsgB, or CsgF in conditions when CsgG is in excess.

CsgE blocks non-specific CsgG-mediated secretion

Examination of the concerted roles of CsgE and CsgG in CsgA secretion is complicated since CsgA is undetectable in strains lacking either of these proteins. Therefore, we developed CsgG-secreted chimeric proteins that remain detectable in the absence of CsgG or CsgE to allow us to study CsgG-mediated secretion. We previously demonstrated that a fusion protein containing the N-terminal 22 residues of mature CsgA specifically interacts with CsgG (Robinson et al., 2006). However, unlike WT CsgA, this CsgA-PhoA fusion protein is not secreted into the culture supernatant, possibly because it is too large to pass the curli subunit secretion apparatus. To test the hypothesis that the N-terminal 22 residues of CsgA are sufficient for extracellular secretion, we fused these residues to the mature N-terminus of the periplasmic protein CpxP to yield the chimera A22-P. CpxP is approximately 17 kDa, the same size as CsgA. Coexpression of CsgG and A22-P resulted in the secretion of the fusion protein (Fig. 4.2A, lanes 4 and 8). No A22-P secretion was observed in the absence of CsgG (Fig. 4.2A lane 7). Surprisingly, WT CpxP was also released into culture supernatants when CsgG was co-expressed (Fig. 4.2A lane 6), indicating that the N-terminal 22 residues of CsgA were unnecessary for secretion of CpxP when CsgG was expressed at high levels. This may indicate that the CsgG translocon

is an ungated pore under these experimental conditions. The idea that overexpressed CsgG forms an ungated pore is consistent with the previous observation that CsgG overexpression renders cells sensitive to the antibiotic erythromycin (Robinson et al., 2006).

Since CsgE had been shown to interact with CsgG and function at the step of secretion (Chapman et al., 2002; Robinson et al., 2006), we determined whether the addition of CsgE altered the secretion profiles described above. Both the chimera *A22-P* and the *cpxP* open reading frames were cloned downstream of *csgG* in pTRC99A, creating artificial operons that allowed the expression of both proteins from the *trc* promoter. When CsgE was coexpressed with A22-P and CsgG, no difference in A22-P secretion was observed (Fig 2B; compare lanes 5 and 6). However, addition of CsgE to cells expressing CpxP and CsgG abolished CpxP secretion (Fig. 4.2B lane 8), indicating that CsgE can inhibit the secretion of non-curli subunit proteins from the curli translocon.

CsgE confers erythromycin resistance to cells overexpressing CsgG

Antibiotic sensitivity assays demonstrated that overexpression of CsgG in *E. coli* results in susceptibility to erythromycin but not vancomycin (Robinson et al., 2006). Our observation that CsgE expression prevented CsgG-mediated CpxP secretion suggested that CsgE might gate the CsgG pore. To determine whether CsgE affects CsgG-dependent erythromycin sensitivity, CsgG was coexpressed with *csgE*. As seen in Figure 3, CsgE significantly increased the growth rate of bacteria overexpressing CsgG in the presence of erythromycin. CsgG has been demonstrated to co-immunoprecipitate with CsgE and CsgF.

One possibility is that the coexpression of either CsgG-interacting protein would confer resistance to erythromycin. CsgF had no effect on erythromycin sensitivity (Fig. 4.3, diamonds). We also tested the ability of cells coexpressing CsgG, CsgE and CsgF to grow in the presence of erythromycin. These cells exhibited a severe growth defect in the presence of erythromycin (data not shown), suggesting that the CsgG pore is in an open state in these conditions.

CsgE and CsgF modulate secretion of A22-P

CsgE is essential for efficient curli assembly and subunit stability when CsgG is expressed from its WT promoter on the chromosome (Chapman et al., 2002; Robinson et al., 2006). However, CsgE was dispensable for secretion of A22-P when CsgG was overexpressed from pTrc99A. CsgG is most likely a limiting factor in the assembly and stability of curli, since increased CsgG expression in otherwise WT cells increases curli assembly and stability (Chapman et al., 2002; Hammer et al., 2007; Loferer et al., 1997; Robinson et al., 2006). To determine whether CsgE contributed to secretion efficiency when CsgG is limiting, we replaced the chromosomal *csgEF* locus with a kanamycin resistance cassette in strain MC4100. The resistance cassette was placed directly upstream of *csgG* in order to drive constitutive *csgG* expression from the chromosome. Low level expression of CsgG was confirmed by western blotting (data not shown) and the strain was transformed with pLR116 (A22-P in pTrc) and either a vector control (pBAD33) or pLR42 (*csgE* in pBAD33). Under these expression conditions, CsgE markedly increased the amount of secreted A22-P indicating that CsgE augments curli subunit secretion when CsgG is limiting (Fig

4, compare lanes 4 and 5). Interestingly, expression of CsgF appeared to inhibit A22-P secretion (Fig. 4.4, compare lanes 4 and 6). These results agree with the previously reported effects of CsgE or CsgF on CsgA stability (Chapman et al., 2002), suggesting that CsgE/CsgF mediated modulation of CsgA secretion occurs through CsgG and the N22 domain of CsgA.

CsgE inhibits self-assembly of CsgA amyloid fibers

The ability of cells expressing both CsgE and CsgG to grow in the presence of erythromycin suggested that CsgE may directly modulate the pore activity of CsgG, but the observation that CsgE increased A22-P secretion raised the possibility that CsgE may also act on CsgA during secretion. We were unable to detect interaction of CsgA or A22-P with CsgE by immunoprecipitation or far-western analysis (data not shown). Interestingly, the few curli fibers produced in *csgE* cells have an aberrant morphology and overexpression of CsgE in WT cells also changes the ultrastructural properties of curli (Chapman et al., 2002; Gibson et al., 2007; Chapman, unpublished observation). One outstanding question in the biosynthesis of curli fibers is how cells prevent amyloid formation on the periplasmic side of the curli assembly apparatus. Since CsgE appeared to modulate the ultrastructural properties of curli and play a role in curlin-specific secretion, we examined the effect of CsgE on polymerization of CsgA. CsgA is soluble and unstructured immediately following purification and after several hours begins to self-assemble into β-sheet rich amyloid fiber aggregates (Chapman et al., 2002). The polymerization of CsgA into fibers can be visualized by sampling CsgA at various time points and viewing these samples by electron

microscopy. The ability of the fibers to bind the amyloid-specific dye, thioflavin T (ThT) can also be used to follow CsgA polymerization over time. Freshly purified CsgA was incubated with or without purified CsgE as described in the Materials and Methods. As shown in Figure 5A, CsgA polymerized into 4- to 6-nm wide amyloid fibers after 24 hours. In contrast, CsgA that was incubated with CsgE failed to form aggregates (Fig. 4.5B). To quantify and monitor the CsgE-inhibition of CsgA polymerization, in vitro polymerization of CsgA fibers with or without CsgE was monitored by real-time ThT polymerization assay (Fig. 4.5C). In a reaction containing 25 μM CsgA, CsgA polymerization entered exponential growth after 270 minutes of incubation at room temperature. In contrast, a reaction containing 22.5 μM of CsgE with or without 25μM CsgA failed to increase ThT fluorescence even after 800 minutes incubation. These results indicate that CsgE can act directly upon CsgA and prevent the self-assembly of CsgA into amyloid fibers.

Discussion

In stark contrast to the disease-associated amyloidogenesis that underlies such neurodegenerative aliments like Alzeihmer's and Parkinson's disease, the assembly of curli fibers is accomplished in a directed manner without any associated toxicity. The curli secretion assembly machine guides the secretion of CsgA and CsgB across the outer membrane where the subunits interact and polymerize into curli amyloid fibers on the cell surface, and never in the periplasm (Chapman et al., 2002; Hammar et al., 1996; Hammer et al., 2007; Chapman, M.R., unpublished observation). In this study, we showed that a small,

CsgG-interacting protein, CsgE, modulates CsgG-mediated secretion. CsgE prevented non-specific secretion while augmenting the secretion of a molecule containing the curli secretion signal peptide. Finally, we found that CsgE can also work directly on CsgA by preventing the self-polymerization of CsgA into amyloid fibers.

Overexpression of the outer membrane lipoprotein CsgG is sufficient to mediate the secretion of the major curli subunit, CsgA, into culture supernatants (Robinson et al., 2006). The concentration of CsgG limits the stability of the curli fiber subunits and overexpression of CsgG increases the stability of CsgA, CsgB and CsgF (Loferer et al., 1997; Robinson et al., 2006; Nenninger 2008, submitted). CsgE is also required for CsgA, CsgB and CsgF stability and efficient curli assembly when CsgG was expressed from its native promoter on the chromosome (Chapman et al., 2002). We found that overexpression of CsgG in *csgE* cells restored stability and assembly of curli fibers and of CsgF surface exposure, suggesting that CsgE functions in the secretion pathway under conditions where CsgG is limiting. We previously demonstrated that overexpression of CsgG conferred erythromycin sensitivity to *E. coli*. This level of CsgG expression also allowed the escape of CpxP, a normally periplasmic protein, into the culture supernatant. Coexpression of CsgE restored erythromycin resistance and prevented the secretion of CpxP, suggesting that CsgE can gate the CsgG pore. Notably, coexpression of CsgE in this system did not prevent secretion of a chimera of CpxP and the CsgA signal peptide, the fusion protein A22-P. Further, under conditions where CsgG concentration was limiting, CsgE expression increased the secretion of A22-P into the culture

supernatant. These results support a model where CsgE gates the CsgG pore and prevents non-specific passage across the outer membrane while facilitating secretion of the curli subunits. The observation that CsgE blocks CsgG-dependent erythromycin sensitivity yet augments curli subunit secretion is not unprecedented. BiP, a chaperone of the eukaryotic endoplasmic reticulum (ER), functions both to assist the secretion of nascent peptides into the ER as well as to seal the luminal side of the translocon before and during translocation (Brodsky et al., 1995; Hamman et al., 1998).

The CsgG secretion protein is spatially restricted into concentrated microdomains along with curli fibers (Epstein 2008, submitted), suggesting that both fiber subunits are concentrated in a similar region of the cellular milleu. This observation raises the question of how the cell prevents polymerization of CsgA in the periplasm prior to secretion. We found that CsgE prevents the self-polymerization of purified CsgA into amyloid fibers. Taken collectively, our data supports a model where CsgE augments CsgA secretion out of cells while simultaneously preventing the aggregation of CsgA. This model suggests that CsgE ensures that secretion of soluble, non-amyloid CsgA precedes fiber formation, thereby preventing formation of periplamic amyloid fibers and abrogating intracellular amyloid toxicity. Future definition of the cross-talk between the activities of CsgE and CsgF will help to unlock the secretes of this unique biogenesis pathway.

Experimental Procedures

Experimental materials

Restriction enzymes, DNA polymerases, and DNA ligases were used in accordance with the manufacturers instructions (Sigma, New England Biolabs). Oligonucleotides were purchased from IDT. Antibiotics were from Sigma Chemical Company.

Bacterial Strains, Plasmids, and Antibodies

Strains, plasmids, and antibodies used in this study are described in Table 4.1.

Growth Conditions

Curli expression was induced by growing bacteria on YESCA agar (per liter: 10 g Casamino acids, 1 g yeast extract, 20 g agar) with or without 20 μg/ml Congo red for 48 hours at 26°C. Expression of pTrc derivatives was induced with 0.1mM IPTG in LB at 37°C shaking. pBAD33 derivatives were induced with 0.04% arabinose in LB shaking. For maintenance of plasmids, bacteria were grown with μg/ml 100 ampicillin, 34 μg/ml chloramphenicol, or 50 μg/ml kanamycin.

Genetic manipulations

The *csgA-cpxP his* fusion was synthesized by overlap PCR using standard PCR protocols. Chromosomal DNA from MC4100 was used as a template. An N-terminal portion encoding residues 1-42 of premature CsgA and the first 20 residues of mature CpxP was amplified with the primers *csgA* F Nco (GTTTCCATGGCGAAACTTTTAAAAGTAGCAGCAATTGCAGC) and *csgA-cpxP* R (CGCCTGAACCGACTTCAGCATTTGGGCC

GCTATTATTACC). A C-terminal region encoding residues 36-42 of CsgA and his-tagged mature CpxP was amplified with the primers *csgA-cpxP* F (GGTAATAATAGCGGCCCAAATGCTGAAGTCGGTTCAGGCG) and *cpxP his* R Pst (GTTTCTGCAGTTAGTGGTGGTGGTGGTGGTGCTGG GAACGTGAGTTGCTAC). The two regions were fused together in a third PCR, and the product was cloned into the Kpn1 and Pst1 sites of pBAD33.
LSR35 was constructed by deleting the *csgEF* locus with a PCR product encoding the kanamycin resistance cassette from pKD13 using the phage λ Red recombinase (Datsenko and Wanner, 2000). The resistance cassette was amplified from pKD13 with the primers *csgE* KO F no FRT (AGCGGTTTCC TGGGCAAACGATAACCTCAGGCGATAAAGCCACGCTGCCGCAAGCACTC) and *csgF* KO R no FRT (AATAAGCGCTGCATGATTATTTT CCTTATGAAGCTGGGGAATAGGAACTTCAAGATCC).

Immunoblot analysis

Bacteria grown on YESCA plates were resuspended in phosphate buffered saline (PBS) and cell number was normalized by taking OD_{600} measurements in a Beckman DU 650 spectrophotometer. Cells were then pelleted and pretreated with (for CsgA and CsgB Western blots) or without formic acid prior to solubilization in SDS loading buffer. Samples were boiled for 5 minutes prior to being electrophoresed through 15% acrylamide gels. Proteins were transferred to nitrocellulose overnight at 17 V in 25 mM CAPS, pH 11.2. Membranes were blocked in TBST containing 1% milk protein and 1% bovine serum albumin (BSA) for 1 hour prior to antibody application. Antibodies were used at the following

concentrations: α CsgA, 1:4000; α CsgB, 1:4000, α CpxP, 1:5000. Horseradish peroxidase-conjugated secondary antibodies (Upstate Biotechnology) were used at a 1:5000 dilution. Detection was performed with Supersignal West Pico chemiluminescent substrate from Pierce. Blots were exposed to Classic Blue autoradiography film from Midwest Scientific.

Electron microscopy

Electron microscopy was performed with a JEOL electron microscope. After growth on YESCA for 48 hours, bacteria were resuspended in PBS and applied to Formvar-coated copper grids for one minute. Specimens were then stained with 0.2% uranyl acetate for 1-2 minutes prior to visualization.

Antibiotic sensitivity assays

E. coli strain LSR11 containing pMC1 (*csgG* in pTrc99a) and either pBAD33, pLR42 (*csgE* in pBAD33), pLR58 (*csgF* in pBAD33) was diluted 1:500 from overnight cultures and grown to an OD600 of 0.05 in LB broth at 37°C shaking. Protein expression was induced with 0.1 mM IPTG and 0.04% arabinose, and 30 μg/ml of erythromycin was added 30' later. OD600 measurements were recorded at 40-minute intervals for 6 hours.

Real time CsgA polymerization assay

CsgA polymerization was monitored *in vitro* by measuring the fluorescence generated when the reaction was mixed with thioflavin-T according to the method described (Wang et al., 2007).

Figure legends

Figure 4.1. Overexpression of CsgG restores stability of CsgA, CsgB, and CsgF to the *csgE* mutant. Bacteria were grown on YESCA agar for 48 hours at 26°C. (A) WT MC4100 and the Δ*csgE* mutant MHR480 (E-) complemented with different plasmids were streaked on Congo red indicator agar. pE, pF, and pG denote *csgE*, *csgF*, and *csgG* under the control of the *csgBA* promoter in pLR1. pE+, pF+, and pG+ represent *csgE*, *csgF*, and *csgG* under the control of the *trc* promoter in p*Trc* 99 A. (B) Western blot analysis of the same strains as in (A). Whole cell lysates were transferred to nitrocellulose and probed with CsgA- and CsgB-specific antisera. (C) Whole cells of wild type (WT, MC4100), *csgE*/vector (MHR480/pLR1), *csgE*/p*csgE* (MHR480/pLR70), *csgE*/vector+ (MHR480/pTrc99a) and *csgE*/p*csgG*+ (MHR480/pMC1) were collected after 48 hours of growth on YESCA agar and analyzed by α-CsgF immunoblot. v = empty vector; "+" indicates an overexpression vector. (D) Whole cells of *csgE*/vector (MHR480/pLR1), *csgE*/p*csgE* (MHR480/pLR70), and *csgE*/p*csgG*+ (MHR480/pMC1) were collected after 48 hours of growth on YESCA agar. Whole cells were treated with 0, 10 or 200 μg/ml of proteinase K (PK), then analyzed by α-CsgF immunoblot. A long exposure of the α-CsgF immunoblot is included to visualize faint bands. α-DsbA immunoblots were used as a positive control for cell integrity. v = empty vector; "+" indicates an overexpression vector.

Figure 4.2. Effects of CsgE on the CsgG-dependent secretion of CpxP and A22-P chimera. Bacteria were grown in LB at 37°C shaking and whole cell and supernatant fractions were subjected to Western blot analysis using CpxP-

specific antisera in these experiments. (A) Wild type CpxP and the A22-P fusion protein were expressed in the presence (G) or absence (-) of CsgG from pMC1 in strain LSR11 (Δ*csg*). (B), lanes 1-4; CsgG and CsgA-CpxP were expressed from the same operon in pLR142 in the presence (G+E) or absence (G) of CsgE from pLR42. (B), lanes 4-8; CsgG and WT CpxP were expressed from pLR210 in the presence or absence of CsgE.

Figure 4.3. Effects of CsgE on erythromycin sensitivity conferred by the overexpression of CsgG. LSR11 containing pMC1 (pG) with either pBAD33, pLR42 (pE), or pLR58 (pF) were grown in LB at 37°C shaking with 30 μg/ml erthromycin and measured by OD600 at 40 minute intervals.

Figure 4.4: CsgE and CsgF have opposing effects on secretion when CsgG is limiting. Bacteria were grown in LB at 37°C shaking and whole cell and supernatant fractions were subjected to Western blot analysis using CpxP-specific antisera. CsgG was expressed at low levels from the chromosome of strain LSR35. CsgA-CpxP was expressed from pLR116 by itself, with CsgE from pLR42, or with CsgF from pLR58.

Figure 4.5. CsgE prevents self-polymerization of CsgA into amyloid fibers. Freshly purified CsgA was incubated alone (A) or in the presence of 22.5 μM CsgE (B) for 24 hours before visualization with transmission electron microscopy (TEM). Typical TEM images are shown. Scale bars equal 500 nm. (C) Real-time monitoring of CsgA self-assembly into amyloid fibers by ThT fluorescence. 25 μM

CsgA was incubated reaction buffer containing ThT either alone (open circles) or with 22.5 μM CsgE (closed diamonds). 22.5 μM CsgE was also incubated in reaction buffer (open triangles).

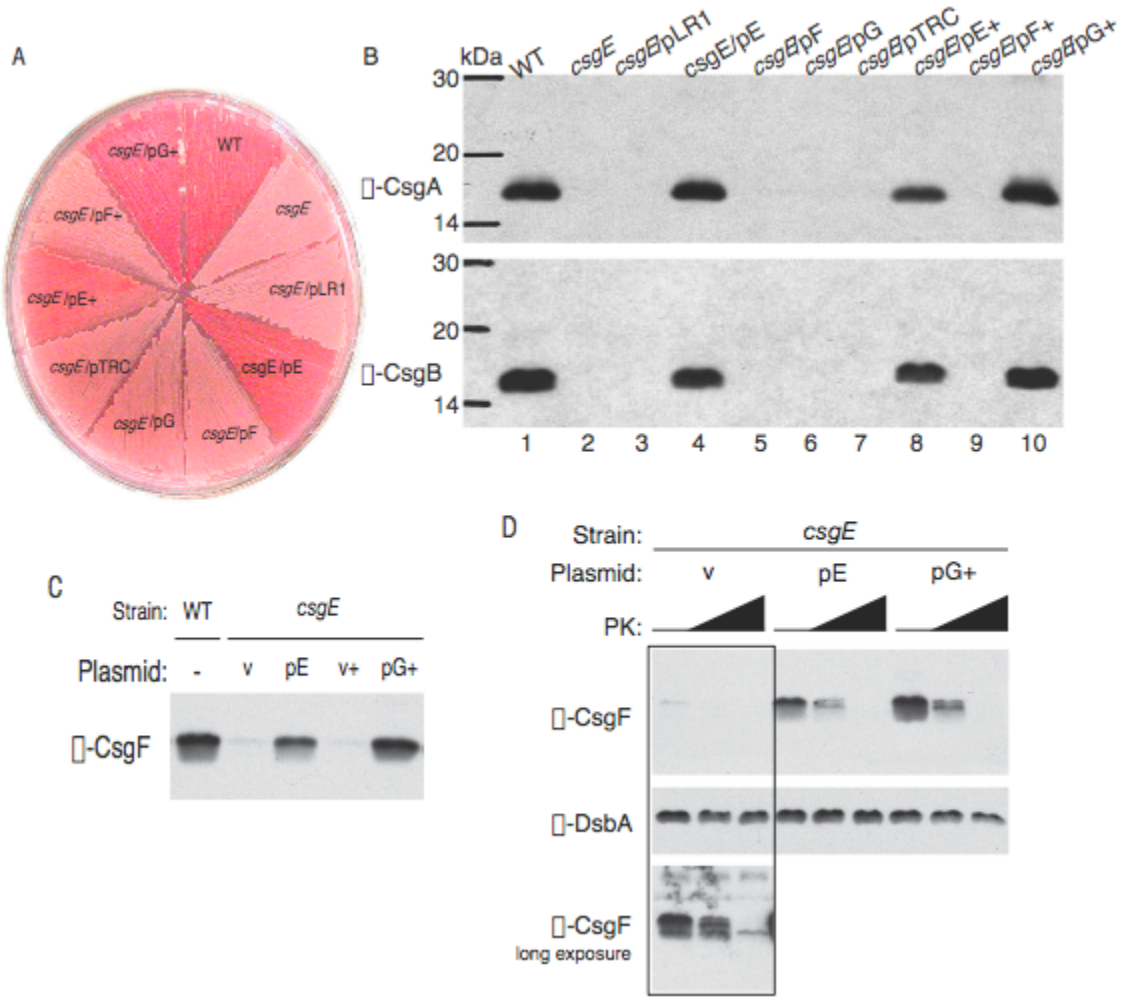

Figure 4.1. Overexpression of CsgG restores stability of CsgA, CsgB, and CsgF to the *csgE* mutant.

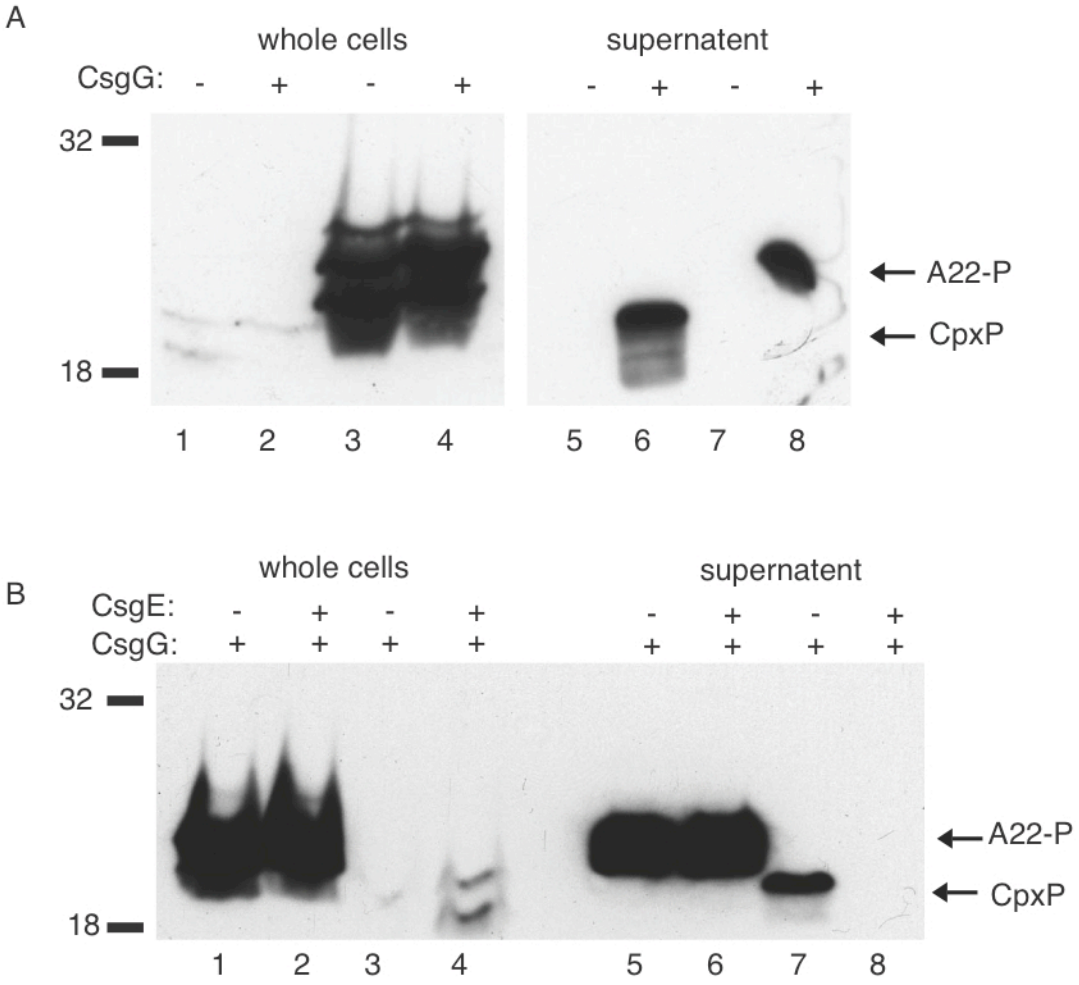

Figure 4.2. Effects of CsgE on the CsgG-dependent secretion of CpxP and A22-P chimera.

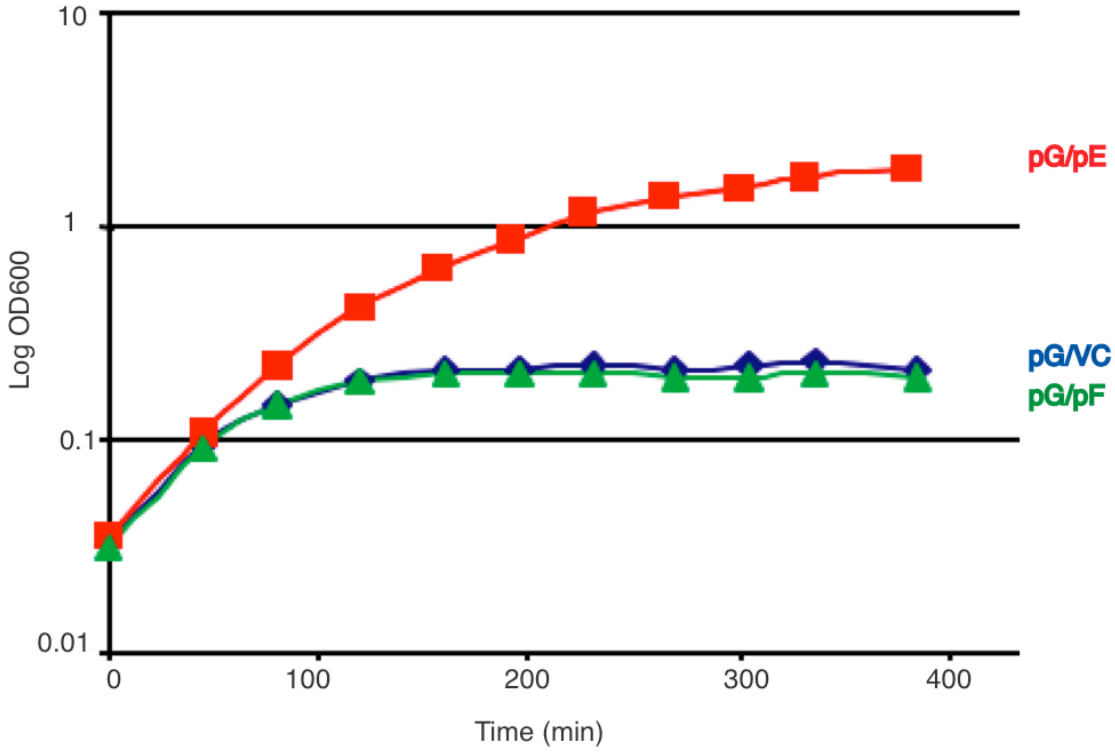

Figure 4.3. Effects of CsgE on erythromycin sensitivity conferred by the overexpression of CsgG.

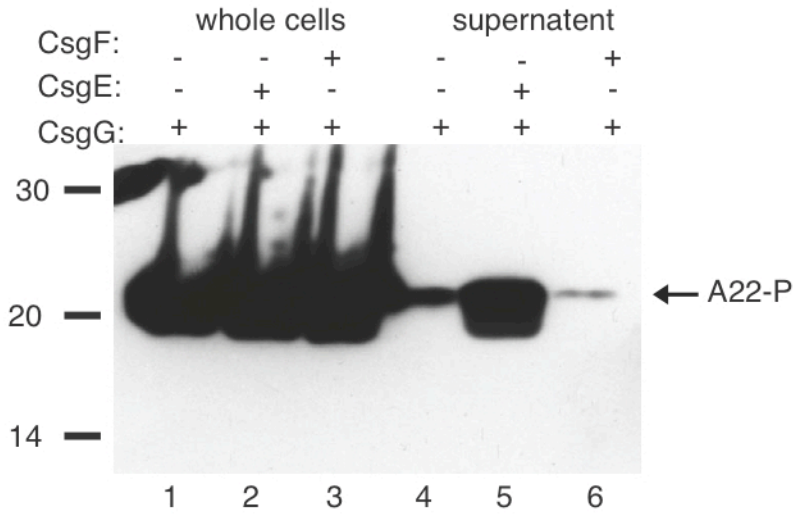

Figure 4.4: CsgE and CsgF have opposing effects on secretion when CsgG is limiting.

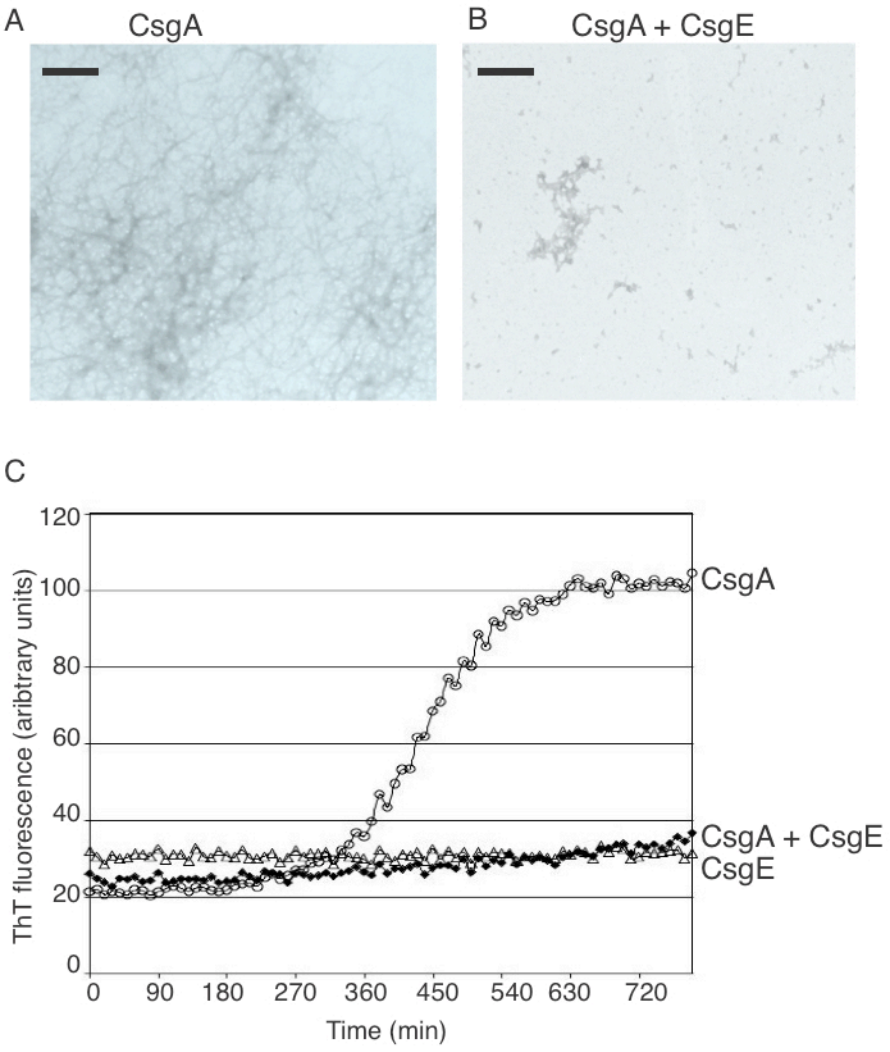

Figure 4.5. CsgE prevents self-polymerization of CsgA into amyloid fibers.

Strains/plasmids/ antibodies	Genotype/features	Source/reference
Strains		
MC4100	F- *araD*139 Δ(*argF-lac*)U169 *rspL*150(Str^r) *relA*1*flbB*5301 *deoC*1 *ptsF*25 *rbsR*	Casadaban, 1976
MHR480	MC4100 Δ*csgE*	Hammar et al, 1996
LSR11	MC4100 Δ*csg*	Chapman et al, 2002
LSR35	MC4100 Δ*csgEF*, *kanR*::*csgG*	This study
LSR1	MC4100 *csgG::Tn*105	Chapter 3
Plasmids		
p*Trc* 99 A	IPTG-inducible expression vector	Pharmacia Biotech
pBAD33	Arabinose-inducible expression vector	Guzman et al,
pLR1	*csgBA* promoter amplified with primers BP/OFBgl2 and BP/ORNcoPst and cloned into the BamH1 and Pst1 sites of pACYC177.	Chapter 2
pLR70	*csgE* cloned into the Nco1 and Pst1 sites of pLR1.	Chapter 3
pLR50	an ORF encoding residues 1-42 of premature CsgA fused to C-terminally his tagged mature CpxP cloned into the Nco1/Pst sites of pBAD33.	This study
pLR62	*cpxP-his* cloned into pBAD33.	This study
pLR15	*csgG* with a Kpn1 site at the 3' terminus cloned into pTrc99 A	This study
pLR142	*csgA-cpxP-his* cloned into the Kpn1/Pst1 sites of pLR15	This study
pLR210	*cpxP-his* cloned into the Kpn1/Pst1 sites of pLR15	This study
pLR116	The Nco/Pst1 fragment of pLR50 cloned into p*Trc* 99 A	Pharmacia Biotech
pLR42	*csgE* cloned into the pBAD33	This study
pLR58	*csgF* cloned into pBAD33	This study
pMC1	*csgG* cloned into pTrc 99 A	Chapman et al, 2002
pLR93	*csgG* cloned into the Nco1/Pst1 sites of pLR1.	Chapter 3
pLR73	*csgF* cloned into the Nco1/Pst1 sites of pLR1.	This study
pLR71	*csgE* cloned into the Nco1/Pst1 sites of p*Trc* 99 A	Chapter 3
pLR74	*csgF* cloned into the Nco1/Pst1 sites of p*Trc* 99 A	This study
pLR29	*csgEFG* amplified from pMC5 with pTrc F Kpn and G R Bgl/Pst and cloned into the Kpn1 and Pst1 sites of pBAD33	This study
Antibodies		
α CsgG	Polyclonal rabbit antiserum to CsgG	This study
ZB-AIII	Purified polyclonal rabbit antiserum to CsgA	Hammar et al, 1996
LR-α CsgB	Polyclonal rabbit antiserum to the peptide (EGSSNRAKIDQTGDY) of CsgB	Chapter 2
α CpxP	Polyclonal rabbit antiserum to CsgB	This study

Table 4.1: Strains, plasmids, and antibodies used in this study.

References

Brodsky, J.L., Goeckeler, J., and Schekman, R. (1995) BiP and Sec63p are required for both co- and posttranslational protein translocation into the yeast endoplasmic reticulum. *Proc Natl Acad Sci U S A* **92**: 9643-9646.

Chapman, M.R., Robinson, L.S., Pinkner, J.S., Roth, R., Heuser, J., Hammar, M., Normark, S., and Hultgren, S.J. (2002) Role of *Escherichia coli* curli operons in directing amyloid fiber formation. *Science* **295**: 851-855.

Gibson, D.L., White, A.P., Rajotte, C.M., and Kay, W.W. (2007) AgfC and AgfE facilitate extracellular thin aggregative fimbriae synthesis in Salmonella Enteritidis. *Microbiology* **153**: 1131-1140.

Gophna, U., Barlev, M., Seijffers, R., Oelschlager, T.A., Hacker, J., and Ron, E.Z. (2001) Curli fibers mediate internalization of Escherichia coli by eukaryotic cells. *Infect Immun* **69**: 2659-2665.

Gophna, U., Oelschlaeger, T.A., Hacker, J., and Ron, E.Z. (2002) Role of fibronectin in curli-mediated internalization. *FEMS Microbiol Lett* **212**: 55-58.

Hamman, B.D., Hendershot, L.M., and Johnson, A.E. (1998) BiP maintains the permeability barrier of the ER membrane by sealing the lumenal end of the translocon pore before and early in translocation. *Cell* **92**: 747-758.

Hammar, M., Arnqvist, A., Bian, Z., Olsen, A., and Normark, S. (1995) Expression of two csg operons is required for production of fibronectin- and congo red-binding curli polymers in Escherichia coli K-12. *Mol Microbiol* **18**: 661-670.

Hammar, M., Bian, Z., and Normark, S. (1996) Nucleator-dependent intercellular assembly of adhesive curli organelles in Escherichia coli. *Proc Natl Acad Sci U S A* **93**: 6562-6566.

Hammer, N.D., Schmidt, J.C., and Chapman, M.R. (2007) The curli nucleator protein, CsgB, contains an amyloidogenic domain that directs CsgA polymerization. *Proc Natl Acad Sci U S A* **104**: 12494-12499.

Loferer, H., Hammar, M., and Normark, S. (1997) Availability of the fibre subunit CsgA and the nucleator protein CsgB during assembly of fibronectin-binding curli is limited by the intracellular concentration of the novel lipoprotein CsgG. *Mol Microbiol* **26**: 11-23.

Olsen, A., Jonsson, A., and Normark, S. (1989) Fibronectin binding mediated by a novel class of surface organelles on Escherichia coli. *Nature* **338**: 652-655.

Olsen, A., Wick, M.J., Morgelin, M., and Bjorck, L. (1998) Curli, fibrous surface proteins of Escherichia coli, interact with major histocompatibility complex class I molecules. *Infect Immun* **66**: 944-949.

Robinson, L.S., Ashman, E.M., Hultgren, S.J., and Chapman, M.R. (2006) Secretion of curli fibre subunits is mediated by the outer membrane-localized CsgG protein. *Mol Microbiol* **59**: 870-881.

Vidal, O., Longin, R., Prigent-Combaret, C., Dorel, C., Hooreman, M., and Lejeune, P. (1998) Isolation of an Escherichia coli K-12 mutant strain able to form biofilms on inert surfaces: involvement of a new ompR allele that increases curli expression. *J Bacteriol* **180**: 2442-2449.

Wang, X., Smith, D.R., Jones, J.W., and Chapman, M.R. (2007) In vitro polymerization of a functional Escherichia coli amyloid protein. *J Biol Chem* **282**: 3713-3719.

Zogaj, X., Bokranz, W., Nimtz, M., and Romling, U. (2003) Production of cellulose and curli fimbriae by members of the family Enterobacteriaceae isolated from the human gastrointestinal tract. *Infect Immun* **71**: 4151-4158.

Chapter V

Conclusion

Curli fiber assembly occurs when soluble CsgA contacts the CsgB nucleator protein on the cell surface. The extracellular nucleation-precipitation assembly pathway to produce functional amyloid fibers is unique among the surface appendages described in Gram-negative bacteria. Critical to this assembly process is the transport of CsgA and CsgB across the outer membrane. We have shown that CsgG mediates secretion of CsgA across the outer membrane, that it can interact with several other proteins in the assembly complex, and forms a denaturation-resistant multimer. CsgG is spatially organized into clusters around curli fibers. We also have found that other *csg*-encoded proteins are required for certain aspects of CsgG assembly and organization in the membrane. Our results suggest a model where curli fiber assembly and secretion are tightly coordinated processes. The concluding chapter of this dissertation will review the major findings of my work, present outstanding questions and preliminary findings, and introduce an integrating model for curli assembly.

CsgG is a multimeric secretion pore in the outer membrane

I have made several observations that support the notion that CsgG can permit secretion across the outer membrane. Overexpression of CsgG resulted

in sensitivity to erythromycin (Chapter II), an antibiotic that is normally prohibited from crossing the outer membrane. The same level of CsgG expression permitted export of CsgA into culture supernatants (Chapter IV). Localization of CsgG to the outer membrane was required to achieve either CsgA secretion or sensitivity to erythromycin (Chapter II). Also consistent with its proposed role as a protein translocon, we found that CsgG spans the outer membrane (Chapter III) and forms a stable, denaturation-resistant oligomeric species (Chapters II and III). The observation that CsgG expression is directly correlated with changes in outer membrane permeability, and can only accomplish these effects when localized to the outer membrane (Chapter II), is highly suggestive that CsgG forms a pore in the outer membrane. However, we cannot yet exclude the possibility that CsgG acts indirectly on some other protein to facilitate CsgA secretion. One method of directly assessing the pore activity of a protein is by measuring the ability of a purified protein to permeabilize artificial membranes. To test the hypothesis that CsgG can form pores in lipid membranes, I measured the ability of CsgG to permeabilize dye-encapsulated liposomes (Fig. 5.1). The dye is self-quenching when compartmentalized into the liposomes, but gives an increased signal when the liposomes are permeabilized. Purified CsgG-his was added to dye-encapsulated liposomes and pore activity was measured as increase in fluorescence. The properties of CsgG present a few challenges to pursuing this method. First, CsgG requires detergent solubilization to permit its release from outer membranes (Chapter I). The detergent itself is capable of permeabilizing the liposomes, which may lead to false-positive readings. Secondly, even in the presence of detergent, CsgG falls

out of solution at concentrations greater than 0.5 mg/ml (Epstein, E.A., unpublished observation). It is unknown what concentration of CsgG will result in incorporation to artificial membranes. These caveats noted, I found that addition of 1 – 3 μg Elugent-solubilized CsgG-his resulted in permeabilization of dye-encapsulated liposomes to a degree greater than the detergent-containing buffer along (Fig. 5.1). This result supports the hypothesis that CsgG can form pores in lipid membranes. This assay may be valuable for future workers to utilize in testing direct pore activity of CsgG mutants, although it may be worthwhile to investigate the solubility of CsgG in various detergents to minimize the contribution of the detergent to the solubilization of liposomes.

Another property shared by many outer membrane secretion proteins is their ability to form ring-shaped multimeric complexes (Brok et al., 1999; Burghout et al., 2004; Collins and Derrick, 2007; Linderoth et al., 1997; Schmidt et al., 2001). Monomeric CsgG has a molecular weight of 30 kDa, but electron microscopic inspection of purified CsgG suggested that it formed a barrel-shaped oligomer (Chapter II). Further, CsgG oligomers were detected in all strains that expressed CsgG (Chapter III). Analytical gel filtration of purified CsgG-his suggested that most CsgG was assembled into an octamer (Fig 5.2A). This agreed with the measurements of the CsgG structures observed by electron microscopy (Chapman, M., unpublished observation). Native gel electrophoresis revealed that in addition to the putative 8-mer, two additional complexes were present when CsgG was overexpressed in the absence of the rest of the proteins in the curli assembly system: a 16-mer and a 24-mer CsgG complex. When CsgG was chromosomally expressed and solubilized from wild-type cells, a high

molecular weight species corresponding to a 24 mer was detected (Fig. 5.2B). This result suggested that the CsgG oligomers formed in WT cells were distinct then those formed when CsgG was expressed singly. Interestingly, partial denaturation by heat treatment of the WT complexes resulted in detection of the 8-mer CsgG complexes (Fig. 5.2B), suggesting that the 24-mer complexes may be composed of 8-mer intermediate molecular weight complexes. The putative 8-mer CsgG complexes were also detected in *csgE* and *csgA* strains after native gel electrophoresis (Fig. 5.2B). Importantly, another method is needed to confirm the exact molecular weight of the CsgG complexes, and native electrophoresis alone cannot alone be considered conclusive for molecular weight determination. Analytical centrifugation to confirm the molecular weight of CsgG oligomers is a technique that merits future investigation – although this technique may be complicated due to the low solubility of CsgG, and the low abundance of CsgG when expressed natively.

Another method I used to qualitatively measure the presence and relative size of the CsgG complex was the mobility of semi-denatured protein upon electrophoresis. Multimeric protein complexes in the bacterial outer membrane migrate slower on SDS-PAGE then their predicted monomeric molecular weights when incompletely denatured (Brok et al., 1999). Chromosomally expressed CsgG solubilized from wild-type cells ran as a single, high molecular weight species that was resistant to denaturation (Chapter III). However, chromosomally expressed CsgG obtained from strains lacking any or all of the other *csg*-encoded proteins, CsgE, CsgF, CsgB, or CsgA, showed an electrophoretic mobility shift to an intermediate molecular weight species (Chapter III). These

results qualitatively agree with our observations of CsgG assembly by native gel analysis. Therefore, regardless of the precise size of the CsgG complex, it seemed clear from these results that CsgG forms a complex whose size, stability, and folding was somehow influenced by the presence or absence of other components of the curli assembly machine.

CsgG: a surface exposed lipoprotein with two predicted transmembrane domains

How is CsgG targeted and assembled into the outer membrane? Most outer membrane localized lipoproteins are transported from the inner membrane to the outer membrane by the concerted efforts of the LolABCDE system. Most known substrates of the Lol system are localized to the inner leaflet of the outer membrane (Tokuda and Matsuyama, 2004). As shown in Chapter II, substitution of the penultimate N-terminal residue of mature CsgG with the Lol avoidance amino acid, aspartate, resulted in detection of CsgG at the inner membrane. This suggested that CsgG is likely a substrate of the Lol system. The inner-membrane localized CsgG construct failed to secrete or stabilize curli subunit proteins. CsgG was first proposed to be located on the inner leaflet of the outer membrane (Loferer et al., 1997), similar to what is seen for most other Lol-transported lipoproteins, but the ability of CsgG to mediate secretion of CsgA into culture supernatants suggested that CsgG might pass through the outer membrane. Indeed, I found that CsgG is exposed to the cell surface (Chapter III). Only one other putative Lol substrate is also exposed to the cell surface: Wza, the polysaccharide translocon (Drummelsmith and Whitfield, 2000). What regions of CsgG could comprise a transmembrane domain? I have utilized various

secondary-structure predication programs to identify potential transmembrane domains of CsgG (data not shown). Most secondary structure prediction software predicts that CsgG has an α-helical transmembrane domain near its C-terminus (Fig. 5.3A). If this putative α-helix comprised a single membrane spanning CsgG transmembrane domain, then we should expect that the C-terminus of CsgG is exposed to the cell surface, if the CsgG N-terminus was inside the cell. However, we found that a C-terminal hexahistidine tag on CsgG was on the inside of the cell (Chapter III). Also, α-helical transmembrane domains appear to be unusual in the outer membrane of Gram-negative bacteria, where most transmembrane domains are comprised of β-barrel architecture. When software that is modeled after known β-barrel outer membrane proteins is used, two short β-strands near the N-terminus of CsgG are predicted to serve as a β-barrel transmembrane domain (Fig. 5.3A; Bagos et al., 2004), with a small extracellular loop between the β-strands.

Targeted mutagenesis of the two CsgG putative membrane-spanning domains is one approach to identify the domains of CsgG that comprise the membrane-spanning regions as well as facilitate formation of CsgG oligomers. I took two approaches to mutating CsgG: alanine- and proline- scanning mutagenesis and deletion/truncation of CsgG. I next tested the stability of the CsgG mutant properties, their ability to support curli formation in a *csgG* strain. Most of the CsgG alleles constructed by these methods resulted in unstable proteins (Table 5.1). For example, alleles of CsgG lacking the C-terminus or either of the C-terminal domains were unstable, as were many alanine and most proline substitutions. However, several CsgG mutants yielded informative results.

I found that most stable CsgG mutants were localized to the outer membrane and exposed to the cell surface (Table 5.1). Finally, I also tested if stable, surface-exposed CsgG mutants would act in a dominant-negative fashion when expressed in WT cells. Since CsgG oligomerizes (Chapter I), dominant negative alleles may be due to formation of interactions between wild type CsgG and the co-expressed CsgG mutant or with other *csg* proteins.

One class of CsgG mutants contained substitutions in the putative N-terminal β-barrel transmembrane domain, such as CsgG-F50A (Fig. 5.3). Interestingly, CsgG-F50A was able to support CsgA stability and secretion out of the cell, although this CsgA did not efficiently assemble into curli fibers (Fig. 5.3B and E). CsgG-F50A was not spatially restricted in the manner seen for wild type CsgG (Fig. 5.3C and Chapter III), which may help explain the low efficiency of curli assembly. Finally, CsgG-F50A was not dominant when expressed in wild type cells (Fig. 5.3F), which may suggest that this protein can not form multimers with WT CsgG. Native gel electrophoresis showed that CsgG-F50A assembled into a 240 kDa complex (Fig. 5.3G), which is consistent with formation of an octomer. However, the high molecular weight CsgG complexes seen in WT cells were not detected. This may indicate that the putative β-barrel domain plays a role in formation of the high molecular weight CsgG complexes that form in WT cells. Importantly, I have been unable to detect the high molecular weight weight CsgG species when WT CsgG is overexpressed in any condition (Chapter III). Therefore, it is likely that the failure of CsgG-F50A to form the high molecular weight species is due to overexpression. Examination of CsgG-F50A at a lower level of expression should help clarify the phenotypes of this mutant.

Only one stable mutant in the putative C-terminal α-helix was generated, CsgG-V227A (Table 5.1 and Fig 5.4). This mutant was stable and localized to the outer membrane, but failed to secrete or stabilize CsgA (Table 5.1 and data not shown). Interestingly, CsgA-V227A did support CsgB-nucleation activity (Fig. 5.4B). This nucleation activity was dependent on the presence of CsgB and CsgF – two proteins essential for cell-associated *in vivo* nucleation of curli fibers. CsgG-V227A was dominant negative when expressed in wild type cells (Fig. 5.5C). This dominance was likely due to interaction of CsgG-V227A with the wild type protein, as CsgG-V227A and WT CsgG readily co-purified (Fig. 5.4D). I used analytical gel filtration chromatography to determine the approximate size of CsgG-V227A oligomers solubilized from outer membrane extracts. Interestingly, CsgG-V227A formed a complex of about 390 kDa, or about 13 CsgG molecules (Fig. 5.4E). WT CsgG formed a complex of calculated to be about 260 kDa by gel filtration chromatography, which is consistent with formation of an octomer.

To test the possibility that the putative extracellular loop was indeed exposed to the cell surface, CsgG variants were constructed that had a hexahistidine epitope inserted into the putative loop region or substituted for six of the least-conserved residues in the putative loop region (Table 5.1 and Fig. 5.5A). The hexahistidine substitution variant, CsgG-SUB was unstable under any expression conditions tested, but the insertion variant, CsgG-LOOP was stable and fractionated with the outer membrane (Table 5.1 and Fig.5.5C). CsgG-LOOP did not complement curli assembly when expressed in wild type cells, and was dominant negative when expressed in wild type cells (Fig. 5.5B). The dominance of CsgG-LOOP may suggest that this protein can interact with wild type CsgG. I

also found that the CsgG hexahistidine insertion variant was exposed to the cell surface (Fig. 5.5D) Unfortunately, the histidine epitope itself was undetectable by any immunoblotting method attempted (data not shown). However, this mutant yielded an interesting clue regarding how CsgF might be tethered to the cell surface. WT CsgG interacts with a cell surface accessory factor, CsgF (Chapter II.) CsgG is also required for the stability and surface localization of CsgF (Nenninger and Hultgren, manuscript submitted). Interestingly, no cell associated CsgF was detected in *csgG* cells expressing CsgG-LOOP, but CsgF was detected in the agar underlying *csgG* cells expressing CsgG-LOOP (Fig. 5.5E.). This result suggests the intriguing possibility that the CsgG extracellular loop also comprises the CsgF-CsgG interacting domain.

Taken collectively, the results obtained from mutagenesis of CsgG suggest that both the β-barrel domain and the α-helix domain are critical for CsgG function. One model supported by my data is that the putative N-terminal β-barrel domain facilitates formation of higher-order CsgG oligomers, but does not affect the secretion function of CsgG (Fig. 5.6). The C-terminal domain appears critical for CsgA secretion as well as formation of lower molecular weight CsgG oligomers. One possibility suggested by this model is that formation of the higher order oligomers is mediated by interaction of CsgG with other proteins, like CsgF, since disruption of the putative extracellular loop resulted un-tethered CsgF from the cell surface. This idea is also supported by the observation that partial denaturation of CsgG yields lower molecular weight CsgG (Chapter III). Future work to define the domain architecture of CsgG will help us to understand how CsgG interacts with other proteins critical for curli assembly.

Spatial restriction of CsgG and non-uniform production of curli fibers

The majority of secreted CsgA is assembled into curli fibers, and very little remains monomeric or unpolymerized(Chapman et al., 2002). In order to address how this process could be so efficient, I developed a testable model. One possibility is that CsgA and CsgB are secreted out of cells at the same location, thereby setting up a scenario where CsgA and CsgB are immediately ready to interact with each other upon exit of the cell and begin the fiber assembly process. Visual inspection of curli-producing cells revealed that curli fibers emanated from a spatially restricted location of a cell, although the precise location varied between cells (Chapter III). Since the transport of CsgA and CsgB out of the cell requires CsgG, we investigated the role of CsgG in the spatial restriction of curli fibers. We found that CsgG was spatially clustered to the region of the cell from where curli fibers emanated from the surface (Chapter III). We also examined the spatial distribution of CsgG in cells lacking the other proteins in the curli assembly system. Surprisingly, we found that CsgG was dispersed over the surface of cells lacking CsgA, CsgB, CsgF, or CsgE. Notably, *csgF* cells display greater levels of secreted, unpolymerized CsgA, suggesting that the dispersed CsgG complex was still able to mediate curlin secretion. Further, we found that fiber assembly was critical for the spatial clustering of CsgG. It is difficult to test exactly which interactions critical for fiber polymerization result in CsgG clustering, since loss of any single protein results in destabilization or mislocalization of multiple other proteins in the curli assembly system. For example, *csgE* cells are drastically depleted in levels of CsgF,

CsgA, and CsgB. It is clear, however, that the clustering of CsgG and polymerization of fibers are tightly coupled and connected processes.

Secretion and fiber assembly also appear to be tightly coupled processes. CsgA and CsgB are undetectable and do not accumulate inside *csgG* cells (Chapman et al., 2002; Loferer et al., 1997). Transcriptional activity of the *csgBA* promoter is significantly decreased in *csgG* cells, but unaffected by loss of any other *csg* protein except CsgD (data not shown). Notably, *csgBA* promoter activity in *csgG* cells is much greater than the activity detected in cells lacking the required activator, CsgD (data not shown). These results suggest that the reduction in CsgA and CsgB protein levels detected when secretion is impaired is due to a combination of negative regulation on the *csgBA* promoter and post-translational degradation of CsgA and CsgB. The mechanism by which CsgA and CsgB are degraded is not known, nor is it clear why *csgBA* promoter activity is reduced in a *csgG* mutant. It is known that CpxP, part of the osmolarity sensing and regulation system, can decrease the expression of the curli genes by inhibiting CsgD expression (Jubelin et al., 2005). One possibility is that CsgA and CsgB do initially accumulate in *csgG* cells, generating periplasmic stress that induces activation of cellular machinery that both clears periplasmic fiber subunits and down-regulates promoter activity. Alternatively, perhaps CsgA and CsgB never reach the periplasm in the absence of CsgG, and cytoplasmic factors mediate the degradation of fiber subunits and repression of *csgBA* transcription. Dissection of the molecular mechanisms underlying regulation and degradation of curli fiber subunits will have implications for how bacteria control amyloid toxicity. An outstanding question in understanding curli fiber biogenesis

is how cells prevent intracellular amyloid assembly and toxicity. It may be that in order to minimize amyloid toxicity a system is established that either secretes the subunits out of the cell or degrades them before the subunits can accumulate.

Interestingly, electron microscopic inspection of wild-type cells revealed that less than 40% of wild-type cells made contacts with curli fibers (Chapter III), and so the number of cells actually producing curli may be even lower. This observation may indicate that there is a cellular cost to producing and assembling curli fibers. I found that every curliated cell had spatially clustered CsgG on its surface (Chapter III). About 30% of all WT cells had clustered CsgG – similar to the number of cells producing curli fibers. With respect to CsgG protein distribution, there were two populations of non-curliated cells. Most non-curliated cells had no evidence of CsgG, while the other cells had somewhat decreased amount of CsgG on the cell surface relative to the level of CsgG observed on curliated cells (Chapter III). This pattern of detection of CsgG was also evident on non-curliated, CsgG-expressing strains like *csgA*: most *csg* mutant cells showed no CsgG while some cells showed randomly distributed CsgG on the cell surface (Chapter III). Therefore, it seems that the non-uniform distribution of CsgG protein among a population of cells is independent of curli assembly or other proteins of the curli biogenesis system. The expression profile of *csgG* in the population remains to be determined. It will be interesting to see if CsgG protein is produced but degraded in non-curliated cells, or if there is non-uniform transcription of *csgG* in the wild-type population.

CsgE function in the curlin secretion and assembly pathway

csgE phenotypes closely resemble the phenotypes of *csgG* cells: the cells are drastically decreased in production of CsgA, CsgB, and CsgF, although CsgG stability is unaffected (Chapman et al., 2002; Nenninger, A., manuscript submitted; Chapter III). Further, CsgG overexpression can suppress CsgE mutant phenotypes, indicating that these proteins function in the same genetic pathway (Chapter IV). Functional analysis of CsgE is complicated. As of this writing, we have failed to reproducibly detect CsgE when it is expressed off its native chromosomal position, although the protein can readily be detected when overexpressed, with or without an epitope tag. Therefore, the subcellular localizations and spatial distribution of natively expressed CsgE are still unknown. Also unclear is if CsgE stability depends on CsgG stability, as is the case for CsgA, CsgB, and CsgF. Despite these challenges, we examined the effects of CsgE on CsgG in an overexpression system. We found that CsgG and CsgE solubilized from outer membranes co-immunoprecipitate (Chapter II). We also found that CsgE expression suppressed CsgG-mediated erythromycin sensitivity (Chapter IV). The ability of CsgG to render cells sensitive to erythromycin suggested that the CsgG pore was ungated when overexpressed without other curli assembly proteins. In fact, we found that the same level of CsgG expression that rendered cells sensitive to erythromycin also resulted in non-specific secretion of periplasmic CpxP into culture supernatants (Chapter IV). CsgA secretion via CsgG is directed by a 22-residue N-terminal signal peptide (Chapter II). This signal peptide can be moved to non-*csg* proteins, like CpxP, and target them to CsgG at the outer membrane. Interestingly, when CsgE was co-expressed with CsgG, CsgA and a CpxP chimera containing the CsgA

secretion signal peptide (N22-P) were secreted out of cells, but the non-specific secretion of wild type CpxP was abolished (Chapters II and IV). We also found that, when CsgG expression was decreased, CsgE augmented secretion of the chimera N22-P (Chapter IV). One possibility, therefore, is that CsgE acts as a specificity factor that gates the CsgG pore while permitting passage of proteins containing the curlin secretion signal peptide. The other two curli-specific proteins that are exported to the cell surface and require both CsgE and CsgG for stability and secretion are CsgB and CsgF. Both CsgB and CsgF contain domains that are very similar to the CsgA N-terminal signal peptide (Chapman, M.R., unpublished observation). It is tempting to speculate that CsgE also helps augment the translocation of CsgF and CsgB across the outer membrane.

This evidence also supports the suggestion that CsgE works directly on CsgG in the cell. Interestingly, co-expression of CsgG and CsgE in *csgA-G* cells resulted in formation of CsgG clusters, while CsgG expressed in *csgA-G* cells failed to cluster (Epstein, E. A., unpublished observation). One possibility, therefore, is that CsgG clusters correspond to a multimeric species and CsgE favors that formation of this CsgG multimeric species. Such a model may help explain why CsgG overexpression suppresses *csgE* phenotypes. If CsgE helps low levels of CsgG to multimerize, then high expression of CsgG could favor multimeriation of CsgG in the absence of CsgE. Further, it is possible that the loss of the CsgG high molecular weight oligomers and clusters in the *csg* mutant strains is due to destabilization or mislocalization of CsgE. Therefore, it is critical to develop methods that will enable the native expression and localization of CsgE to be determined in each of the *csg* mutant strains.

CsgA self-assembly readily occurs with purified protein *in vitro*, but polymerized CsgA is never detected in cells lacking the nucleation protein CsgB, regardless of the level of CsgA expression. Much of this control is at the level of the CsgA protein itself, which has specific residues that favor or prohibit *in vivo* amyloid assembly (Wang and Chapman, 2008; Wang et al., 2008; Wang et al., 2007). However, it is also possible that other curli assembly factors modulate curlin self-assembly. We found that CsgE specifically inhibits self-assembly of CsgA polymers *in vitro* (Chapter IV). It remains to be seen if this effect occurs under physiological conditions, but from this data we can envision a model where CsgE gates the periplasmic face of the CsgG pore and prevents internal amyloid assembly. After secretion is accomplished, CsgA would not be localized near CsgE and so CsgA would be free to interact with CsgB and assemble into curli fibers. Obviously, this model assumes that CsgE is on the inside of the cell. Until *in vivo* analyses with CsgE are possible, there are still *in vitro* assays that would be very informative and help us order the secretion and assembly pathway. In particular, it would be very informative to test the *in vitro* ability of CsgB to nucleate CsgA into fibers in the presence of CsgE.

The MOO model for curli biogenesis

The evidence I have presented in this dissertation presents a two-part model for how cells accomplish controlled curli amyloid fiber assembly (Fig 5.7). First, CsgG is transported by the Lol system to outer membrane. During or after transport, CsgG forms a lower molecular weight oligomer (the *csg*-independent CsgG oligomer), is assembled into the outer membrane, and exposes a surface

domain. These steps are independent of any other curli-specific gene. Second, at the outer membrane CsgG is gated and grouped together with other components of the curli assembly machine, giving rise to multimers of the initial CsgG oligomers (MOO). CsgE and CsgF production proceeds CsgG due to the order of genes on the *csgDEFG* operon and, since CsgD is required for transcriptional activation of the *csgBA* operon, it is likely that a complex of CsgE, CsgF, and CsgG forms at the outer membrane prior to CsgA and CsgB entrance to the periplasm. CsgE promotes the export of at least CsgA out of the cell, while prohibiting intracellular amyloid assembly. The roles of CsgG and CsgE appear to be tightly linked, and an initial CsgG-CsgE interaction could favor formation of the CsgG multimer. Importantly, the collective interactions of all the curli assembly proteins are required to cluster the CsgG multimer in wild type cells, and clustering both requires and facilitates the interaction of CsgA and CsgB. Many questions regarding CsgG assembly and subunit secretion remain to be addressed. The most important of these is definition of the topology and domain architecture of CsgG and mapping of the regions of CsgG that enable the numerous protein-protein interactions made by this interesting protein. Increasing our understanding of how the curli assembly complex forms will help us understand how nature harnesses the power of amyloid formation and directs it to beneficial uses.

Experimental Procedures

Dye leakage assay

2.5 mg each of phosphatidyl choline and phosphatidyl ethanolamine were rehydrated into a film containing 50mM Carboxyfluorescein in 10mM NaPi (pH 7.4) with 100 mM NaCl. Samples were vortexed and sonicated to homogeneity and subjected to several freeze-thaw cycles to increase dye entrapment efficiency. After a final freeze cycle, samples were sonicated for about 10 minutes to generate small unilamellar vesicles. Free dye was removed from the preparation by running the sample on G-50 sephadex column in 10mM NaPi (pH 7.4) with 100 mM NaCl. Liposomes were diluted to 20 mM HEPES, pH 7.4, with 300 mM NaCl and fluorescence measured at excitation wavelength at 490 nm before and after adding 0.2% Triton-X100. Dye entrapment is confirmed when seeing a 5 – 10 fold increase in fluorescence after addition of detergent. Liposomes in 20mM HEPES-300mM NaCl were combined with 20μL 20mM HEPES-300mM NaCl-0.5% Elugent (HNE) or HNE containing soluble CsgG-his purified as described in Chapter II, and fluorescence emission at 517 nm monitored for several minutes.

CsgG solubilization, electrophoresis, and chromatography

Cells were fractionated by detergent extraction as described in Chapter II. Cell-free suspensions were generated by lysis of cell suspensions with two passages through a French press at 14,000 psi and removal of unbroken cells centrifugation at 3000xg for 15 minutes. Proteins in the cell free suspensions were solubilized with 0.5% Elugent. Elugent-soluble proteins from the sarkosyl-insoluble outer membrane fraction or the cell-free suspension were resolved by 5% stacking/13% or 8%-SDS-PAGE or by non-denaturing electrophoresis on a

4-12% Tris-Glycine gel (Invitrogen). CsgG-his and CsgG-V127A-HA were solublized from outer membranes as described above and outer membrane extract was subjected to analytical gel filtration chromatography using standard techniques. Briefly, samples and standards were applied to a Superdex 200 HR 10/30 column (Pharmcia Biotech) connected to an FPLC system with a mobile phase of HNE buffer. Molecular weight standards obtained from Sigma were suspended in HNE and elution volume determined. Void volume was determined by application of Blue Dextran 2000 (Sigma) to the column, and samples running at or greater than the void volume were pooled and probed for CsgG. No CsgG was detected in the void volume.

Figure Legends

Figure 5.1 CsgG-mediated permeabilization of artificial membranes. Liposomes containing the dye carboxy fluorescein were diluted into 180 μL 20 mM HEPES (pH 7.4)-0.3M NaCl and 20μL HNE buffer containing purified CsgG-his or buffer alone was added to give 1μg, 2 μg, or 3μg final concentration CsgG-his. Fluorescence was monitored continuously at excitation = 490nm and emission = 517 nm to measure dye release. Addition of mellitin (positive control for pore formation) is indicated by the *.

Figure 5.2 Size determination of CsgG oligomers (A) Analytical gel filtration of purified CsgG-his. 0.5mL fractions were collected and were western blotted with α-CsgG antibodies to determine the volume CsgG eluted from the column. Arrows indicate the two pools of CsgG detected after gel filtration. **(B)** Cells were

grown on YESCA plates at 26°C for 40 hours to induce expression of the *csg* genes. Blue native gel electrophoresis was used to resolve outer membranes from WT cells, *csgBACcsgDEFG* cells overexpressing CsgG (pCsgG), *csgA*, and *csgB* cells, as indicated. WT samples were also preheated at 95°C for ten minutes before loading onto the native gel. After electrophoresis, samples were blotted to a nitrocellulose membrane and blotted with α-CsgG antibodies.

Figure 5.3 Phenotypes of CsgG-F50A. (A) Schematic diagram of CsgG showing the Sec translocation signal, the acylated cysteine, the LoI recognition signal (star), and two predicted transmembrane domains (β TM and α TM). Location of 50th amino acid is indicated with the arrowhead. **(B)** LSR1 (*csgG*) containing the empty vector (pTRC99A), or vector containing either wild type CsgG (pMC1) or CsgG-F50A (pF50A) were plated on YESCA plates supplemented with curli-binding dye Congo red and grown in curli inducing conditions before photography. **(C)** Typical indirect immunofluorecence image obatained after probing cells with antibodies against CsgG and α-rabbit-Alexa488 secondary antibody. Shown is a merged image of the Alexa488 signal and DAPI-stained cell nucleoide (blue), although no Alexa488 signal is evident. **(D)** Intact cell dot blotting with α-CsgG antibodies of WT cells or *csgG* cells expressing CsgG-F50A (LSR1/pF50A). **(E)** Western blot with α-CsgA antibodies of cells and underlying media. Samples were boiled in SDS sample buffer with (+) or without (-) pretreatment with formic acid (FA) before loading samples onto the gel. **(F)** MC4100 or C600 containing plasmids to express CsgG-F50A or the functional CsgG allele CsgG-E23G-F50A were grown on Congo red-containing YESCA

plates to measure curli assembly. LSR11 and LSR12 are complete curli operon deletion strains derived from MC4100 or C600, respectively. **(G)** CsgG-F50A was solubulized from membranes and resolved by blue native gel electrophoresis before transferring to nitrocellulose membrane and probing with α-CsgG antibodies.

Figure 5.4 Phenotypes of CsgG-V227A. (A) Schematic diagram of CsgG showing the Sec translocation signal, the acylated cysteine, the LoI recognition signal (star), and two predicted transmembrane domains (β TM and α TM). Location of 227th amino acid is indicated with the arrowhead. **(B)** Ability of *csgG* expressing CsgG-V227A to support polymerization or nucleation activity was measured by the interbacterial complementation assay. *csgG*/pV227A was streaked across *csgA* or *csgB* cells and then the cross-streaks grown in curli-inducing conditions and curli production measured as Congo red binding. **(C)** Congo red binding of indicated strains. **(D)** Outer membranes were collected from cells expressing CsgG-HA, or CsgG-HA and CsgG-V227A-6xhis. Outer membranes (O) were applied to NiNTA column and the following fractions collected: flow through (ft), wash (w), and CsgG-V227A-his was eluted with 100 mM Imidazole (E1–S). Fractions were analyzed by western blotting with α-HA antibodies. **(E)** 0.5mL fractions obtained after analytical gel filtration chromatography of CsgG-his or CsgG-V227A-HA were resolved by SDS-PAGE before western blotting with α-CsgG antibodies. Approximate sizes of CsgG complexes were determined by comparison to molecular weight standards.

Figure 5.5 Phenotypes of CsgG-LOOP. (A) Schematic diagram of CsgG showing the Sec translocation signal, the acylated cysteine, the LoI recognition signal (star), and two predicted transmembrane domains (β TM and α TM). Residues encoding a hexahistidine epitope were inserted where indicated by the arrowhead. **(B)** Indicated strains were plated on Congo red containing YESCA plates and grown in curli inducing conditions. **(C)** Equal numbers of whole cells of the indicated strains were suspended in SDS-sample buffer and heated at 95°C for 10 minutes before SDS-PAGE and western blotting with α-CsgG antibodies. **(D)** Cells were grown on YESCA plates for 26°C for 40 hours to induce expression of the *csg* operons before spotting equal numbers of cells onto a nitrocellulose membrane and probing with α-CsgG antibody. **(E)** After growing cells in curli inducing conditions, whole cells or cells and the underlying agar were heated in SDS-containing sample buffer before SDS-PAGE and western blotting with α-CsgF antibodies.

Figure 5.6 Model of CsgG domain architecture. Shown is one model for how CsgG may assemble into the outer membrane and possible functional domains. CsgG-F50A is not dominant with WT CsgG, suggesting that the putative N-terminal β-barrel domain may also be critical for forming higher-order CsgG oligomers. CsgF becomes released from the surface of *csgG*/CsgG-LOOP cells, suggesting that CsgF may interact with the putative extracellular loop domain. CsgG-V227A fails to secrete or stabilize CsgA, although it is assembled into the outer membrane and interacts with WT CsgG. One possibility is that the C-terminal putative α-helix is critical for CsgA stability or secretion.

Figure 5.7 Model of CsgG assembly. CsgG assembly can be divided to two phases: those steps that are independent of other curli specific genes, and the steps that require the other *csg* proteins. First, CsgG is transported across the outer membrane by the Sec translocation system and is transported to the outer membrane by the LolABCDE system. CsgG oligomerization into the lower molecular weight oligomer, which forms independently of any other *csg* encoded protein, forms either at the outer membrane or possibly in the periplasm. Exposure of the CsgG surface domain is independent of any other *csg* protein. CsgE may interact with CsgG and favor formation of a clustered multimeric species, while acting to promote restritic CsgG-mediated secretion to *csg* proteins and prevent internal amyloid assembly. Other *csg* encoded proteins interact with CsgG at the outer membrane and all the curli assembly machinery is needed to achieve clustering of CsgG into focalized microdomains.

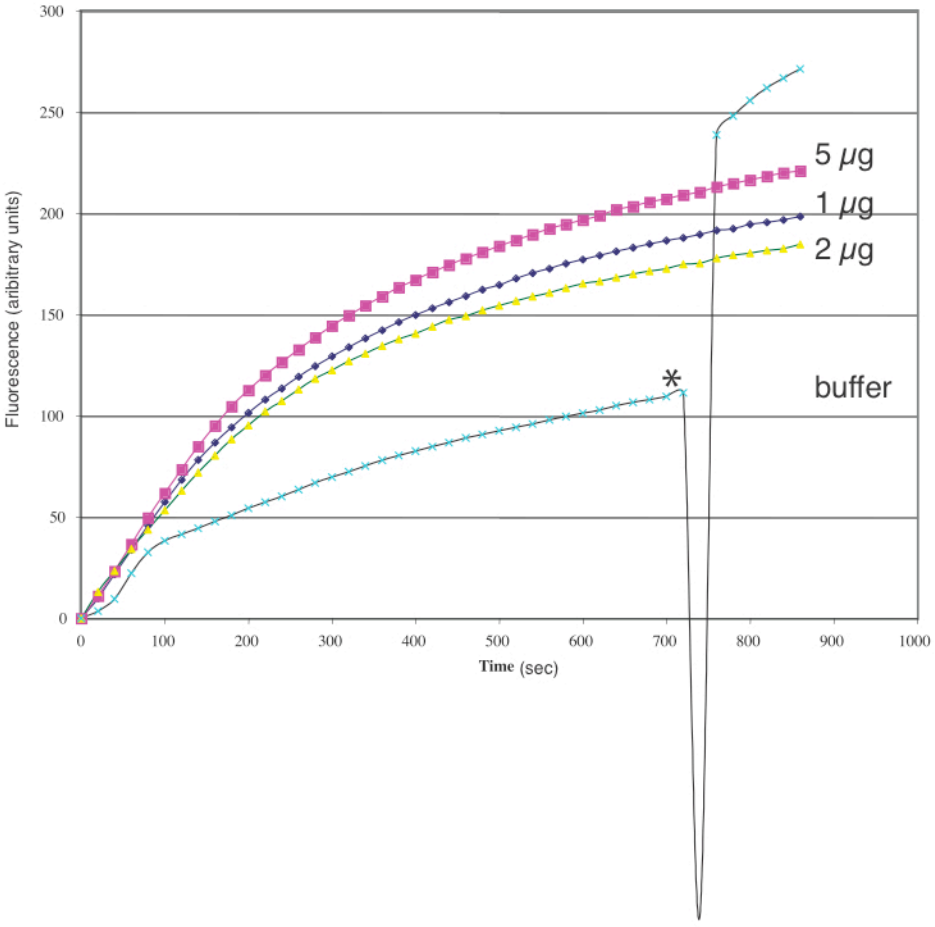

Figure 5.1 CsgG-mediated permeabilization of synthetic membranes.

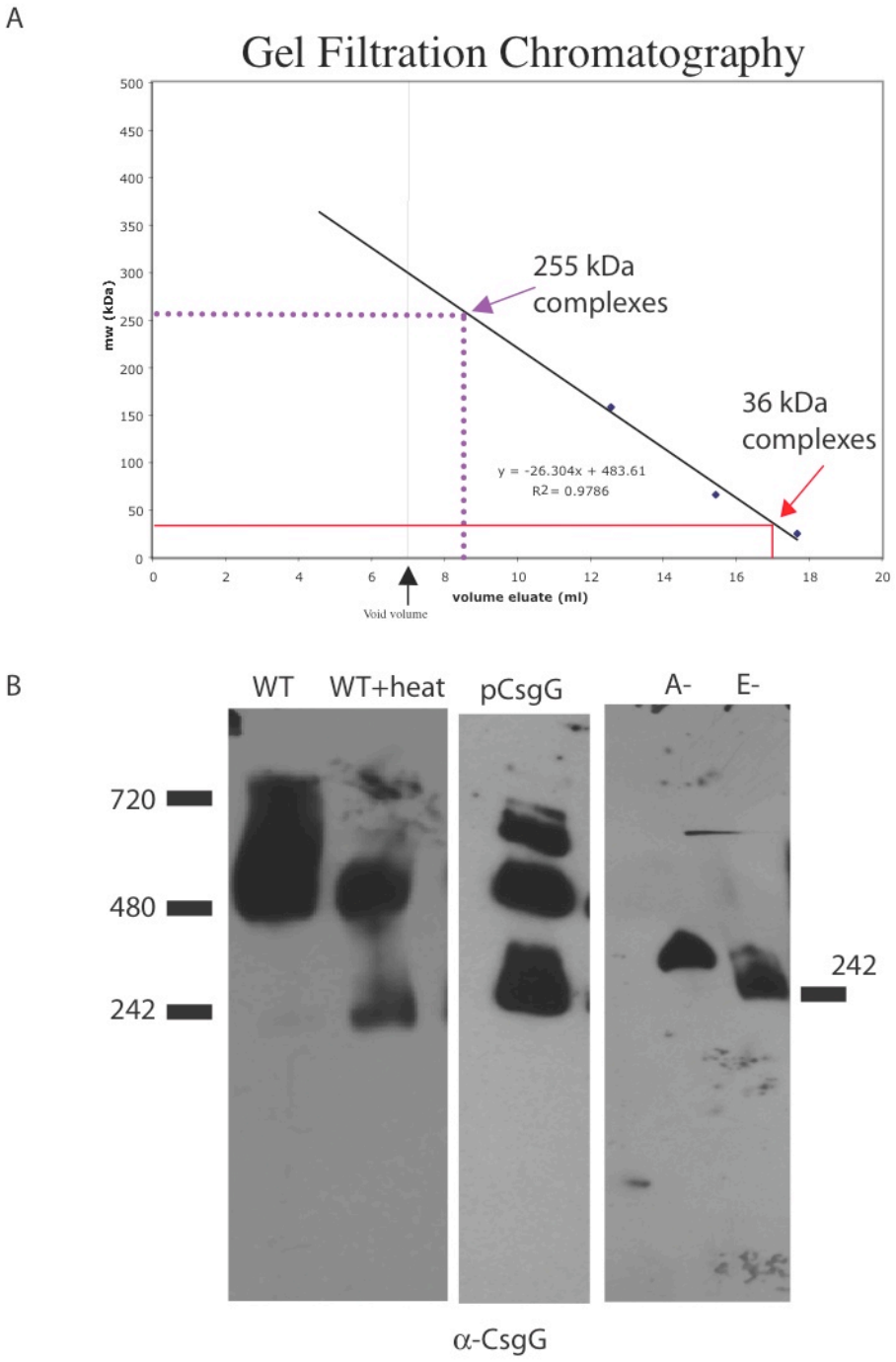

Figure 5.2 Size determination of CsgG oligomers.

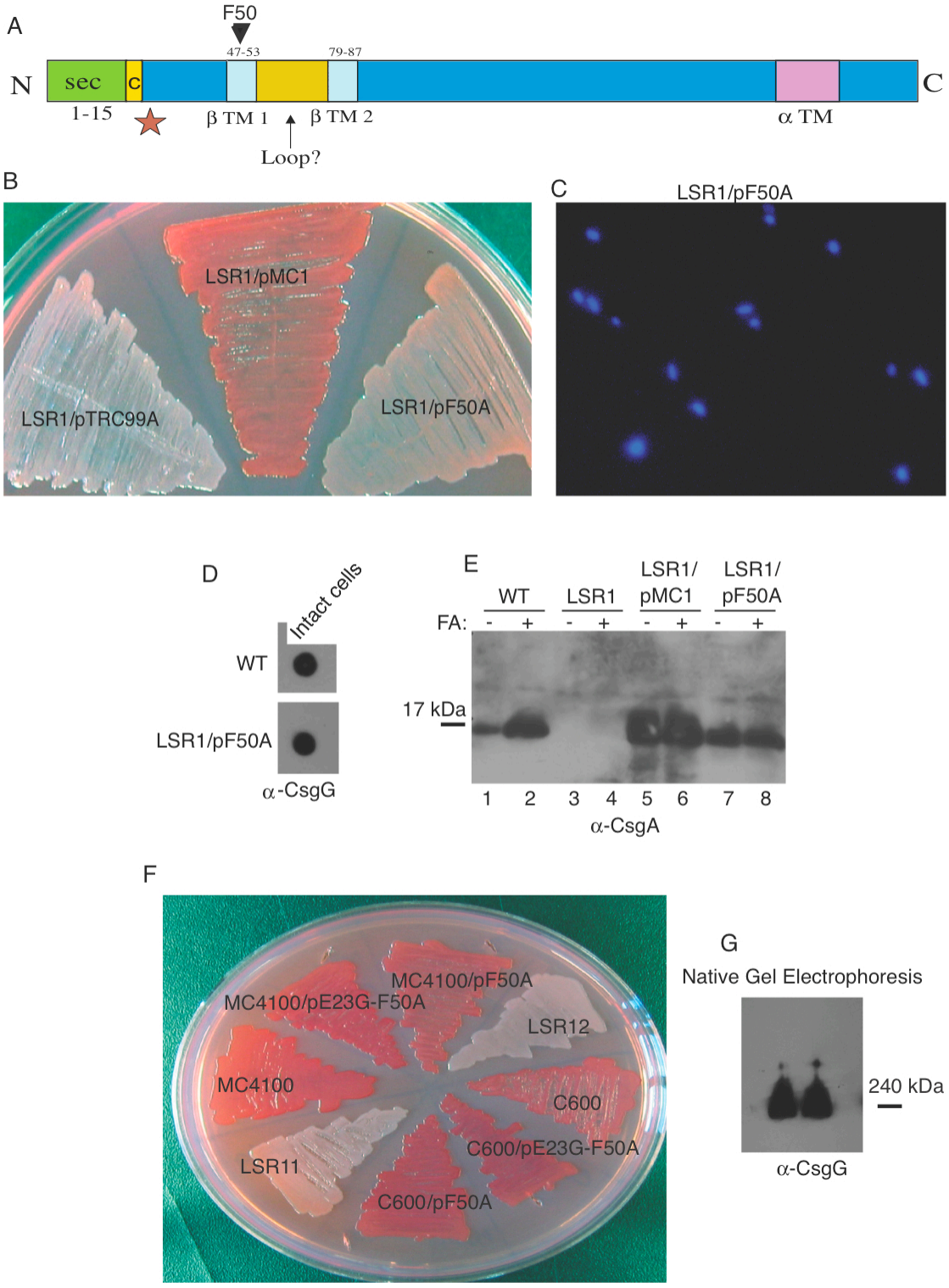

Figure 5.3 Phenotypes of CsgG-F50A.

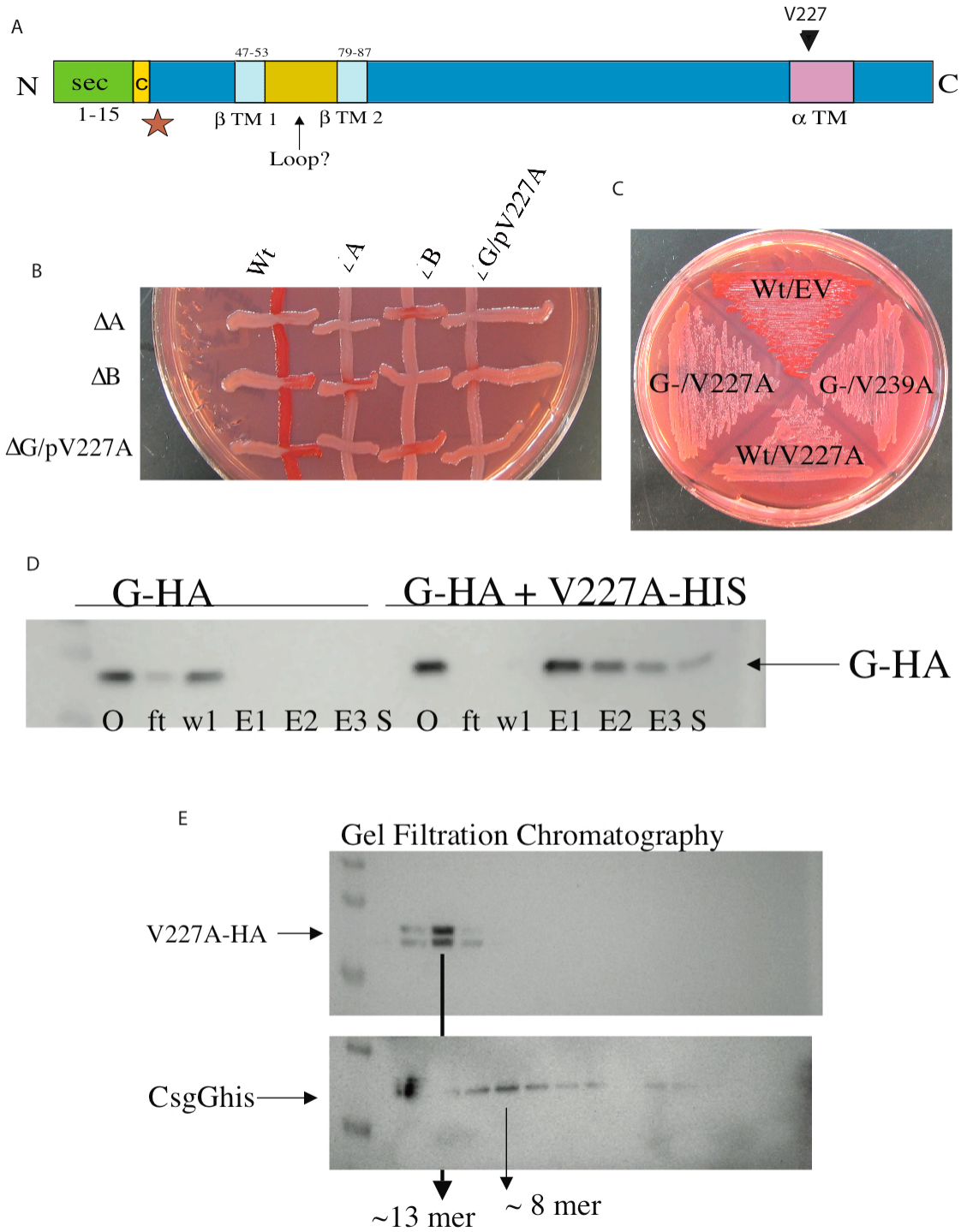

Figure 5.4 Phenotypes of CsgG-V227A.

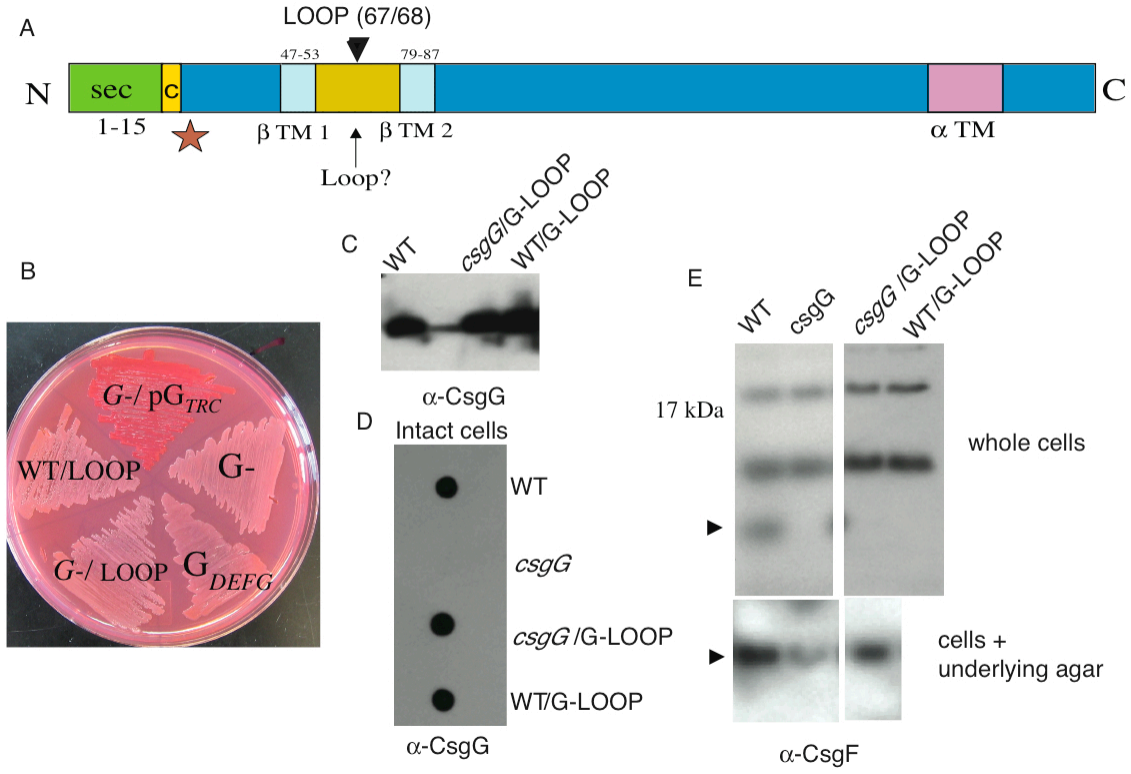

Figure 5.5 Phenotypes of CsgG-LOOP.

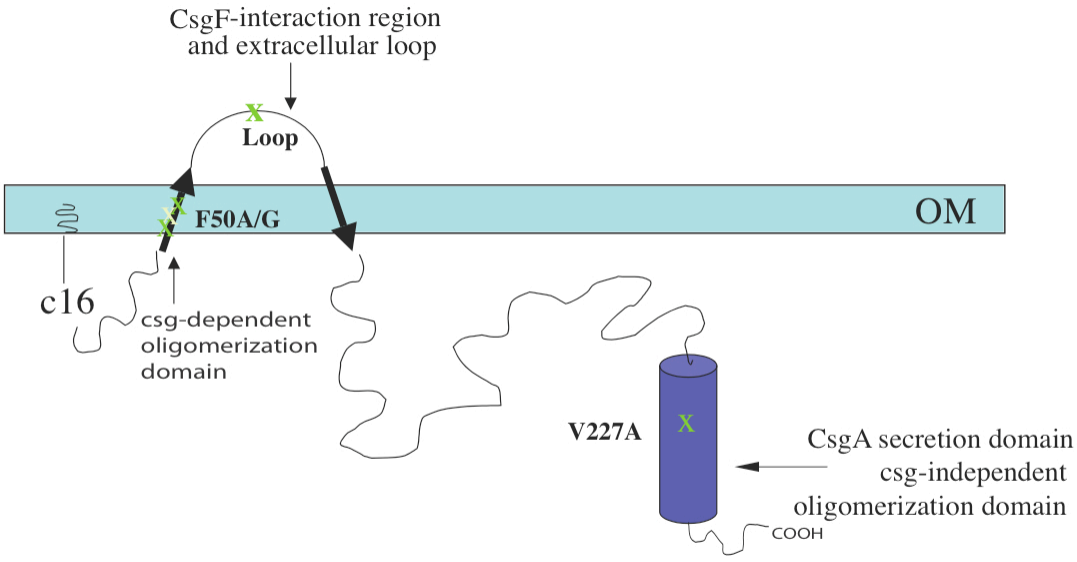

Figure 5.6 Model of CsgG domain architecture.

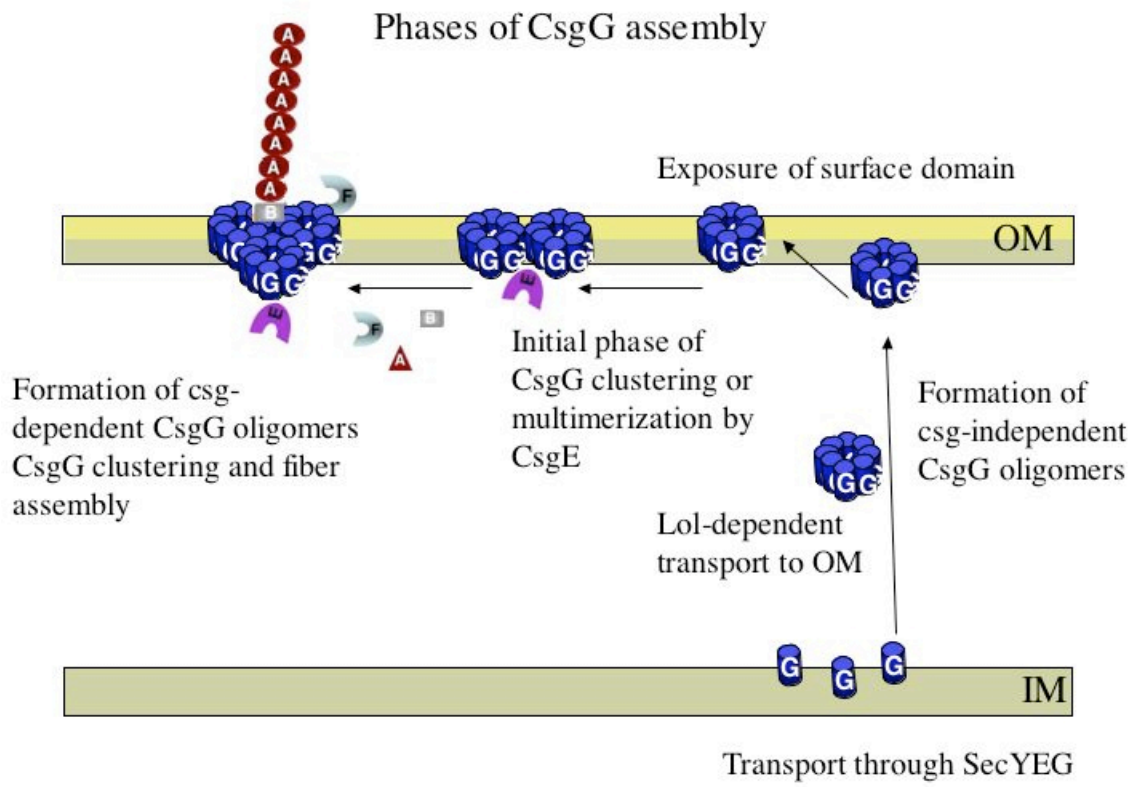

Figure 5.7 Model of the two phases of CsgG assembly.

CsgG mutant	Description	Stability*	CR binding	Surface exposed?	Dominant negative?
CsgG	Wild type CsgG allele	**+++**	**CR+**	**Yes**	
CsgG-L17D	Mutation of +2 residue to the Lol avoidance signal (Chapter II).	**+**	**CR-**	**No**	**No**
CsgGss	Replacement of native OM targeting sequences with periplasmic localization signal (Chapter II)	+	**CR-**	**No**	**Yes**
CsgG-LOOP	6x-his inserted between residues 67 and 68 of the putative extracellular loop immature protein.	**+++**	**CR-**	**Yes**	**Yes**
CsgG-SUB	6x-his substituted for residues 63-68 (FKPYPA) of the putative extracellular loop.	**-**	**CR-**	n.t.	n.t.
CsgG-DNTM	Missing residues 53 to 78 (the entire putative extracellular loop).	**-**	**CR-**	n.t.	n.t.
CsgG-CTRUNC	Missing residues 227 – 281 (including the putative α-helix).	**-**	**CR-**	n.t.	n.t.
CsgG-G47P	Proline scan of putative β-barrel transmembrane domain.	+++	**CR+**	**Yes**	n.t.
CsgG-I49P	Proline scan of putative β-barrel transmembrane domain.	**-**	**CR-**	n.t.	n.t.
CsgG-I49A	Alanine scan of putative β-barrel transmembrane domain.	+++	**Delayed CR+**	**Yes**	**No**
CsgG-F50A (or G)	Alanine scan of putative β-barrel transmembrane domain.	**+++**	**-**	**Yes**	**No**
CsgG-E23G/F50A	Alanine scan of putative β-barrel transmembrane domain.	**+++**	**CR+**	**Yes**	n.t.
CsgG-V51A	Alanine scan of putative β-barrel transmembrane domain.	**+++**	**CR+**	**Yes**	n.t.
CsgG-V51P	Proline scan of putative β-barrel transmembrane domain.	**-**	**CR-**	n.t.	n.t.
CsgG-V53A/P	Pro/Ala scan of putative β-barrel transmembrane domain.	**-**	**CR-**	n.t.	n.t.
CsgG-V227A	Alanine scan of putative α-helical transmembrane domain.	**+**	**CR-**	**Yes**	**Yes**
CsgG-V239A	Alanine scan of putative α-helical transmembrane domain.	**-**	**CR-**	n.t.	**No**

Table 5.1: Phenotypes of selected CsgG mutants.

* *csgG* cells containing plasmids encoding wild type CsgG or the various mutants were grown on YESCA plates for 48 hours at 26°C. Proteins were expressed from *trc* promoter in pTRC99A and stability measured by western blotting whole cell lysates using polyclonal rabbit α-CsgG antibody. Undetectable protein level is indicated with the **–** sign and level of expression similar to wild-type CsgG (expressed from *trc* promoter) indicated by **+++**. Some phenotypes were not tested (n.t.).

References

Bagos, P.G., Liakopoulos, T.D., Spyropoulos, I.C., and Hamodrakas, S.J. (2004) PRED-TMBB: a web server for predicting the topology of beta-barrel outer membrane proteins. *Nucleic Acids Res* **32**: W400-4.

Brok, R., Van Gelder, P., Winterhalter, M., Ziese, U., Koster, A.J., de Cock, H., Koster, M., Tommassen, J., and Bitter, W. (1999) The C-terminal domain of the Pseudomonas secretin XcpQ forms oligomeric rings with pore activity. *J Mol Biol* **294**: 1169-1179.

Burghout, P., van Boxtel, R., Van Gelder, P., Ringler, P., Muller, S.A., Tommassen, J., and Koster, M. (2004) Structure and electrophysiological properties of the YscC secretin from the type III secretion system of Yersinia enterocolitica. *J Bacteriol* **186**: 4645-4654.

Chapman, M.R., Robinson, L.S., Pinkner, J.S., Roth, R., Heuser, J., Hammar, M., Normark, S., and Hultgren, S.J. (2002) Role of *Escherichia coli* curli operons in directing amyloid fiber formation. *Science* **295**: 851-855.

Collins, R.F., and Derrick, J.P. (2007) Wza: a new structural paradigm for outer membrane secretory proteins? *Trends Microbiol* **15**: 96-100.

Drummelsmith, J., and Whitfield, C. (2000) Translocation of group 1 capsular polysaccharide to the surface of Escherichia coli requires a multimeric complex in the outer membrane. *EMBO J* **19**: 57-66.

Jubelin, G., Vianney, A., Beloin, C., Ghigo, J.M., Lazzaroni, J.C., Lejeune, P., and Dorel, C. (2005) CpxR/OmpR interplay regulates curli gene expression in response to osmolarity in Escherichia coli. *J Bacteriol* **187**: 2038-2049.

Linderoth, N.A., Simon, M.N., and Russel, M. (1997) The filamentous phage pIV multimer visualized by scanning transmission electron microscopy. *Science* **278**: 1635-1638.

Loferer, H., Hammar, M., and Normark, S. (1997) Availability of the fibre subunit CsgA and the nucleator protein CsgB during assembly of fibronectin-binding curli is limited by the intracellular concentration of the novel lipoprotein CsgG. *Mol Microbiol* **26**: 11-23.

Schmidt, S.A., Bieber, D., Ramer, S.W., Hwang, J., Wu, C.Y., and Schoolnik, G. (2001) Structure-function analysis of BfpB, a secretin-like protein encoded by the bundle-forming-pilus operon of enteropathogenic Escherichia coli. *J Bacteriol* **183**: 4848-4859.

Tokuda, H., and Matsuyama, S. (2004) Sorting of lipoproteins to the outer membrane in E. coli. *Biochim Biophys Acta* **1693**: 5-13.

Wang, X., and Chapman, M.R. (2008) Sequence determinants of bacterial amyloid formation. *J Mol Biol* **380**: 570-580.

Wang, X., Hammer, N.D., and Chapman, M.R. (2008) The molecular basis of functional bacterial amyloid polymerization and nucleation. *J Biol Chem* **283**: 21530-21539.

Wang, X., Smith, D.R., Jones, J.W., and Chapman, M.R. (2007) In vitro polymerization of a functional Escherichia coli amyloid protein. *J Biol Chem* **282**: 3713-3719.